BULLETIN DE L'ACADÉMIE
POLONAISE DES SCIENCES
Cl. III — Vol. V, No. 5, 1957

MATHEMATICS

On the Approximate Solution of Non-Linear Functional Equations

by

M. ALTMAN

Presented by W. ORLICZ on February 23, 1957

For approximate solutions of non-linear operator equations in Banach spaces L. V. Kantorovitch [1] has given an iterative method, which is an extension of Newton's well-known classical method. Other authors have also examined Newton's method and its applications. However, in all these investigations it is supposed that the Fréchet differential, which appears in Newton's method, possesses a continuous inverse. The examination of the existence of this inverse transformation and the evaluation of its norm are the greatest difficulties connected with the application of the above mentioned method.

But generally the solution of non-linear operator equations in Banach spaces can be reduced to a solution of non-linear functional equations in these spaces. In the present note we give an iterative method for approximate solutions of non-linear functional equations in Banach spaces.

Let X be a Banach space and let $F(x)$, $x \in X$, be a non-linear continuous functional defined on the closed sphere $S(x_0,r)$ of X with centre x_0 and radius r.

Consider the non-linear functional equation

$$F(x)=0. \tag{1}$$

We suppose that $F(x)$ is differentiable in the sense of Fréchet in the sphere $S(x_0,r)$ and denote the Fréchet differential of $F(x)$ by $f(x)=F'(x)$.

Define a sequence of elements of X as follows:

Put $f_0=f(x_0)=F'(x_0)$ and choose an element y of X such that $f_0(y)\neq 0$.

$$x_1=x_0-\frac{F(x_0)}{f_0(y)}\,y, \qquad x_{n+1}=x_n-\frac{F(x_n)}{f_0(y)}\,y. \tag{2}$$

This sequence defines the approximate solution of Eq. (1) by theorem given below.

THEOREM 1. *Let us assume that the following conditions are satisfied*:

$$(3)\qquad |F(x_0)|\leqslant D,\quad \frac{\|y\|}{|f_0(y)|}\leqslant B,\quad \|F'(x)-F'(x_0)\|\leqslant C,\quad F'(x_0)\neq 0$$

for all x *of* $S(x_0,r)$,

$$BC<1 \quad \text{and} \quad BD\leqslant r(1-BC).$$

Then the sequence (x_n) *defined by formula* (2) *converges to a solution* x^* *of Eq.* (1) *and* $x^*\in S(x_0,r)$.

Proof. It follows from (2) that

$$(4)\qquad f_0(x_n-x_{n+1})=F(x_n);$$

hence we get the identity

$$(5)\qquad f_0(x_n-x_{n+1})=F(x_n)-F(x_{n-1})-f_0(x_n-x_{n-1}).$$

Thus, we have by (2), (4) and (5)

$$(6)\qquad \|x_{n+1}-x_n\|=\frac{\|y\|}{|f_0(y)|}\,|F(x_n)-F(x_{n-1})-F'(x_0)(x_n-x_{n-1})|.$$

The analogue of Lagrange's formula applied to (6) gives by (3)

$$(7)\qquad \|x_{n+1}-x_n\|\leqslant B\sup\|F'(\bar{x})-F'(x_0)\|\,\|x_n-x_{n-1}\|,$$

where $\bar{x}=x_{n-1}+t(x_n-x_{n-1})$ and $0\leqslant t\leqslant 1$.

It follows from conditions (3) and (7) that the sequence (x_n) is contained in the sphere $S(x_0,r)$ and converges to an element x^* which also belongs to $S(x_0,r)$. Since $F(x_n)\to 0$, as $n\to\infty$ by (4), and $F(x)$ is continuous, x^* is a solution of Eq. (1).

Remark 1. For the error estimate we have the following evident formula

$$\|x_n-x^*\|\leqslant\frac{(BC)^nBD}{1-BC}.$$

Let us assume that the Fréchet differential $F'(x)$ satisfies the Lipschitz condition in a sphere $S(x_0,r)$. Using the same method as in Theorem 1 we can prove the following

THEOREM 2. *Let us suppose that the following conditions are satisfied*: *There exists a constant* K *such that*:

1° $B^2KD<\frac{1}{4}$.

2° *The Fréchet differential* $F'(x)$ *satisfies the Lipschitz condition with the constant* K *in the sphere* $S(x_0,r)$, *where*

$$r=\frac{1-\sqrt{1-4B^2KD}}{2BK}.$$

Then the sequence (2) *converges to a solution of Eq.* (1). *This solution belongs to sphere* $S(x_0,r)$.

Remark 2. It is sufficient to assume that the Fréchet differential $F'(x)$ satisfies the Lipschitz condition in the sphere $S(x_0,r)$, where $r=2BD$.

Let us now consider Eq. (1) under the assumption that there exists the second Fréchet differential $F''(x)$, the norm of which is bounded in some sphere $S(x_0,r)$, i. e., $\|F''(x)\| \leqslant K$ for $x \in S(x_0,r)$.

THEOREM 3. *Let us assume that the following conditions are satisfied: There exists a constant* K *such that:*

1° $B^2KD<\sqrt{2}-1$;

2° *The second Fréchet differential* $F''(x)$ *exists and satisfies the condition*

$$\|F''(x)\| \leqslant K$$

in the sphere $S(x_0,r)$, *where*

$$r=\frac{1+B^2KD-\sqrt{1-B^2KD-B^4K^2D^2}}{2BK}.$$

Then the sequence (2) *converges to a solution of Eq.* (1). *This solution belongs to sphere* $S(x_0,r)$.

Remark 3. It is sufficient to assume that the second Fréchet differential $F''(x)$ satisfies condition 2° for $r=2BD$.

The iterative process given by formula (2) is defined by the use of the Fréchet differential $F'(x)$ at the fixed point $x=x_0$. We shall now consider this process, replacing $F'(x_0)$ by $F'(x_n)$ for $n=0,1,2,\ldots$ Putting $f_n=f(x_n)=F'(x_n)$, we define a sequence of elements of X as follows:

$$x_1=x_0-\frac{F(x)}{f_0(y_0)}\,y_0, \qquad x_{n+1}=x_n-\frac{F(x_n)}{f_n(y_n)}\,y_n, \tag{8}$$

where the elements $y_n \in X$ are so chosen that $\|y_n\|=1$, $|f_n(y_n)| \geqslant \|f_n\|-\varepsilon$, and ε is a sufficiently small positive number defined below.

Let us now consider Eq. (1) under the assumption that there exists the second Fréchet differential $F''(x)$, the norm of which is bounded in the sphere $S(x_0,r)$, i. e., $\|F''(x)\| \leqslant K$ for $x \in S(x_0,r)$.

THEOREM 4. *Let us assume that the following conditions are satisfied:*

1° $|F(x_0)| \leqslant D$;

2° *there exist two constants* B *and* K *such that*

$$h_0=B^2KD<2;$$

3° *the Fréchet differential* $F'(x)$ *exists and satisfies the condition*

$$\sup_x \|F'(x)\|^{-1}=A<B$$

in the sphere $S(x_0,r)$, *where*

$$r=BD\sum_{n=0}^{\infty}\left(\frac{h_0}{2}\right)^{2^n-1}; \tag{9}$$

4° *the second Fréchet differential exists and satisfies the condition*

$$\|F''(x)\| \leqslant K$$

in the same sphere $S(x_0,r)$. *If, in addition, the positive number* ε *is so chosen that*

$$0 < \varepsilon < \max(A^{-1}, A^{-1}-B^{-1}),$$

then the sequence (8) *converges to a solution of Eq.* (1). *This solution belongs to sphere* $S(x_0,r)$.

Proof. It follows immediately from (8) that

$$f_n(x_n - x_{n+1}) = F(x_n). \tag{10}$$

Hence, we have the identity

$$f_n(x_n - x_{n+1}) = F(x_n) - F(x_{n-1}) - f_{n-1}(x_n - x_{n-1}). \tag{11}$$

As a consequence of (8), (10), and (11), we obtain

$$\|x_{n+1} - x_n\| = \frac{1}{|f_n(y_n)|}\,|F(x_n) - F(x_{n-1}) - f_{n-1}(x_n - x_{n-1})|.$$

Hence, using the analogue of Taylor's formula, we have by conditions 3° and 4°

$$\|x_{n+1} - x_n\| \leqslant \frac{BK}{2}\,\|x_n - x_{n-1}\|^2. \tag{12}$$

Since $\|x_1 - x_0\| = \dfrac{|F(x_0)|}{|f_0(x_0)|} < BD$ by 3°, we get by (12)

$$\|x_{n+1} - x_n\| \leqslant BD\left(\frac{B^2KD}{2}\right)^{2^n-1} = BD\left(\frac{h_0}{2}\right)^{2^n-1}. \tag{13}$$

The inequality

$$\|x_{n+1} - x_0\| \leqslant \|x_1 - x_0\| + \|x_2 - x_1\| + \ldots + \|x_{n+1} - x_n\| \leqslant BD\sum_{k=0}^{n}\left(\frac{h}{2}\right)^{2^k-1} < r$$

shows that the sequence of elements x_n is contained in the sphere $S(x_0,r)$.

The convergence of the sequence of elements x_n to an element x^* results from the inequality

$$\|x_n - x_{n+p}\| \leqslant BD\sum_{k=n}^{n+p-1}\left(\frac{h}{2}\right)^{2^k-1} < r\left(\frac{h}{2}\right)^{2^n-1}.$$

It follows from condition 4° that the sequence of $\|f_n\|$ is bounded. Hence, by (10), $F(x_n) \to 0$ as $x_n \to x^*$ and x^* is a solution of Eq. (1).

INSTITUTE OF MATHEMATICS, POLISH ACADEMY OF SCIENCES

REFERENCES

[1] L. V. Kantorovitch, *On Newton's method* (in Russian), Trudy Mat. Inst. im. Steklova, **28** (1949), 104.

BULLETIN DE L'ACADÉMIE
POLONAISE DES SCIENCES
Cl. III — Vol. V, No. 5, 1957

MATHEMATICS

Concerning Approximate Solutions of Non-Linear Functional Equations

by

M. ALTMAN

Presented by W. ORLICZ on February 23, 1957

Paper [1] contains an iterative method for solving non-linear functional equations in Banach spaces. This method may also be regarded as an extension of Newton's well-known classical method. But this extension is essentially different from that given by L. V. Kantorovitch [2].

The present note concerns the examination of the above method under different conditions. The fundamental role for Newton's method as given by Kantorovitch is played by the Fréchet differential. For the convergence of this process it is supposed that the Fréchet differential possesses a continuous inverse. The examination of the existence of this inverse transformation and the estimate of its norm presents the greatest difficulty for the application of Kantorovitch's method. These difficulties are obviated in our method. The present note contains also as an illustration an elementary example, for which our method is applicable, but Kantorovitch's method is in principle inapplicable, since in this case no inverse of the Fréchet differential exists.

Let X be a Banach space and let $F(x)$, $x \in X$, be a non-linear continuous functional defined on the closed sphere $S(x_0, r)$ of X with centre x_0 and radius r.

Consider the non-linear functional equation

$$F(x) = 0. \tag{1}$$

We suppose that $F(x)$ is differentiable in the sense of Fréchet in the sphere $S(x_0, r)$, and we denote by $f(x) = F'(x)$ the Fréchet differential of $F(x)$.

Putting $f_n = f(x_n) = F'(x_n)$ we choose a sequence of elements $y_n \in X$ such that

$$\|y_n\| = 1, \quad f_n(y_n) = \|f_n\| \qquad n = 0, 1, 2, \ldots \tag{2}$$

provided that such a choice is possible.

The iterative process for solving Eq. (1) is defined as in [1]:

$$x_1 = x_0 - \frac{F(x_0)}{f_0(y_0)}\, y_0, \qquad x_{n+1} = x_n - \frac{F(x_n)}{f_n(y_n)}\, y_n. \tag{3}$$

Moreover, let us assume that there exists the second Fréchet differential $F''(x)$ of $F(x)$ the norm of which is bounded in the sphere $S(x_0,r)$, i. e., there exists a constant K such that $\|F''(x)\| \leqslant K$ for every x of $S(x_0,r)$.

Conditions of the convergence of process (3) which are also sufficient conditions for the existence of a solution of Eq. (1) are given by the following

THEOREM 1. *Let us assume that the following conditions are satisfied:*

1° *for the Fréchet differential $f_0 = F'(x_0)$ at the initial approximate solution x_0 the inequality*

$$1/\|f_0\| \leqslant B_0 \tag{4}$$

is fulfilled;

2° *the error estimate for the first approximate solution is known and*

$$\|x_1 - x_0\| \leqslant |F(x_0)|/\|f_0\| \leqslant \eta_0; \tag{5}$$

3° *there exists a constant K such that the norm of the second Fréchet differential is bounded by it in the sphere $S(x_0,r)$, i. e.,*

$$\|F''(x)\| \leqslant K \quad \text{for} \quad x \in S(x_0,r); \tag{6}$$

4° *the constants B_0, η_0 and K satisfy the inequality*

$$h_0 = B_0\eta_0 K \leqslant \tfrac{1}{2}; \tag{7}$$

$$r = \frac{1-\sqrt{1-2h_0}}{h_0}\,\eta_0. \tag{8}$$

Then Eq. (1) *has a solution x^* which belongs to sphere $S(x_0,r)$ and the sequence of approximate solutions x_n defined by process* (3) *converges to x^*. For the error estimate we have the formula*

$$\|x_n - x^*\| \leqslant \frac{1}{2^{n-1}}\,(2h_0)^{2^{n-1}}\eta_0. \tag{9}$$

Proof. It follows immediately from (3) that

$$f_n(x_n - x_{n+1}) = F(x_n). \tag{10}$$

Hence, we have the identity

$$f_n(x_n - x_{n+1}) = F(x_n) - F(x_{n-1}) - f_{n-1}(x_n - x_{n-1}). \tag{11}$$

As a consequence of (2), (3), (10) and (11) we obtain

$$\|x_{n+1} - x_n\| = \frac{1}{\|f_n\|}\,|F(x_n) - F(x_{n-1}) - f_{n-1}(x_n - x_{n-1})|. \tag{12}$$

Hence, using the analogue of Taylor's formula, we have

$$\|x_{n+1}-x_n\| \leqslant \frac{K}{2\|f_n\|}\|x_n-x_{n-1}\|^2. \tag{13}$$

We shall now estimate the norm $\|f_1\|=\|F'(x_1)\|$:

$$\|F'(x_1)\| \geqslant \|F'(x_0)\|-\|F'(x_0)-F'(x_1)\| = \|F'(x_0)\|\cdot\left(1-\frac{\|F'(x_0)-F'(x_1)\|}{\|F'(x_0)\|}\right).$$

Hence, using the analogue of Lagrange's formula, we have by (4)

$$\|F'(x_1)\| \geqslant \|F'(x_0)\|\cdot(1-B_0K\eta_0) = \|F'(x_0)\|\cdot(1-h_0).$$

Thus, we obtain

$$\|f_1\|^{-1} \leqslant \frac{1}{1-h_0}\,\frac{1}{\|f_0\|} \leqslant \frac{B_0}{1-h_0} = B_1. \tag{14}$$

For $n=1$, (13) gives by (5) and (14)

$$\|x_2-x_1\| \leqslant \frac{1}{2}\cdot\frac{1}{1-h_0}\cdot B_0K\eta_0^2 = \frac{1}{2}\,\frac{h_0\eta_0}{1-h_0} = \eta_1. \tag{15}$$

Condition (7) is satisfied for $x=x_1$:

$$h_1 = B_1K\eta_1 = \frac{B_0}{1-h_0}\cdot\frac{1}{2}\cdot\frac{h_0\eta_0K}{1-h_0} = \frac{h_0^2}{2(1-h_0)^2} \leqslant 2h_0^2 \leqslant \frac{1}{2}. \tag{16}$$

Thus, conditions 1°-4° are satisfied for $x=x_1$ replacing the numbers B_0,η_0 and h_0 by B_1,η_1 and h_1. Hence, we can define by induction the approximate solution x_n and the corresponding numbers B_n,η_n and h_n, which satisfy the formulae analogous to (5), (14), (15) and (16):

$$\|x_{n+1}-x_n\| \leqslant \eta_n, \tag{5'}$$

$$B_n = \frac{B_{n-1}}{1-h_{n-1}}, \tag{14'}$$

$$\eta_n = \frac{1}{2}\cdot\frac{h_{n-1}\eta_{n-1}}{1-h_{n-1}}, \tag{15'}$$

$$h_n = \frac{1}{2}\,\frac{h_{n-1}^2}{(1-h_{n-1})^2}. \tag{16'}$$

Using the same argument as Kantorovitch [2] we obtain from (5'), (14'), (15') and (16')

$$\|x_{n+p}-x_n\| \leqslant \frac{1}{2^{n-1}}(2h_0)^{2^{n-1}}\eta_0. \tag{17}$$

The same argument shows that all the approximate solutions x_n are contained in the sphere $S(x_0,r)$ defined by (8). It follows from (17)

that the sequence (x_n) converges to an element x^* of the sphere $S(x_0,r)$. It follows from (10) that x^* is a solution of Eq. (1) since the linear functionals f_n are bounded.

Formula (9) results from (17).

Remark 1. Condition (7) can be replaced by the following:

$$h_0 = B_0^2 DK \leqslant \tfrac{1}{2}, \tag{7'}$$

where D is a constant such that $|F(x_0)| \leqslant D$.

Remark 2. It is convenient in practice to verify that condition (6) is satisfied in a constant sphere containing the sphere $S(x_0,r)$, where the radius is defined by (8). For this purpose we can take, for instance, the sphere $S(x_0,r)$, where $r = 2\eta_0$ or $r = 2B_0 D$.

Now let H be a real Hilbert space and let $S(x_0,r)$ be a closed sphere of H. Consider the non-linear operator equation

$$P(x) = 0, \tag{18}$$

where $P(x)$ is a non-linear continuous operator defined on $S(x_0,r)$ with values in H. Let us assume that $P(x)$ is differentiable in the sense of Fréchet in the sphere $S(x_0,r)$ and denote by $P'(x)$ the Fréchet differential of $P(x)$.

Putting $F(x) = \|P(x)\|^2$ we reduce Eq. (18) to Eq. (1). Process (3) can here be defined as follows:

$$\begin{aligned} x_1 &= x_0 - \frac{\|P(x)\|^2}{2\|Q(x_0)\|^2} Q(x_0), \\ x_{n+1} &= x_n - \frac{\|P(x_n)\|^2}{2\|Q(x_n)\|^2} Q(x_n), \end{aligned} \tag{19}$$

where $Q(x) = \overline{P}'(x) P(x)$ and the linear operator $\overline{P}'(x)$ is the adjoint of $P'(x)$. Suppose that there exists the Fréchet differential $Q'(x)$ in the sphere $S(x_0,r)$, and $Q'(x)$ is bounded, i. e., there exists a constant K such that $\|Q'(x)\| \leqslant K$ for every x of $S(x_0,r)$.

Theorem 1 can be formulated as follows:

THEOREM 2. *Let us assume that the following conditions are satisfied:*

1° $Q(x_0) = \overline{P}'(x_0) \neq 0$;

2° *there exists a constant K such that*

$$\|Q'(x)\| \leqslant K \quad \text{for every } x \text{ of } S(x_0,r);$$

3° $$\frac{\|P(x_0)\|^2 K}{\|Q(x_0)\|^2} \leqslant 2h_0 \leqslant 1,$$

where r is defined by (8).

Then Eq. (18) *possesses a solution x^* which belongs to sphere $S(x_0,r)$ and the sequence of approximate solutions x_n defined by process* (19) *converges to x^*. The error estimate is given by formula* (9).

Remark 3. The radius of the sphere $S(x_0,r)$, where r is defined by (9), can be replaced by $r=2\eta_0$, where

$$\frac{\|P(x_0)\|^2}{\|Q(x_0)\|^2}\leqslant 2\eta_0.$$

As an illustration of Theorem 2 we give the following elementary example which shows that Kantorovitch's method is not applicable in this case:

Consider the system of equations

$$f\equiv u^2+u+v+3/2=0,$$
$$g\equiv u^2+u-v-1=0.$$

Put $x=(u;v)$, $x_0=(-1/2;-1)$, $P(x)=\big(f(u,v);\ g(u,v)\big)$. After simple computations we obtain

$$Q(x)=P'(x)P(x)=(4u^3+6u^2+3u+1/2;2v+5/2).$$

The linear operator $P'(x)$ is defined by the matrix

$$\begin{pmatrix}2u+1, & 1\\ 2u+1, & -1\end{pmatrix}.$$

Thus we see that the linear operator $P'(x_0)$ has no inverse, hence the method of Kantorovitch is not applicable. But we shall show that the conditions of Theorem 2 are satisfied.

The linear operator $Q'(x)$ is defined by the matrix

$$\begin{pmatrix}12u^2+12u+3, & 0\\ 0 & , 2\end{pmatrix}.$$

Since $\|P(x_0)\|^2=1/8$ and $\|Q(x_0)\|=1/2$, we have $2\eta_0=1/8:\ 1/2=1/4$. It is easy to see that $\|Q'(x)\|=2$ in the sphere $S(x_0,2\eta_0)$. Thus we have $K=2$.

Condition 3^0 is also satisfied since

$$(\tfrac{1}{8}\cdot 2):\tfrac{1}{4}=2h_0=1.$$

INSTITUTE OF MATHEMATICS, POLISH ACADEMY OF SCIENCES

REFERENCES

[1] M. Altman, *On the approximate solution of non-linear functional equations*, Bull. Acad. Polon. Sci. Cl. III, in this issue p. 457.

[2] L. V. Kantorovitch, *On Newton's method* (in Russian), Trudy Mat. Inst. im. V. A. Steklova, **28** (1949), 104.

BULLETIN DE L'ACADÉMIE
POLONAISE DES SCIENCES
Cl. III — Vol. V, No. 5, 1957

MATHÉMATIQUE

Sur un système d'équations intégrales non-linéaires de seconde espèce à une infinité de fonctions inconnues à singularité forte

par

D. PRZEWORSKA-ROLEWICZ

Présenté par S. MAZUR le 26 Février 1957

Cette communication a pour but d'établir l'existence de la solution du système suivant d'équations intégrales non-linéaires à une infinité de fonctions inconnues à singularité forte:

$$\varphi_n(t)=\int_L \frac{K_n(t,\tau,\varphi_1(\tau),\varphi_2(\tau),\ldots)}{\tau-t}\,d\tau\,, \tag{1}$$

où $n=1,2,\ldots$ et où L est un ensemble fini de lignes fermées disjointes, situées dans le plan de la variable complexe et ayant la tangente continue.

L'équation de la forme (1), mais à une seule fonction inconnue, a été résolue par Guséinov [1] dans le cas particulier où la ligne L se réduisait à un segment rectiligne et par Pogorzelski [3], [4] d'abord dans le cas de la fonction K holomorphe et, plus tard, dans le cas où cette fonction n'était assujettie qu'à la condition d'Hölder.

L'existence de la solution du système (1) à une infinité de fonctions inconnues sera déduite du théorème suivant de Tichonov [5] sur le point invariant d'une transformation dans l'espace métrique:

"Dans un espace métrique linéaire, local convexe et complet (c'est-à-dire dans un espace de type B_0) toute transformation continue d'un ensemble convexe, fermé et compact en son sous-ensemble a au moins un point invariant".

THÉORÈME: *Admettons que*

1° *L est un ensemble fini de lignes fermées disjointes, situées dans le plan de la variable complexe et ayant la tangente continue;*

2° *$K_n(t,\tau,u_1,\ldots)$ est pour tout $n=1,2,\ldots$ une fonction définie dans la région $t\in L$; $\tau\in L$; $|u_n|<R$ et satisfaisant dans cette région à la condition d'Hölder de la forme*

$$|K_n(t,\tau,u_1,\ldots)-K_n(t',\tau',u_1',\ldots)|\leq h_n[|t-t'|^\nu+|\tau-\tau'|^\mu+\sum_{i=1}^{\infty}\alpha_{ni}|u_i-u_i'|]\,, \tag{2}$$

où $0 < \mu < \nu \leqslant 1$ *et où* $\sum_{i=1}^{\infty} a_{ni}$ *sont les séries arbitraires aux termes positifs dont les sommes sont inférieures à l'unité;*

3° $0 < h_n < 1/D$ **) pour* $n = 1, 2, \ldots$;

4° *les constantes du problème satisfont pour* $n = 1, 2, \ldots$ *à l'inégalité*

$$\frac{h_n D}{1 - D h_n} < \frac{R \sup_L |K_n| - I h_n}{I h_n}, \quad \text{où} \quad I = \sup_L \int_L \frac{dl_\tau}{|\tau - t|^{1-\mu}}. \tag{3}$$

Ces hypothèses admises, le système (1) *a au moins une solution* $\varphi_1^*(t)$, $\varphi_2^*(t), \ldots$ *dont les termes satisfont à la condition d'Hölder avec l'exposant* μ.

Démonstration. Considérons l'espace E composé de toutes les suites $\Phi = \{\varphi_n(t)\}$ de fonctions continues de la variable complexe définies sur L et admettons-y une suite dénombrable de pseudonormes homogènes $\|\Phi\|_n = \sup_L |\varphi_n(t)|$. La métrique peut être définie, par exemple, comme la somme d'une série

$$\varrho(\Phi, \Psi) = \sum_{i=1}^{\infty} \frac{1}{2^i} \frac{\|\Phi - \Psi\|_i}{1 + \|\Phi - \Psi\|_i}.$$

On sait que l'espace E est alors du type B_0.

Considérons dans E l'ensemble Z défini par les conditions:

$$|\varphi_n(t)| \leqslant R, \tag{4}$$

$$|\varphi_n(t) - \varphi_n(t')| \leqslant \varkappa |t - t'|^\mu, \tag{5}$$

où $n = 1, 2, \ldots$, le coefficient $\varkappa$ étant arbitrairement fixé à l'intérieur d'un intervalle qui sera déterminé plus loin.

On peut montrer que l'ensemble Z est convexe, fermé et compact. Considérons enfin une transformation de Z donnée par la formule

$$\psi_n(t) = \int_L \frac{K_n(t, \tau, \varphi_1(\tau), \ldots)}{\tau - t} d\tau, \quad \text{où} \quad n = 1, 2, \ldots, \tag{6}$$

qui fait correspondre à tout point $\Phi = \{\varphi_n\}$ de l'ensemble Z un point $\psi = \{\psi_n\}$ de l'espace E.

---

*) La constante D figure dans le théorème suivant de Plemelj-Privalov [2] qui sera appliqué dans la démonstration:

"Si $f(t, \tau)$ est une fonction complexe de deux variables t, $\tau \in L$, assujettie à la condition d'Hölder de la forme

$$|f(t, \tau) - f(t', \tau')| \leqslant q[|t - t'|^\nu + |\tau - \tau'|^\mu] \quad \text{où} \quad 0 < \mu < \nu \leqslant 1, \tag{*}$$

la fonction F déterminée par l'intégrale impropre de Cauchy

$$F(t) = \int_L \frac{f(t, \tau)}{\tau - t} d\tau$$

satisfait à la condition d'Hölder de la forme

$$F(t) - F(t') \leqslant q D |t - t'|^\mu, \tag{**}$$

où la constante D ne dépend que des lignes formant l'ensemble L".

Nous allons démontrer que la transformation (6) est continue, à savoir que $\varrho(\psi^{(m)},\psi)\to 0$ si $\varrho(\Phi^{(m)},\Phi)\to 0$. Il suffit de montrer que la convergence uniforme d'une suite $\{\varphi_n^{(m)}\}$ vers φ_n implique, pour tout $n=1,2,\ldots$, celle de la suite $\{\psi_n^{(m)}\}$ des fonctions qui viennent correspondre à $\varphi_n^{(m)}$ vers la fonction ψ_n qui correspond à φ_n. On a en effet pour $n=1,2,\ldots$

$$\psi_n^{(m)}(t)-\psi_n(t)=\int_L \frac{K_n(t,\tau,\varphi_1^{(m)}(\tau),\ldots)-K_n(t,\tau,\varphi_1(\tau),\ldots)}{\tau-t}\,d\tau=$$

$$=\pi i\left[K_n(t,t,\varphi_n^{(m)}(t),\ldots)-K_n(t,t,\varphi_1(t),\ldots)\right]+$$

$$+\int_L \frac{K_n(t,\tau,\varphi_1^{(m)}(\tau),\ldots)-K_n(t,\tau,\varphi_1^{(m)}(t),\ldots)}{\tau-t}\,d\tau+$$

$$-\int_L \frac{K_n(t,\tau,\varphi_1(\tau),\ldots)-K_n(t,t,\varphi_1(t),\ldots)}{\tau-t}\,d\tau$$

et la première différence I_1 satisfait à l'inégalité

$$|I_1|\leqslant \pi h_n\sum_{i=1}^{\infty}\alpha_{ni}|\varphi_i^{(m)}(t)-\varphi_i(t)|\,.$$

Il existe un nombre M_n suffisamment grand pour que l'on ait $\sum_{i=M_n}^{\infty}\alpha_{ni}\leqslant\frac{\varepsilon}{16R\pi h_n}$; $(n=1,2,\ldots)$ et pour que l'on puisse choisir un nombre N_n de façon à avoir

$$|\varphi_i^{(m)}(t)-\varphi_i(t)|\leqslant\varepsilon/8\pi h_n \quad\text{pour}\quad m>N_n \quad\text{et}\quad i=1,2,\ldots M_n-1\,.$$

On a donc $|I_1|<\varepsilon/4$ pour $m>N_n$ et $n=1,2,\ldots$

Pour la seconde différence I_2, considérons un cercle Λ de centre t et de rayon ϱ suffisamment petit pour qu'il n'y ait qu'un seul arc l, partie d'une ligne de L, et décomposons I_2 en deux sommandes:

$$I_2=I_2^{l}+I_2^{L-l}\,,$$

l'intégration s'étendant sur l'arc l et sur les lignes de $L-l$.

Pour chaque $m=1,2,\ldots$ et aussi pour la limite, l'inégalité suivante se trouve satisfaite:

$$\left|\int \frac{K_n(t,\tau,\varphi_1^{(m)}(\tau),\ldots)-K_n(t,t,\varphi_1^{(m)}(t),\ldots)}{\tau-t}\,d\tau\right|\leqslant h_n(1+\varkappa)\int_l\frac{dl_\tau}{|\tau-t)^{1-\mu}}\leqslant\frac{\varepsilon}{4}\,,$$

si l'arc l est suffisamment petit. Par conséquent, $|I_2^{l}|\leqslant\varepsilon/2$.

Dans l'intégrale I_2^{L-l}, le point t est situé à l'extérieur du domaine de l'intégration. On peut donc choisir pour ε et pour chaque n un nombre M_n' tel que $m>M_n'$ entraîne $|I_2^{L-l}|<\varepsilon/4$.

On a donc finalement pour tout $n=1,2,\ldots$

$$(7)\qquad |\psi_n^{(m)}(t)-\psi_n(t)|\leqslant\varepsilon,\quad\text{lorsque}\quad m>\max(N_n,M_n')\,.$$

Nous allons démontrer que l'ensemble Z' des points transformés Ψ fait partie de l'ensemble Z. En effet,

$$\psi_n(t)=\int_L \frac{K_n(t,\tau,\varphi_1(\tau),\ldots)-K_n(t,t,\varphi_1(t),\ldots)}{\tau-t}\,d\tau+\pi i K_n(t,t,\varphi_1(t),\ldots),$$

d'où

$$|\psi_n(t)|\leqslant h_n(1+\varkappa)I+\pi \sup_L |K_n| \quad \text{pour} \quad n=1,2,\ldots \tag{8}$$

Pareillement,

$$|K_n(t,\tau,\varphi_1(\tau),\ldots)-K_n(t',\tau',\varphi_1(\tau'),\ldots)|\leqslant h_n(1+\varkappa)[|t-t'|^\nu+|\tau-\tau'|^\mu],$$

$$|\psi_n(t)-\psi_n(t')|\leqslant h_n(1+\varkappa)D|t-t'|^\mu \quad \text{pour} \quad n=1,2,\ldots \tag{9}$$

en vertu du théorème précité de Plemelj-Privalov. In en résulte que le point transformé ψ appartient à l'ensemble Z lorsque les constantes satisfont pour $n=1,2,\ldots$ aux inégalités

$$h_n(1+\varkappa)D\leqslant\varkappa \quad \text{et} \quad h_n(1+\varkappa)I+\pi \sup_L |K_n|\leqslant R,$$

c'est-à-dire

$$0<\frac{h_nD}{1-h_nD}\leqslant\varkappa\leqslant\frac{R-\pi \sup_L |K_n|-h_nI}{h_nI}. \tag{10}$$

Or un nombre $\varkappa$ satisfaisant à (10) existe en vertu de (4).

Toutes les conditions du théorème de Tichonov étant ainsi satisfaites, il existe au moins une solution $\varphi_1^*(t),\varphi_2^*(t),\ldots$ dont les termes satisfont à la condition d'Hölder avec l'exposant μ et le coefficient $\varkappa$.

On peut étendre le théorème au cas général $|u_n|\leqslant R_n$. Il suffit à ce but d'admettre que $\varphi_n(t)=\frac{R_n}{r}\bar{\varphi}_n(t)$,

$$\sum_{i=1}^{\infty} a_{ni}R_i\leqslant R<\frac{R_n}{h_nD}, \quad \frac{Rh_nD}{R_n-Rh_nD}<\frac{R_n-\pi \sup_L |K_n|-h_nI}{h_nI}$$

pour $n=1,2,\ldots$ et d'appliquer le théorème du cas où $\bar{\varphi}_n(t)$ sont les fonctions inconnues.

ÉCOLE POLYTECHNIQUE, VARSOVIE

OUVRAGES CITÉS

[1] A. I. Guséinov, *Sur une équation intégrale* (en russe), Izw. AN SSSR, **12** (1948), 193.

[2] N. I. Muskhelishvili, *Singular integral equations*. P. Noordhoff N. V. Groningen-Holland, 1953, p. 42.

[3] W. Pogorzelski, *Sur l'équation intégrale non-linéaire de seconde espèce à forte singularité*, Ann. Pol. Math. (1954).

[4] W. Pogorzelski, *Badanie równań całkowych mocno-osobliwych metodą punktu niezmienniczego*. Biuletyn WAT im. J. Dąbrowskiego, **18** (1955).

BULLETIN DE L'ACADÉMIE
POLONAISE DES SCIENCES
Cl. III — Vol. V, No. 5, 1957

MATHEMATICS

On a Certain Class of Linear Metric Spaces

by

S. ROLEWICZ

Presented by S. MAZUR on February 26, 1957

Let X be a linearly-metric space, i. e., a linear and metric space in which the operations x_1+x_2, tx are continuous. As we know, a homogeneous norm equivalent to the metric exists in space X if, and only if, there exists in that space a bounded and convex neighbourhood of element 0. If there exists in space X a norm $\|x\|$ that is p-homogeneous, i. e., such that $\|tx\|=t^p\|x\|$, where $0<p\leqslant 1$, and equivalent to the metric, then in any case there exists in space X a bounded neighbourhood of element 0; e. g., it is the set of those x for which $\|x\|<1$. In the present note we shall prove that, conversely, if there exists in space X a bounded neighbourhood of element 0, then there exists in that space a p-homogeneous norm equivalent to the metric for a certain p such that $0<p\leqslant 1$; it will be observed that if $\|x\|$ is a p-homogeneous norm in space X, then $\|x\|^{q/p}$ is a q-homogeneous norm in that space for $0<q\leqslant p$.

1. Suppose that there exists in the linearly-metric space X a bounded neighbourhood of element 0. Denote by $\mathfrak{A}$ the class of those bounded neighbourhoods A of element 0 for which $tA\subset A$ for $|t|\leqslant 1$; such neighbourhoods exist because if B is any bounded neighbourhood of element 0, then the sum A of all the sets tB, where $|t|\leqslant 1$, is a neighbourhood with the required properties *).

By the *concavity module* $c(A)$ *of the neighbourhood* $A\in\mathfrak{A}$ we shall understand the infimum of the set of all numbers $s>0$ such that $A\oplus A\subset sA$; the infimum $c(X)$ of the set of all numbers $c(A)$, where $A\in\mathfrak{A}$, will be called *the concavity module of space* X. We easily find that we always have $c(A)\geqslant 2$ and, moreover, $c(A)=2$ if, and only if, the neighbourhood A is convex. In the sequel we shall make use of the observation that if a linearly-metric space Y is isomorphic with space X, then $c(Y)=c(X)$, and if Y is a subspace of space X, then $c(Y)\leqslant c(X)$.

*) By tA we understand the set of elements tx, where $x\in A$, and by $A\oplus B$ — the set of elements x_1+x_2, where $x_1\in A$, $x_2\in B$.

THEOREM. *If* $0 < p < p_0 = \log_{c(X)} 2$, *then there exists in space* X *a* p*-homogeneous norm equivalent to the metric.*

Proof. There exists an $A \in \mathfrak{A}$ such that $c(A) < s = 2^{1/p}$. If $r = \sum_{k=-m}^{n} \varepsilon_k 2^k > 0$, where $\varepsilon_k = 0$ or 1 for $k = -m, -m+1, \ldots, n$ and m, n are natural, then let $U(r) = \varepsilon_{-m} s^{-m} A \oplus \varepsilon_{m+1} s^{-m+1} A \oplus \ldots \oplus \varepsilon_n s^n A$. The neighbourhoods $U(r)$ of element 0 defined in this way for dyadic fractions $r > 0$ are such that $U(r_1) + U(r_2) \subset U(r_1 + r_2)$ and $(-1)\,U(r) = U(r)$ always hold. Hence, and from the observation that A is a bounded neighbourhood of element 0, it follows in a known manner that if $\|x\|^*$ denotes the infimum of the set of all dyadic fractions $r > 0$ such that $x \in U(r)$, then $\|x\|^*$ is a norm in space X equivalent to the metric [1]; moreover, $\|s^\alpha x\|^* = (s^\alpha)^p \|x\|$ for integer α, and $\|tx\|^* \leqslant \|x\|^*$ for $0 \leqslant t \leqslant 1$. These last properties imply that if a given number $\vartheta > 0$ is written in the form $\vartheta = s^\alpha w$, where α is an integer, $1 \leqslant w < s$, then $\|\vartheta x\|^*/\vartheta^p = \|wx\|^*/w^p \leqslant \|wx\|^* \leqslant \|sx\|^* = 2\|x\|^*$. The formula $\|x\| = \|\sup_{\vartheta > 0} \|\vartheta x\|^*/\vartheta^p$ defines in space X such a functional that $\|x\|^* \leqslant \|x\| \leqslant 2\|x\|^*$ and $\|tx\| = t^p \|x\|$. In order to prove that $\|x\|$ is a p-homogeneous norm equivalent to the metric it is thus sufficient to show that $\|x_1 + x_2\| \leqslant \leqslant \|x_1\| + \|x_2\|$. This follows from the fact that, according to the above, there exists a $v \in \langle 1, s \rangle$ such that $\|x_1 + x_2\| = \|v(x_1 + x_2)\|^*/v^p$, and we have $\frac{\|v(x_1+x_2)\|^*}{v^p} = \frac{\|vx_1\|^*}{v^p} + \frac{\|vx_2\|^*}{v^p} \leqslant \|x_1\| + \|x_2\|$.

Remark 1. The inverse theorem is true in the following form: If there exists in the linearly-metric space X a norm equivalent to the metric and such that $\|tx\| \geqslant t^p \|x\|$ for $t \geqslant 1$ for a certain $p > 0$, then there exists a bounded neighbourhood A of element 0 such that $c(A) \leqslant 2^{1/p}$. Indeed, the sphere $A = \underset{x}{E}(\|x\| < 1)$ is a bounded neighbourhood of element 0 such that $tA \subset A$ for $|t| \leqslant 1$ and $c(A) \leqslant 2^{1/p}$, because $A \oplus A \subset \underset{x}{E}[\|x\| < 2] \subset 2^{1/p} A$.

Remark 2. The following example, given by A. Pełczyński, proves that our restriction in the theorem to the numbers $p < p_0$ is essential, i. e., that on the whole there exists no p_0-homogeneous norm equivalent to the metric. Namely, let p_n be an increasing sequence of positive numbers tending to the number $p_0 \leqslant 1$ and let us choose natural numbers k_n and $u_n > 0$ in such a way that $k_n \cdot u_n^{p_0} \leqslant 1/2^n$, $k_n u_n^{p_n} \geqslant 1$. Let $q_n = p_1$ for $1 \leqslant n \leqslant k_1$, $q_n = p_{m+1}$ for $\sum_{i=1}^{m} k_i < n \leqslant \sum_{l=1}^{m+1} k_l$ and denote by X an F-space consisting of numerical sequences $x = (\xi_n)$ such that $\|x\| = \sum_{n=1}^{\infty} |\xi_n|^{q_n} < +\infty$. If $0 < p < \bar{p} < p_0$, then the formula $\|x\|^* = \sum_{n=1} |\xi_n|^{\sup(\bar{p}, q_n)}$ defines in space X a norm equivalent to the norm $\|x\|$ and such that $\|tx\|^* \geqslant t^{\bar{p}} \|x\|^*$ for $t \geqslant 1$. Thus, in virtue of Remark 1 and of the theorem, there exists

in space X a p-homogeneous norm equivalent to the norm $\|x\|$. But the assumption of the existence in space X of a p_0-homogeneous norm $\|x\|_0$ equivalent to the norm $\|x\|$ easily leads to a contradiction. For setting $\xi_n^0 = u_n$ in the case of $q_n = p_m$ and $e_n = (\varepsilon_{nm})$, where $\varepsilon_{nm} = 1$ for $n = m$, $\varepsilon_{nm} = 0$ for $n \neq m$, we should have $\sum_{n=1}^{\infty} \|\xi_n^0 e_n\|_0 = \sum_{n=1}^{\infty} |\xi_n^0|^{p_0} \|e_n\|_0 \leqslant \sup_n \|e_n\|_0$, and since $\|e_n\| = 1$, and consequently the sequence (e_n) is bounded, we should have $\sup_n \|e_n\|_0 < +\infty$ and from the convergence of the series $\sum_{n=1} \xi_n^0 e_n$ it would follow that its sum is $x_0 = (\xi_n^0)$, which gives a contradiction because $x_0 \notin X$.

2. We shall determine the concavity module for certain concrete spaces:

(a) A space l^p, where $0 < p < 1$, consisting of numerical sequences $x = (\xi_n)$ such that $\|x\| = \sum_{n=1}^{\infty} |\xi_n|^p < +\infty$. In virtue of Remark 1 we have in any case $c(l^p) \leqslant 2^{1/p}$. In order to prove that $c(l^p) = 2^{1/p}$ it suffices to show, in accordance with the theorem, that for $q > p$ there exists in space l^p no q-homogeneous norm $\|x_0\|$ equivalent to the norm $\|x\|$. This follows by reasoning analogical to that of Remark 2. Taking a sequence $x_0 = (\xi_n^0)$ such that $\sum_{n=1}^{\infty} |\xi_n^0|^p = +\infty$, $\sum_{n=1}^{\infty} |\xi_n^0|^q < +\infty$, we should have $\sum_{n=1}^{\infty} \|\xi_n^0 e_n\|_0 = \sum_{n=1}^{\infty} |\xi_n^0|^q \|e_n\|_0 \leqslant$ $\leqslant \sup_n \|e_n\|_0 \cdot \sum_{n=1}^{\infty} |\xi_n^0|^q < +\infty$; from the convergence of the series $\sum_{n=1}^{\infty} \xi_n^0 e_n$ it would follow that its sum is x_0, contrary to the fact that $x_0 \notin l^p$.

(b) A space L^p, where $0 \leqslant p < 1$, composed of measurable functions $x = x(t)$ in the interval $\langle 0,1 \rangle$ such that $\|x\| = \int_0^1 |x(t)|^p dt < +\infty$. By Remark 1 we again have $c(L^p) \leqslant 2^{1/p}$. In order to ascertain that $c(L^p) = 2^{1/p}$, it suffices to observe that the space l^p is isomorphic with a substance of the space L^p, i. e., $c(L^p) \geqslant c(l^p) = 2^{1/p}$.

Conclusion. There exists no linearly-metric space X in which there is a bounded neighbourhood of element 0 and which contains isomorphically each of the spaces l^{p_n} (or L^{p_n}), where $0 < p_n < 1$, $p_n \to 0$.

INSTITUTE OF MATHEMATICS, POLISH ACADEMY OF SCIENCES

REFERENCES

[1] S. Kakutani, *Über die Metrisation der topologischen Gruppen*, Proc. Imp. Acad. Tokyo, **12** (1936).

BULLETIN DE L'ACADÉMIE
POLONAISE DES SCIENCES
Cl. III — Vol. V, No. 5, 1957

MATHEMATIK

Invariante Riemannsche Metriken in homogenen Räumen

von

A. GOETZ

Vorgelegt von A. MOSTOWSKI den 2. März 1957

In einer früheren Arbeit [1] habe ich eine notwendige und hinreichende Bedingung (K) dafür angegeben, dass in einem homogenen Raum mit erstem Abzählbarkeitsaxiom eine invariante Metrik existiert. In der vorliegenden Note untersuche ich den Fall einer Lieschen Gruppe und gebe eine notwendige und hinreichende Bedingung für die Existenz einer invarianten Riemannschen Metrik.

1. Es sei G eine $n+s$-gliedriege Liesche Gruppe, die in einem n-dimensionalen topologischen Raum $\mathcal{M}$ transitiv wirkt. Wir setzen voraus, wie in [1], dass

I. Die Funktion $\varphi_P(x)=xP$ stetig in $G\times\mathcal{M}$ ist.

II. Die Abbildung φ_P der Gruppe G auf $\mathcal{M}$ bei fixiertem $P\in\mathcal{M}$ offen ist.

Mit H_P bezeichnen wir die Untergruppe der Transformationen, die den Punkt P unbewegt lassen, d. h. $H_P=\{x: xP=P\}$.

Die Untergruppe H_P ist bekanntlich eine s-gliedrige Liesche Gruppe, der Raum $\mathcal{M}$ ist mit G/H_P homöomorph und ist eine n-dimensionale analytische Mannigfaltigkeit. Die Abbildung φ_P ist analytisch.

Eine Riemannsche Metrik in $\mathcal{M}$ ist bestimmt, indem man in den linearen Tangentenräumen in allen Punkten von $\mathcal{M}$ skalare Produkte definiert. Die Metrik ist invariant in Bezug auf G, wenn jede Transformation $x\in G$ die Tangentenvektoren in P in Tangentenvektoren in xP so überführt, dass die skalaren Produkte übereinstimmen.

2. Die Liesche Algebra $\mathfrak{g}$ der Gruppe G werden wir als Raum der Vektoren betrachten, die zu G im Einheitselement e tangential sind. Die zu H_P tangentialen Vektoren bilden eine Unteralgebra $\mathfrak{h}_P$. $\mathfrak{g}$ ist ein $n+s$-dimensionaler und $\mathfrak{h}_P$ ein s-dimensionaler linearer Raum. Die Elemente (Vektoren) aus der Lieschen Algebra $\mathfrak{g}$ bezeichnen wir mit $\boldsymbol{u}$, $\boldsymbol{v}$ usw.

Jedem $a\in G$ ordnen wir den inneren Automorphismus $x\to axa^{-1}$ der Gruppe G zu. Diesem Automorphismus entspricht eine lineare Trans-

formation $\mathrm{ad}(a)$ der Lieschen Algebra $\mathfrak{g}$. Die Abbildung $a \to \mathrm{ad}(a)$ ist eine lineare Darstellung von G, die sogenannte adjungierte Darstellung.

Es ist klar, dass die Gruppe $\mathrm{ad}(H_P)$ die Unteralgebra $\mathfrak{h}_P$ invariant lässt, d. h.

$$\mathrm{ad}(H_P)\mathfrak{h}_P \subset \mathfrak{h}_P . \tag{1}$$

Als Elemente (Vektoren) des n-dimensionalen Raumes $\mathfrak{g}/\mathfrak{h}_P$ (mit fetten Buchstaben $\boldsymbol{U}$, $\boldsymbol{V}$ u.s.w. bezeichnet) betrachten wir Klassen von Vektoren aus $\mathfrak{g}$. Zu derselben Klasse gehören Vektoren, deren Differenz in $\mathfrak{h}_P$ liegt.

Infolge (1) können wir die Gruppe $\mathrm{ad}(H_P)$ als Gruppe linearer Transformationen des Raumes $\mathfrak{g}/\mathfrak{h}_P$ betrachten. In der Tat gehören die Vektoren $\boldsymbol{u}$ and $\boldsymbol{v}$ derselben Klasse $\boldsymbol{U}$ an, so gibt es einen Vektor $\boldsymbol{h} \in \mathfrak{h}_P$, für welchen $\boldsymbol{u} = \boldsymbol{v} + \boldsymbol{h}$. Für jedes $h \in H_P$ haben wir dann $\mathrm{ad}(h)\boldsymbol{u} = \mathrm{ad}(h)\boldsymbol{v} + \mathrm{ad}(h)\boldsymbol{h}$, da aber $\mathrm{ad}(h)\boldsymbol{h} \in \mathfrak{h}_P$, gehören auch $\mathrm{ad}(h)\boldsymbol{u}$ und $\mathrm{ad}(h)\boldsymbol{v}$ derselben Klasse an, die wir mit $\mathrm{Ad}(h)\boldsymbol{U}$ bezeichnen. $\mathrm{Ad}(h)$ bedeutet die Transformation von $\mathfrak{g}/\mathfrak{h}_P$, die durch die Transformation $\mathrm{ad}(h)$ induziert wird.

3. Fixieren wir jetzt einen Punkt $P_0 \in \mathcal{M}$. Es bedeute $\boldsymbol{U}_P$ einen in P zu $\mathcal{M}$ tangentialem Vektor, und $Q(t)[-\alpha < t < +\alpha, Q(0) = P]$ bedeute eine differenzierbare Kurve in $\mathcal{M}$ mit dem Tangentialvektor $\boldsymbol{U}_P$ (d. h. $(dQ/dt)_{t=0} = \boldsymbol{U}_P$). Es sei weiter x ein Element aus $\varphi_{P_0}^{-1}(P)$ (d. h. $xP_0 = P$). Die Kurve $Q_1(t) = x^{-1}Q(t)$ ist dann differenzierbar und $Q_1(0) = P_0$. Es ist dann in G eine solche differenzierbare Kurve $q(t)$ vorhanden, dass

$$\varphi_{P_0}\big(q(t)\big) = x^{-1}Q(t) . \tag{2}$$

Die Kurve $q(t)$ ist durch $x^{-1}Q(t)$ nicht eindeutig bestimmt, da die Bedingung (2) auch alle Kurven $q(t)h(t)$ erfüllen, wo $h(t)$ differenzierbar und in H_{P_0} enthalten ist.

Diese Kurven bestimmen in $\mathfrak{g}$ Tangentenvektoren, die sich voneinander um Vektoren aus $\mathfrak{h}_{P_0}$ unterscheiden, und deswegen eindeutig Vektoren aus $\mathfrak{g}/\mathfrak{h}_{P_0}$ bestimmen. Es ist auch leicht einzusehen, dass diese Konstruktion von der Wahl der Kurve $Q(t)$ nicht abhängt, sondern nur von $\boldsymbol{U}_P$ und von der Wahl der Transformation $x \in \varphi_{P_0}^{-1}(P)$. Wir haben damit dem Paare U_P, x einen Vektor aus $\mathfrak{g}/\mathfrak{h}_{P_0}$, den wir mit $\boldsymbol{U}_x$ bezeichnen, zugeordnet.

Wenn wir jetzt dieselbe Konstruktion für ein anderes Element aus $\varphi_{P_0}^{-1}(P)$, sagen wir xh, $h \in H_{P_0}$, durchführen, so wird $h^{-1}x^{-1}Q(t)$ die entsprechende Kurve durch P_0 sein; die entsprechende Kurve in G sei zum Beispiel $h^{-1}q(t)h$. In $\mathfrak{g}/\mathfrak{h}_{P_0}$ bekommen wir den Vektor $\boldsymbol{U}_{xh}$, der aus dem Vorigen mittels Transformation $\mathrm{Ad}(h^{-1})$ entsteht, d. h.

$$\boldsymbol{U}_{xh} = \mathrm{Ad}(h^{-1})\boldsymbol{U}_x . \tag{3}$$

4. Hilfssatz 1. *Existiert in einem n-dimensionalen linearen Raum $\mathfrak{L}$ eine beschränkte Nullumgebung* $\mathfrak{u}$, *die in Bezug auf eine Gruppe Γ linearer Transformationen invariant ist, d. h. $\Gamma\mathfrak{u}\subset\mathfrak{u}$, so existiert in $\mathfrak{L}$ ein skalares Produkt, das invariant in Bezug auf Γ ist.*

Beweis. Wählen wir eine Basis von n-linear unabhängigen Vektoren, so sind die Transformationen durch gemeinsam beschränkte Matrizen dargestellt. Wäre es anders, so müsste es eine Folge $\{A_k\}$ von Matrizen

$$A_k=\begin{pmatrix} a_{11}^{(k)} & \dots & a_{1n}^{(k)} \\ \cdot & \dots & \cdot \\ \cdot & \dots & \cdot \\ a_{n1}^{(k)} & \dots & a_{nn}^{(k)} \end{pmatrix}$$

und solche Indizes i, j, dass $a_{ij}^{(k)} \underset{k\to\infty}{\to} \infty$, existieren. Es sei zum Beispiel $a_{11}^{(k)} \to \infty$. Dann ist die Folge der Transformation des Vektors $\{\alpha, 0, \dots, 0\}$ für jedes $\alpha \neq 0$ unbeschränkt, was im Widerspruch mit $\Gamma\mathfrak{u}\subset\mathfrak{u}$ steht.

Die abgeschlossene Hülle $\bar{\Gamma}$ von Γ in der vollen Gruppe der linearen Transformationen ist deswegen kompakt. In der Tat, in jeder Folge von Matrizen aus Γ gibt es eine konvergente Unterfolge, und die Grenze muss eine nichtausgeartete Matrix sein, da sonst die Folge der reziproken Matrizen unbeschränkt wäre.

Nach einem bekannten Satze von H. Weyl ([2], 3, S. 225) existiert in $\mathfrak{L}$ ein in Bezug auf $\bar{\Gamma}$ invariantes skalares Produkt.

Hilfssatz 2. *Existiert in* $\mathfrak{g}$ *eine solche beschränkte Nullumgebung* $\mathfrak{u}$, *dass*

$$\mathrm{ad}(H_{P_0})\mathfrak{u}\subset\mathfrak{u}+\mathfrak{h}_{P_0}, \tag{4}$$

so existiert in $\mathfrak{g}/\mathfrak{h}_{P_0}$ ein in Bezug auf $\mathrm{Ad}(H_{P_0})$ invariantes skalares Produkt.

Beweis. Die Nullumgebung $\mathfrak{U}=\mathfrak{u}+\mathfrak{h}_{P_0}$ in $\mathfrak{g}/\mathfrak{h}_{P_0}$ ist beschränkt und invariant gegen $\mathrm{Ad}(H_{P_0})$ und man kann Hilfssatz 1 anwenden.

Satz. *Eine in Bezug auf G invariante Riemannsche Metrik in $\mathfrak{M}$ existiert dann und nur dann, wenn die folgende Bedingung erfüllt ist:*

(K_1) *In der Lieschen Algebra* $\mathfrak{g}$ *der Gruppe G existiert eine solche beschränkte Nullumgebung* $\mathfrak{u}$, *dass für irgendein $P_0 \in \mathfrak{M}$*

$$\mathrm{ad}(H_{P_0})\mathfrak{u}\subset\mathfrak{u}$$

ist.

Es ist klar, dass dasselbe für jeden anderen Punkt $P \in \mathfrak{M}$ gilt.

Beweis. Die Bedingung ist hinreichend.

Nach dem Hilfssatz 2 existiert in $\mathfrak{g}/\mathfrak{h}_{P_0}$ ein in Bezug auf $\mathrm{Ad}(H_{P_0})$ invariantes skalares Produkt. Wir bezeichnen es mit $(\boldsymbol{U},\boldsymbol{V})$. Es seien $\boldsymbol{U}_P$ und $\boldsymbol{V}_P$ zwei Vektoren, die in P zu $\mathfrak{M}$ tangential sind. Das skalare Produkt $(\boldsymbol{U}_P,\boldsymbol{V}_P)_P$ dieser Vektoren definieren wir mittels der Formel

$$(\boldsymbol{U}_P,\boldsymbol{V}_P)_P=(\boldsymbol{U}_x,\boldsymbol{V}_x), \tag{5}$$

wo U_x und V_x Vektoren aus $\mathfrak{g}/\mathfrak{h}_{P_0}$ sind, die für U_P und V_P wie in 3, bestimmt wurden.

Nach (3) und nach der Invarianz in Bezug auf $\mathrm{Ad}(H_{P_0})$ des skalaren Produktes in $\mathfrak{g}/\mathfrak{h}_{P_0}$ ist diese Definition von der Wahl von $x \in \varphi_{P_0}^{-1}(P)$ unabhängig. In der Tat, für jedes $h \in H_{P_0}$ haben wir

$$(U_{xh}, V_{xh}) = (\mathrm{Ad}(h^{-1})U_x, \mathrm{Ad}(h^{-1})V_x) = (U_x, V_x).$$

Aus der Konstruktion der skalaren Produkte in den einzelnen Tangentenräumen folgt leicht, dass bei einer Transformation $x \in G$ die Tangentenvektoren in P in Tangentenvektoren in xP mit gleichem skalarem Produkt überführt werden. Deswegen bestimmen die skalaren Produkte $(U_P, V_P)_P$ eine invariante Riemannsche Metrik in $\mathcal{M}$.

Die Bedingung ist notwendig. Es folgt aus derselben Konstruktion, dass wenn es eine invariante Riemannsche Metrik gibt, in $\mathfrak{g}/\mathfrak{h}_{P_0}$ ein in Bezug auf $\mathrm{Ad}(H_{P_0})$ invariantes skalares Produkt existieren muss. Dann bilden die Vektoren U aus $\mathfrak{g}/\mathfrak{h}_{P_0}$ mit $(U,U) \leqslant 1$ eine beschränkte invariante Nullumgebung, und es gibt in $\mathfrak{g}$ eine beschränkte Nullumgebung $\mathfrak{u}$, für welche (4) gilt.

Ist H_{P_0} zusammenhängend, so kann die Bedingung (K_1) durch eine äquivalente „lokale" Bedingung (K_2) ersetzt werden. Diese lautet:

(K_2) *Es existiert in* $\mathfrak{g}$ *eine beschränkte Nullumgebung* $\mathfrak{u}$, *für die*

$$[\mathfrak{h}_{P_0}, \mathfrak{u}] \subset \mathfrak{u} + \mathfrak{h}_{P_0}$$

ist, wo $[u,v]$ *das schiefe Produkt der Lieschen Algebra bedeutet.*

MATHEMATISCHES INSTITUT DER POLNISCHEN AKADEMIE DER WISSENSCHAFTEN

SCHRIFTTUM

[1] A. Goetz, *Invariante Metriken in homogenen Räumen*, Bull. Acad. Polon. Sci., Cl. III, **5** (1957), 139.

[2] L. S. Pontriagin, *Stetige Gruppen* (russisch), 2. Auflage, Moskau, 1954.

BULLETIN DE L'ACADÉMIE
POLONAISE DES SCIENCES
Cl. III — Vol. V, No. 5, 1957

MATHEMATICS

On Quasi Normed Spaces

by

M. PAVEL (Bucarest)

Presented by K. BORSUK on March 6, 1957

Introduction

1. The purpose of this paper is to establish some results upon linear spaces in which a quasi norm has been introduced and which are complete for the distance defined with it.

I. General properties

2. Definition 2.1. Let E be a linear space over a scalar field Φ (real or complex). A transformation $x \to \|x\| = p(x)$ is a quasi norm if it is subject to the following conditions: 1° $\|x+y\| \leqslant \|x\| + \|y\|$, $x \in E$, $y \in E$; 2° $\|\lambda x\| = |\lambda|^r \|x\|$, $\lambda \in \Phi$, $x \in E$, $0 < r \leqslant 1$; 3° $\|x\| = 0$ if, and only if, $x = 0$. If $x \to \|x\|$ is a quasi norm and if we denote

$$d(x,y) = \|x-y\|, \quad x \in E, \quad y \in E, \tag{+}$$

then d is a distance on E, as one can easily verify. If $\lim_{n\to\infty} x_n = x$, $\lim_{n\to\infty} y_n = y$, $\lim_{n\to\infty} \lambda_n = \lambda$, $\lim_{n\to\infty} \mu_n = \mu$, then obviously $\lim_{n\to\infty} (\lambda_n x_n + \mu_n y_n) = \lambda x + \mu y$. From the preceding relation, it follows that the linear space E with the distance $(+)$ makes up a linear topological space. We will call E a quasi normed space.

Definition 2.2. A linear space on which a quasi norm (1°, 2°, 3°) has been defined and which is complete for the distance $(+)$ will be called a (QN) space.

It is obvious that a Banach space is a (QN) space. We will now produce some examples of (QN) spaces which are not necessarily Banach spaces.

Example 2.1. Let L^r be the set of Lebesgue measurable functions f, defined on $[0,1]$ and for which $|f|^r$ is integrable. If we denote $\|f\| = \int_0^1 |f(x)|^r dx$, then $f \to \|f\|$ is a quasi norm and $(L^r, f \to \|f\|)$ is a (QN) space [1].

It is also known [2] that the quasi norm considered by Hyers [3] is formally similar for a locally bounded space with that from the spaces L^p, $0<p<1$.

Example 2.2. Let l^r be the set of real numbers' sequences (x_n) with $\sum |x_n|^r<\infty$. If we denote, for $x=(x_n)$, $\|x\|=\sum |x_n|^r$, then $x\to\|x\|$ is a quasi norm and l^r with this quasi norm makes up a (QN) space. We obtain a similar example, but more general, of a (QN) space, if we consider a family $\Phi_0=(E_n)_{1\leqslant n<\infty}$ of Banach spaces, denoting by $l^r(\Phi_0)$ the totality of the sequences $x=(x_n)$ for which $\sum p_n(x_n)^r<\infty$, and defining $\|x\|=\sum |x_n|^r$. This is also a quasi norm and with $l^r(\Phi_0)$ it makes up a (QN) space. If $E_n=R$ for each n, then we obtain Example 2.2.

3. Let us consider a (QN) space E and its quasi norm $x\to\|x\|$. Let us observe that, if $r\geqslant 1$ in condition 2°, and if $p(x)=\|x\|^{1/r}$, then $p(x)$ is a norm which makes up with E a Banach space. If we consider now the case in which condition 2° would be replaced by condition

$$(++) \qquad \|\lambda x\|=\varphi(|\lambda|)\|x\|,$$

where φ is a continuous function defined on the set R_+ of all real $\geqslant 0$ numbers, and if we suppose that the other conditions 1° and 3° are verified and that E is a linear topological space for the distance d, then it is easy to prove that the considered space is a (QN) space, excepting the trivial case in which r is the constant 1.

4. THEOREM 4.1. *If $(E_i)_{1\leqslant i\leqslant n}$ is a finite family of (ON) spaces, with powers $r_1,\dots,r_n$ and if for every $x=(x_i)_{1\leqslant i\leqslant n}\in\prod_i^n E_i=E$ we set $p(x)=$ $=p_1(x_1)^{s_1}+\dots p_n(x_n)^{s_n}$, where $s_i=r_1\dots r_{i-1}r_{i+1}\dots r_n$, and p_i is the quasi norm in E_i $(1\leqslant i\leqslant n)$, then the space (E,p) is a (QN) space and the topology of E is identical with the product topology of the spaces E_i.*

Proof. Condition 1° of the quasi norm can easily be verified by deriving it from the inequality $|a+b|^q<|a|^q+|b|^q$ for $0<q\leqslant 1$ [4]. Condition 2° results from the choice of s_i. Condition 3° is obvious. As concerns the last assertion of the theorem, it is enough to observe that, if $x_k=(x_i^k)_{1\leqslant i\leqslant n}$, $x=(x_i)_{1\leqslant i\leqslant n}$, then $\lim_{n\to\infty} p(x_k-x)=0$ if, and only if, $\lim_{k\to\infty} p(x_i^k-x_i)=0$ for every i.

THEOREM 4.2. *Given a (QN) space E and a closed subspace N. If for every $\dot{x}\in E/N$ we set $\|\dot{x}\|=\inf_{x\in\dot{x}}\|x\|$, then $\dot{x}\to\|\dot{x}\|$ is a quasi norm and $(E/N,$ $\dot{x}\to\|\dot{x}\|)$ is a (QN) space.*

We omit the proof of this theorem, since it can be given in an usual way.

One may also prove that, if E is a linear space on which a quasi norm $x\to\|x\|$ with the power r has been defined, then the space E may

be considered as a dense subspace of a (QN) space $\hat{E}$ having the following properties: 1) E is dense in $\hat{E}$; 2) the restriction of the quasi norm defined in $\hat{E}$ at the space E coincides with the quasi norm defined originally in E.

II. Linear transformations

5. Let E, F be two (QN) spaces, with powers r, s and T a linear (additive and homogeneous) transformation which maps E into F.

THEOREM 5.1. *The necessary and sufficient condition for the continuity of a linear transformation T is that there exists a positive number a, for which the following inequality holds*:

$$\|T(x)\|_s \leqslant a\|x\|_r^{s/r}. \tag{5.1}$$

We omit the proof of this theorem.

6. Let $\mathcal{L}(E,F)$ be the set of continuous linear transformations, which map E into F, these being two (QN) spaces with the same power r. Let us observe that in $\mathcal{L}(E,F)$ the operations $T+S$, λT defined by $(T+S)(x) = T(x)+S(x)$, $(\lambda T)(x)=\lambda T(x)$ have a sense, and $\mathcal{L}(E,F)$ with two operations makes up a linear space. The mapping $T\to\|T\|$ is a quasi norm in $\mathcal{L}(E,F)$, as one can easily verify, and $(\mathcal{L}(E,F),\ T\to\|T\|)$ is a (QN) space.

7. As concerns the extension of linear transformations which map a (QN) space into another, with the same power r, one can easily prove that the main results [6], [7] about extensions and projections [8] in Banach spaces are true in (QN) spaces too.

III. Resolvent and spectrum

8. Definition 8.1. E is a (QN) algebra with power r, if it is an algebra as well as a (QN) space with power r and if, in addition, for every $x\in E,\ y\in E,\ \|xy\|\leqslant\|x\|\|y\|$.

One of the most important examples of (QN) algebras is the set $\mathcal{L}(E)$ of all linear continuous transformations of a (QN) space E into itself, if we notice that in $\mathcal{L}(E)$ takes place, besides $T+S$, λT, also the operation TS defined by $(TS)(x)=T[S(x)]$, and that $\|TS\|\leqslant\|T\|\|S\|$. In what follows, we will take into consideration only (QN) algebras E which possess a unit element e. In our postulates, there is no mention of inverses, but the distinction between elements which have inverses and those which do not is essential in what follows.

Let us now consider the inverse of the element $\lambda e-x$, $x\in E$, $\lambda\in C$, as a function of λ. Defining regular and singular elements as usually

one can get the distribution of regular elements, as in Banach algebras [9], by

THEOREM 8.1. *Every element x in the sphere $\|x-e\|<1$ is regular and for such an x: $x^{-1}=e+\sum_{n=1}^{\infty}(e-x)^n$.*

THEOREM 8.2. *The regular elements form an open set $\mathcal{G}$ in E.*

THEOREM 8.3. *The inverse x^{-1} is a continuous function of x in $\mathcal{G}$.*

9. Let us now consider the inverse of $\lambda e-a$ a function of λ for a fixed a, $a\in E$. Accordingly, as $\lambda e-a$ is regular or singular, we will say, as usually, that λ belongs to the resolvent set $\varrho(a)$ or to the spectrum $\sigma(a)$ of a; for $\lambda\in\varrho(a)$, the inverse of $\lambda e-a$ exists, it is called the resolvent of a and is denoted by $R(\lambda;a)$.

THEOREM 9.1. *The resolvent set is open. $R(\lambda;a)$ is a holomorphic *) function of λ.*

Proof. If $\lambda_0\in\varrho(a)$, then $(\lambda_0 e-a)^{-1}$ exists. For every λ which is subject to the inequality

$$|\lambda_0-\lambda|^r<\|R(\lambda_0;a)\|^{-1}, \tag{9.2}$$

the series

$$(\lambda_0 e-a)^{-1}\Big[e+\sum_{n=1}^{\infty}(\lambda_0-\lambda)^n(\lambda_0 e-a)^{-n}\Big] \tag{9.3}$$

is convergent and defines an element in E. A simple calculus proves that this is the inverse of $\lambda e-a$. It follows that if $\lambda_0\in\varrho(a)$, then the circle determined by (9.2) is contained in $\varrho(a)$; hence the resolvent set $\varrho(a)$ is an open set for every $a\in E$. (9.3) shows that the inverse is a holomorphic function in the resolvent set.

We get for the resolvent a stronger result, than that given by (9.1), by

THEOREM 9.2. *For every $a\in E$*

$$(\lambda e-a)^{-1}=\frac{e}{\lambda}+\sum_{n=1}^{\infty}\frac{a^n}{\lambda^{n+1}} \quad \text{for} \quad |\lambda|^r>\gamma, \quad \text{where} \quad \gamma=\lim_{n\to\infty}\sqrt[n]{\|a^n\|}.$$

Proof. The convergence of the series in the right member of the first equality can be easily verified for those values of λ which are sub-

*) A transformation f of a domain D of the complex plane into a (QN) algebra E is holomorphic in D, if the function f can be developped around every point $\zeta\in D$ in a power series with coefficients in E: $f(\zeta_0)=\sum_{n=0}^{\infty}(\zeta_0-\zeta)^n a_n$; one can easily verify that this series is convergent in the greatest circle with its centre in ζ included in the holomorphy domain of f and with the radius given by:

$$\frac{1}{\varrho}=[\limsup_{n\to\infty}\|a_n\|^{1/n}]^{1/r}. \tag{9.1}$$

ject to $|\lambda'|>\gamma$ and a direct calculus shows that the sum of the series is $(\lambda e-a)^{-1}$.

10. In (QN) spaces one may do the extension of holomorphic scalar functions to holomorphic vector functions. Given a (QN) algebra E, a power series $\sum_{n=0}^{\infty} a_n z^n$, $a_n \in E$, $z \in E$, defines a holomorphic mapping of $\|z\|<\varrho$ to E; with $\frac{1}{\varrho}=\limsup_{n\to\infty} \sqrt[n]{\|a_n\|}$. If $f(\lambda)$ is holomorphic inside the circle

$$|\lambda-\lambda_0|<\frac{1}{\limsup_{n\to\infty}\left|\frac{f^{(n)}(\lambda_0)}{n!}\right|^{1/n}},$$

then we will call, as usually,

$$f(x)=\sum_{n=0}^{\infty}\frac{f^{(n)}(\lambda_0)}{n!}(x-\lambda_0 e)^n \tag{10.1}$$

the principal extension of $f(\lambda)$ in the sphere

$$\|x-\lambda_0 e\|<\frac{1}{\limsup_{n\to\infty}\left|\frac{f^{(n)}(\lambda_0)}{n!}\right|^{r/n}}.$$

THEOREM 10.1. *If $f(\lambda)$ is holomorphic in a domain Δ of the complex plane and if $\mathcal{D}_\Delta$ is the union of all spheres*

$$\|x-\lambda_0 e\|<\frac{1}{\limsup_{n\to\infty}\left|\frac{f^{(n)}(\lambda_0)}{n!}\right|^{r/n}},$$

such that the circle

$$|\lambda-\lambda_0|<\frac{1}{\limsup_{n\to\infty}\left|\frac{f^{(n)}(\lambda_0)}{n!}\right|^{1/n}}$$

is in Δ, then the principal extension of $f(\lambda)$ is uniquely determined by the preceeding definition in D_Δ and is a holomorphic function of x in $\mathcal{D}_\Delta$.

Proof. Let $f(x;\lambda_0 e)$ be the power series in formula (10.1). It is obvious that this is a holomorphic function of x in the sphere of definition. As concerns the fact that the various power series $f(x;\lambda_0 e)$ are elements of the same holomorphic function – this can be proved like in Banach spaces.

11. From the last considerations, it results that it is possible to develop a spectral theory in quasi normed spaces. A second problem which is open is to find the class of linear topological non-locally convex spaces whose topology can be defined by means of a family of semi-quasi norms.

REFERENCES

[1] M. M. Day, *The spaces L^p with $0<p<1$*, Bull. Amer. Math. Soc. **46** (1940), 816.

[2] D. G. Bourgin, *Linear topological spaces*, Am. Jour. Math. **65** (1943), 637.

[3] D. H. Hyers, *Locally bounded linear topological spaces*, Revista de Ciencias **41** (1939), 555.

[4] N. Bourbaki, *Utilisation des nombres réels en topologie générale*, Paris, 1948, p. 40.

[5] S. Banach, *Théorie des opérations linéaires*, Varsovie, 1932, p. 54.

[6] N. Bourbaki, *Espaces d'applications linéaires continues*, Paris, 1955.

[7] A. Sobczyk, *On the extension of linear transformations*, Trans. Am. Math. Soc. **55** (1944).

[8] K. Borsuk, *Sur les rétractes*, Fund. Math. **17** (1931), 152.

[9] E. Hille, *Functional analysis and semi-groups*, New York, 1948, p. 92.

BULLETIN DE L'ACADÉMIE
POLONAISE DES SCIENCES
Cl. III — Vol. V, No. 5, 1957

MATHEMATICS

Uniform Distribution on a Sphere

by

M. KAC

Presented by H. STEINHAUS on March 13, 1957

THEOREM. *S being the sphere* $x^2+y^2+z^2=1$ *we assume the projections of a moving point* $P(t)$ *on the diameters of* S *to cover them uniformly as the time* t *runs through* 01; $P(t)=(x(t), y(t), z(t))$ *is supposed to be continuous. Then* $P(t)$ *covers* S *uniformly.*

This assertion means that

$$(*) \qquad \left| \sum_t \{P(t) \in R\} \right| = |R|/4\pi$$

for every region R on S; $|\ |$ reads as linear respectively as superficial measure.

Now, our theorem has been proved implicitly by Archimedes if R in (*) is understood as a circular region. The extension to all $R \subset S$ by elementary geometry is very cumbersome. An analytical proof of our theorem for all regions R on S is as follows:

Proof. The assumption signifies for real a, b, c, $a^2+b^2+c^2>0$, that

$$\frac{ax(t)+by(t)+cz(t)}{\sqrt{a^2+b^2+c^2}}$$

has the same distribution as $2t-1$. This implies the identity of characteristic functions of both functions:

$$(1) \qquad \int_0^1 e^{i(ax(t)+by(t)+cz(t))}\,dt = \frac{\sin\sqrt{a^2+b^2+c^2}}{\sqrt{a^2+b^2+c^2}} = f(a,b,c)\,.$$

On the other hand one verifies directly

$$(2) \qquad \frac{1}{4\pi}\int_S\int e^{i(ax+by+cz)}\,ds = \frac{\sin\sqrt{a^2+b^2+c^2}}{\sqrt{a^2+b^2+c^2}} = f(a,b,c)\,,$$

where ds is an element of S and x,y,z the integration variables. The formula

$$\iint_S e^{i(ax+by+cz)}ds = H\left(\frac{1}{i}\frac{\partial}{\partial\vartheta}, \frac{1}{i}\frac{\partial}{\partial b}, \frac{1}{i}\frac{\partial}{\partial c}\right)\iint_S e^{i(ax+by+cz)}ds \tag{3}$$

for any polynomial $H(x,y,z)$ is also easily verified. Now, joining (1), (2) and (3), we get

$$\frac{1}{4\pi}\iint_S e^{i(ax+by+cz)}H(x,y,z)\,ds = H\left(\frac{1}{i}\frac{\partial}{\partial a}, \frac{1}{i}\frac{\partial}{\partial b}, \frac{1}{i}\frac{\partial}{\partial c}\right) f(a,b,c) = \tag{4}$$

$$= H\left(\frac{1}{i}\frac{\partial}{\partial a}, \frac{1}{i}\frac{\partial}{\partial b}, \frac{1}{i}\frac{\partial}{\partial c}\right)\int_0^1 e^{i(ax(t)+by(t)+cz(t))}\,dt =$$

$$= \int_0^1 e^{i(ax(t)+by(t)+cz(t))}\cdot H\big(x(t),y(t),z(t)\big)\,dt\,.$$

The first and last integral in (4) being equal we obtain for $a\to 0$, $b\to 0$, $c\to 0$

$$\int_0^1 H\big(x(t),y(t),z(t)\big)\,dt = \frac{1}{4\pi}\iint_S H(x,y,z)\,ds\,. \tag{5}$$

Consider now a sequence $\{H_n(x,y,z)\}$ of spherical harmonics converging for $n\to\infty$ to 1 in R and to 0 in the interior of $S-R$; there exists such a sequence, moreover, it can be chosen as to be uniformly bounded on S. Putting H_n for H in (5) we get for $n\to\infty$

$$\Big|\mathop{E}_t\{P(t)\in R\}\Big| = |R|/4\pi\,.$$

The converse of our theorem is an immediate consequence of the Archimedean theorem already alluded to and stating the equality of surfaces of a sphere and of the circumscribed cylinder.

CORNELL UNIVERSITY, ITHACA, N. Y., U. S. A.

BULLETIN DE L'ACADÉMIE
POLONAISE DES SCIENCES
Cl. III — Vol. V, No. 5. 1957

MATHEMATICS

(h**F**)-Spaces and the Banach Inversion Property

by

W. SŁOWIKOWSKI

Presented by S. MAZUR on March 20, 1957

Introduction

It is known [3] that the classes of ($\mathbf{B}_0$)-spaces [2] and of ($\mathbf{DB}_0$)-spaces belong to the class of linear locally convex spaces with the *Banach Inversion Property*, i. e., to a class **K** of linear, locally convex spaces such that every one-to-one linear continuous mapping of $X \in \mathbf{K}$ onto $Y \in \mathbf{K}$ is bicontinuous.

In this paper are considered the more general classes of linear spaces and linear locally convex topological spaces with the Banach Inversion Property. These spaces are called (h**F**)-spaces and locally convex (h**F**)-spaces, respectively.

hF-spaces

A linear space X is called (h**F**)-*space* if there is a fixed sequence (X_p), $p=1,2,\ldots$ of linear subspaces of X and a sequence of F-norms *) $|x|_p$, which are defined on X_p, respectively, such that the following conditions are fulfilled:

1. The X_p spaces with F-norms $|x|_p$ are (**F**)-spaces, i. e., linear, topological, complete metric spaces with a distance function $\varrho_p(x,y)=|x-y|_p$ [1].
2. $X_p \subset X_{p+1}$ and $\lim_n |x_n|_p = 0$ implies $\lim_n |x_n|_{p+1} = 0$ for every $(x_n) \subset X_p$.
3. $X = \bigcup X_p$.

We shall say that the sequence (X_p) of (**F**)-spaces induces in X an (h**F**)-topology. A sequence $(x_n) \subset X$ is called *h-convergent* to x_0 (it will be written $x_n \xrightarrow{h} x_0$), if there is such a p that $x_n, x_0 \in X_p$ and $\lim_n |x_n - x_0|_p = 0$; (x_n) is called *h*-convergent* to (x_0) (it will be written $x_n \xrightarrow{h^*} x_0$), if every

*) The functional $|x|$ is named F-norm if $|x+y| \leqslant |x|+|y|$, $|-x|=|x|$ and $|x|=0$ is equivalent to $x=0$.

subsequence x_{m_n} has a subsequence $x_{m_{k_n}}$ such that $x_{m_{k_n}} \overset{h}{\to} x_0$; (x_n) is called *h*-bounded*, if for every sequence $0 < t_n \to 0$, $t_n x_n \overset{h^*}{\to} 0$.

Let X and Y be (h**F**)-spaces and U a linear transformation of X into Y. The transformation U is called *h-continuous* if for every $(x_n) \subset X$, $x_n \overset{h}{\to} 0$ implies $Ux_n \overset{h}{\to} 0$; U is called *h*-continuous* if for every $(x_n) \subset X$, $x_n \overset{h^*}{\to} 0$ implies $Ux_n \overset{h^*}{\to} 0$; U is named *h-closed* if for every $(x_n) \subset X$, $x_n \overset{h}{\to} x_0$ and $U x_n \overset{h}{\to} y_0$ implies $Ux_0 = y_0$.

THEOREM 1. *If for every* $(x_n) \subset X$, $x_n \overset{h}{\to} 0$ *implies h*-boundedness of the sequence* (Ux_n) *then* U *is h*-continuous.*

THEOREM 2. *If* U *is h-continuous and maps the space* X *onto the space* Y, *then for every* $(y_n) \subset Y$ $y_n \overset{h}{\to} 0$, *there is* $(x_n) \subset X$ $x_n \overset{h}{\to} 0$, *such that* $y_n = U x_n$.

THEOREM 3. *The following conditions are equivalent*:

1. U *is h-continuous.*
2. U *is h*-continuous.*
3. U *is h-closed.*

Theorem 2 implies that the class of (h**F**)-spaces has the Banach Inversion Property, i. e., every h-continuous one-to-one linear mapping of (h**F**)-space X onto (h**F**)-space Y has the h-continuous inversion.

(h**F**)-locally convex spaces

Let Z be an (h**F**)-space. Further, let (τ) denote a locally convex b-topology in Z. (We write b-topology for bornological topology).

We shall say that *the topology* (τ) *is compatible with the* (h**F**)*-topology*, if the following conditions are satisfied:

(a) if $(x_n) \subset Z$ and $x_n \overset{h}{\to} 0$, then $x_n \to 0$ in (τ) topology;

(b) if $(x_n) \subset Z$ and (x_n) is bounded in (τ) topology, then (x_n) is h*-bounded.

Let us consider two (h**F**)-spaces X and Y with locally convex b-topologies (τ_1), and (τ_2) which are compatible with (h**F**)-topologies respectively. If we denote by U a linear transformation of the space X into the space Y, then we have the following

THEOREM 4. *The transformation* U *is h-continuous if, and only if, it is continuous as the transformation of the space* X *with* (τ_1) *topology into the space* Y *with* (τ_2) *topology.*

If two locally convex b-topologies of an (h**F**)-space Z are compatible with the (h**F**)-topology of Z, then the Theorem 4 implies the equivalence of these topologies, i. e., bicontinuity of identical mapping of Z with the former topology onto Z with the latter one. This means that

in Z a locally convex b-topology compatible with the (h**F**)-topology of Z can be introduced in exactly one way.

An (h**F**)-space X is called a locally convex (h**F**)-space if there can be introduced in X the locally convex b-topology which is compatible with (h**F**)-topology of X.

THEOREM 5. *The space X is a locally convex (h**F**)-space if, and only if, every sequence bounded with respect to every linear h-continuous functional defined on X is h*-bounded.*

Let X and Y denote locally convex (h**F**)-spaces and U a linear transformation of X into Y. Then the following theorem holds:

THEOREM 6. *The transformation U is continuous if, and only if, it is h-continuous.*

COROLLARY. *If U is closed (i. e., if $x_n \to x_0$ and $Ux_n \to y_0$ implies $Ux_0 = y_0$), then U is continuous.*

Thus, every continuous one-to-one mapping of a locally convex (h**F**)-space X onto a locally convex (h**F**)-space Y has the continuous inverse mapping, and so the class of locally convex (h**F**)-spaces has the Banach Inversion Property.

INSTITUTE OF MATHEMATICS, POLISH ACADEMY OF SCIENCES

REFERENCES

[1] S. Banach, *Théorie des opérations linéaires*, Warsaw, 1932.

[2] S. Mazur and W. Orlicz, *Sur les espaces métriques linéaires (I)*, Studia Mathematica **10** (1948), 184.

[3] W. Słowikowski, *On a certain specification of* (**DF**) *linear locally convex spaces*, Bull. Acad. Polon. Sci., Cl. III, **5** (1957), 387.

BULLETIN DE L'ACADÉMIE
POLONAISE DES SCIENCES
Cl. III — Vol. V, No. 5, 1957

THEORETICAL PHYSICS

On the Lagrangian in Special Relativity Theory

by

L. INFELD

Presented on March 14, 1957

1. Introduction

This paper deals with the Lagrangian in relativistic mechanics. Recently an interesting paper by G. Szamosi [1] appeared on the same subject. The treatment given here is, we believe, more general and simple.

2. The proper relativistic Lagrangian

We assume that a relativistic Lagrangian $\mathcal{L}$ is given: either through the physics of some problem, or, as a natural generalisation of the Lagrangian in classical mechanics. That is,

$$\mathcal{L} = \mathcal{L}(x_\mu, x'_\mu) . \tag{2.1}$$

Here

$$x'_\mu = \frac{dx_\mu}{ds}; \qquad dx_\nu dx_\nu = -ds^2 = \sum_{\nu=1}^{4} (dx_\nu)^2; \qquad x_4 = it \tag{2.2}$$

(c = velocity of light = 1).

When the integral of (2.1) with respect to ds is varied, we have to take into account the fact that x'_ν are not arbitrary. They fulfil the condition

$$x'_\nu x'_\nu + 1 = 0 . \tag{2.3}$$

To obtain a proper Lagrangian in which the x_ν's can be treated as independent from each other, we have to multiply the last equation by a Lagrangian factor and add to (2.1). This is the essential idea of this paper. The proper Lagrangian $\mathcal{L}^*$ is

$$\mathcal{L}^* = \mathcal{L} + \frac{\lambda}{2}(x'_\nu x'_\nu + 1) \tag{2.4}$$

and the variational principle of relativistic mechanics is

$$\delta \int \mathcal{L}^* ds = 0 . \tag{2.5}$$

The variation has to be performed with respect to the x_ν's and λ. Thus, as our equations of motion we have

$$\frac{\partial \mathcal{L}}{\partial x_\nu} - \left(\frac{\partial \mathcal{L}}{\partial x'_\nu}\right)' - (\lambda x'_\nu)' = 0 , \tag{2.6}$$

$$\tfrac{1}{2}(x'_\nu x'_\nu + 1) = 0 . \tag{2.7}$$

These are the five equations to determine the $x_\mu(s)$ and $\lambda(s)$. From these equations we can find λ as a function of x_ν, x'_ν. Indeed, multiplying (2.6) by x'_ν we find, because of (2.7):

$$\lambda' = \left(\frac{\partial \mathcal{L}}{\partial x'_\nu}\right)' x'_\nu - \frac{\partial \mathcal{L}}{\partial x_\nu} x'_\nu . \tag{2.8}$$

If $\mathcal{L}$ does not depend explicitly on s, which we shall assume, this equation can be integrated, giving the following result, which is important for all further applications:

$$\boxed{\lambda = \frac{\partial \mathcal{L}}{\partial x'_\nu} x'_\nu - \mathcal{L}} . \tag{2.9}$$

Here the constant of integration has been left out since it can always be absorbed by the Lagrangian.

We shall put this value for λ into (2.6) and obtain in this way the proper relativistic equations of motion in which λ is eliminated and only the original Lagrangian appears:

$$\left(\frac{\partial \mathcal{L}}{\partial x_\nu}\right) - \left(\frac{\partial \mathcal{L}}{\partial x'_\nu}\right)' - \left(\frac{\partial \mathcal{L}}{\partial x'_\varrho} x'_\varrho x'_\nu\right)' + (\mathcal{L} x'_\nu)' = 0 . \tag{2.10}$$

The only conditions that $\mathcal{L}$ must fulfil for the equation to be valid, is its explicit independence of s. If we call the left-hand side of (2.10) Ω_ν, we can easily verify that

$$\Omega_\nu x'_\nu = 0 \tag{2.11}$$

is fulfilled identically for arbitrary $\mathcal{L}$.

In the simpler case in which $\mathcal{L}$ depends only on x_μ, (2.10) becomes

$$-(\mathcal{L} x'_\nu)' = \frac{\partial \mathcal{L}}{\partial x_\nu} . \tag{2.12}$$

Since the right-hand side of this equation is usually interpreted as the "force", then $-\mathcal{L}$ should be interpreted as the proper relativistic rest mass. For $\mathcal{L} = -m = \text{constant}$ we have simply $m x''_\nu = 0$, that is, the law of inertia.

3, Special cases

As our first special case we shall take that of a particle under the influence of a potential force

$$\mathcal{L} = -m - \varphi; \qquad \varphi = \varphi(x_\mu). \tag{3.1}$$

Although we do not need a knowledge of λ for the equations of motion, let us write it down from (2.9)

$$\lambda = m + \varphi. \tag{3.2}$$

The equations of motion (2.12) are indeed simple:

$$\left((m+\varphi)x_\nu'\right)' = -\frac{\partial \varphi}{\partial x_\nu}. \tag{3.3}$$

Thus, $(m+\varphi)$ is the proper relativistic rest mass depending on the external field The consequences of this equation were thoroughly investigated by J. Werle [2], [3], who discovered a new relativistic effect coming from (3.3). If φ is negative, that is in the case of attraction, an impregnable core is formed near the centre of force and (near the centre of force) the attraction changes into repulsion. For the sake of completeness we shall discuss briefly this interesting phenomenon, which, to our knowledge, is little known.

Let us assume that φ does not depend on x_y. Then the fourth equation can be immediately integrated, giving

$$\frac{m+\varphi}{\sqrt{1-v^2}} = \text{constant}, \tag{3.4}$$

where v is the three-dimensional velocity.

We shall explain the character of the new relativistic phenomenon, further specialising our assumptions. Let us assume in (3.4)

$$\varphi = -\frac{g^2}{r}; \qquad \text{constant} = m, \tag{3.5}$$

where g^2 is some constant and r the (3-dimensional) distance from the centre of force. Then (3.4) takes the form

$$\frac{m - g^2/r}{\sqrt{1-v^2}} = m. \tag{3.6}$$

For $r = \infty$, we have $v = 0$; this means that the particle is falling to the centre of force and for small velocities (3.6) becomes the usual energy integral of classical motion. For $v = 1$, that is for the velocity of light, the numerator must also be zero, that is, for

$$g^2/r_0 = m; \qquad r_0 = g^2/m, \tag{3.7}$$

the proper rest mass vanishes. Up to this point, that is in the region C (for $r>r_0$) the motion was accelerated until the particle obtained the velocity of light. For $r<r_0$ the numerator becomes negative. But taking the negative square root we obtain a positive quotient. Thus (3.6) is fulfilled for $r<r_0$ and $v<1$. In the second region B (for $r<r_0$) we have

$$\frac{g^2/r-m}{\sqrt{1-v^2}}=m\,;\qquad r<r_0 \tag{3.8}$$

decelerated motion. Finally, the particle stops if $v=0$, that is for $\bar{r}=\frac{r_0}{2}$ because

$$\frac{2g^2}{r_0}-m=m\,. \tag{3.9}$$

Thus, the sphere of radius $\bar{r}=\frac{r_0}{2}$ divides the second region, B, from the third, A $\left(\text{for } r<\frac{r_0}{2}\right)$, which cannot be penetrated.

Thus we see that a particle freely falling from $r=\infty$ is attracted in the region C to the centre of force, reaches the velocity of light at its lower boundary, is repulsed in the region B, stops at its lower boundary, to be repulsed towards the region C again.

The same features of a motion under the influence of potential forces, depending only on the space co-ordinates, also appear in the more general case in which $\varphi(r)$ is any negative monotonically decreasing function, and the constant of integration in (3.4) is arbitrary.

Our discussion, based on the two possible values of the square root shows that in integrating the fourth equation (3.3), we take the absolute values, that is

$$\left|\frac{m+\varphi}{\sqrt{1-v^2}}\right|=|\text{constant}|\,. \tag{3.10}$$

If we take the square root to be, say, only positive, then the character of the motion changes. Then, in the case of const. $=m$ and $\varphi=-g^2/r$, both regions B and A would be impregnable, and the particle, on reaching the sphere with radius r_0, would be reflected from it. But this interpretation seems more artificial than the previous one. J. Werle used the first interpretation to explain the existence of repulsive nuclear forces if the particles are very near each other.

Now we shall discuss the second special case, that of a charge e in an electromagnetic field characterised by the potential vector $A_\mu(x)$.

We take

$$\mathcal{L}=-m+eA_\nu x'_\nu\,. \tag{3.11}$$

Then (2.9) gives us simply

$$\lambda=m \tag{3.12}$$

and (2.10):

$$mx''_\nu = e(A_{\varrho,\nu} - A_{\nu,\varrho})x'_\varrho ; A_{\nu,\varrho} = \frac{\partial A_\nu}{\partial x_\varrho}. \tag{3.13}$$

These are the usual equations of motion for a charged particle in a given electromagnetic field.

INSTITUTE OF PHYSICS, POLISH ACADEMY OF SCIENCES

REFERENCES

[1] G. Szamosi, Acta Phys. Hung. **6** (1956), 207.

[2] J. Werle, *The problem of "equivalent" potentials in classical equations of motion*, Bull. Acad. Polon. Sci. Cl. III, **1** (1953), 281.

[3] P. E. Kunin and J. M. Taxar, Latvijas PSR. Zinatnu Akad. Vestis **52** (1951), No. 11.

BULLETIN DE L'ACADÉMIE
POLONAISE DES SCIENCES
Cl. III — Vol. V, No. 5, 1957

EXPERIMENTAL PHYSICS

Parameter of Disorder p and the Interlayer Distance d_{002} in Highly Graphitised Artificial Graphites

by

M. LEFELD

Presented by A. SOŁTAN on February 12, 1957

As shown by the investigations of Warren, Franklin and others, artificial graphites obtained by the heat treatment of carbon black have a structure intermediate between the structure of carbon black and the structure of perfect graphite. In the case of carbon black we have to do with a "random layer structure" in which the layers consisting of atoms of carbon situated at the corners of hexagonal rings are arranged parallelly, but are entirely randomly oriented with respect to a displacement in the plane of the layer and rotation about the normal to the layer, the distances between them being equal. During the heat treatment process these layers fall into order, forming in the end the structure of perfect graphite. The changes in the order of the layers effect changes in the X-ray diffraction pattern. The lines (hkl) with $l \neq 0$ do not appear on the rentgenograms of the carbon black (as the investigations of Biscoe and Warren [2] and others showed) disregarding reflections of the type $00l$) and two-dimensional lattice reflections of the type (hk); they do, however, appear on the rentgenograms of the artificial graphites, their sharpness increasing together with the increase in order. The parameter of disorder p, which is defined as the probability of the occurrence of any disorientation between two neighbouring layers, is a quantity characterising the degree of order of a given sample.

In order to check to what extent a given substance is ordered, the distribution of the intensity of the radiation diffracted in the reciprocal space (expressed as a function of the reciprocal lattice variable) should be examined.

The axes a^* and b^* of the reciprocal plane lattice correspond to the crystallographic axes lying in the plane of the graphite layer and denoted by a and b. Axis c^* is, in this case, perpendicular to axes a^* and b^*. For a set of parallel and equidistant layers having a random

orientation with respect to the neighbouring layers, the reciprocal lattice may be represented as a set of rods parallel to axis c^* and passing through points whose positions are given by the vectors $\vec{s}_0 = h\vec{a}^* + k\vec{b}^*$ (where h and k are integral indices), and the set of points lying on axis c^*.

So long as the graphite layers are entirely randomly oriented there will be no maxima on the rods (hk) (besides the points ($hk0$) and rod (00)). If, however, we are dealing with a set of layers oriented with respect to one another, there will occur on those rods having constants h and k and variable l, more or less diffuse maxima corresponding to the lines (hkl).

In order for the X-rays to be reflected in a direction making an angle 2θ with the direction of the primary beam, the sphere of reflection of radius $1/\lambda$, passing through the origin of the reciprocal lattice must also pass through other points of the same lattice. This is equivalent to the fact that the end of the vector $\vec{s}$ $\left(\text{whose length is } |\vec{s}| = \frac{2\sin\theta}{\lambda}\right)$ will lie on the rods parallel to axis c^* at a point corresponding to any more or less diffuse maximum (hkl). For powdered samples consisting of sets of unoriented parallel layers the intensity of the reflected radius is proportional to $\frac{1}{s(s^2 - s_0^2)^{1/2}}$ $(s_0 = |\vec{s}_0| = \frac{2\sin\theta}{\lambda}$, where $\vec{s}_0$ is a vector giving the position of the point ($hk0$) on the rods passing through this point and parallel to axis c^*, and $s = |\vec{s}| = \frac{2\sin\theta}{\lambda}$, where $\vec{s}$ gives the position of any other point on this axis [3], [4]). In the case of artificial graphites, where there appears a mutual orientation of layers, the function giving the intensity distribution of the scattered radiation as a function of s must be multiplied by a function dependent on the degree of order of the layers and given by

$$I = \frac{1 - U^2}{1 + U^2 - 2U\cos\varphi}, \tag{1}$$

where $U = 1 - p$ and $\varphi = \pi l$ (l is a variable taking values that are not necessarily integral and changing in accordance with the direction of the axis c^* and given by $d(s^2 - s_0^2)^{1/2}$, where d is the interlayer distance). In Fig. 1 we see how the shape of the (hkl) line given by Eq. (1) in reciprocal space changes for different parameters of disorder p.

Investigating a number of artificial graphites, Franklin [1] showed that the interlayer distance d_{002} of well crystallised graphite is constant and equal to 3.354 Å; in the case of non-graphitic carbons having the structure of carbon black this distance is also constant, but equal to 3.44 Å. In respect to carbons undergoing graphitisation she found that the mean interlayer distance, measured from the position of the maximum line (002), is intermediate between these two values; this distance decreases with an increase in the order. The subject of the present work

was to study the changes of interlayer distance for changes in the degree of order for several samples of synthetic graphites whose structure is close to the structure of perfect graphite, that is, in a region with a small value of p.

In order to determine the parameter of disorder p for the substances investigated, the shape of the (112) lines was determined in the reciprocal space (after introducing the necessary corrections) in accordance with the previously discussed method used by R. E. Franklin. For individual samples, the parameter p was determined by comparison with

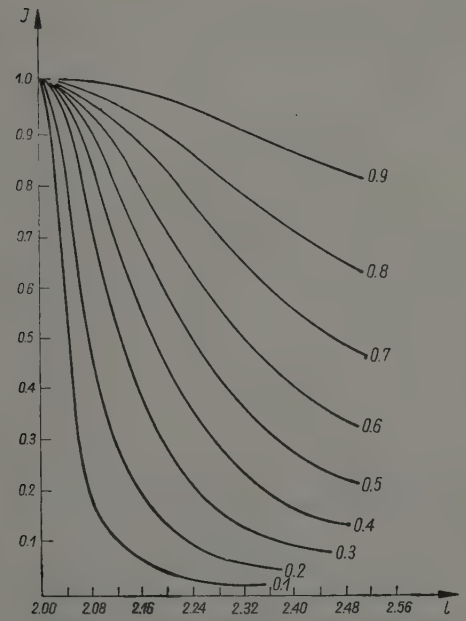

Fig. 1

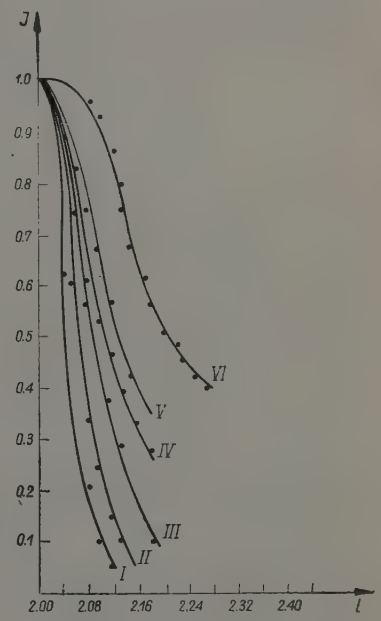

Fig. 2

the theoretical curves. The interlayer distance d_{002} for these substances was determined by using NaCl as a standard, the accuracy obtained being ± 0.004 Å.

Fig. 2. shows the shapes of the lines (112) in reciprocal space for the five graphite samples investigated in this work (sample I was Ceylon graphite, and the remaining samples were artificial graphites). Table I gives the obtained interlayer distances d_{002} together with the parameters of disorder p determined by the shape of the lines.

On the basis of these results it may be seen that there is a linear relationship between d_{002} and p for values of p in the range 0.05 to 0.5 (for the samples investigated in this case).

A decrease in the distance d_{002} is accompanied by an increase in the order (or decrease in the disorder parameter p). For these samples this is in accordance with the results of Bacon [5]. This relation is illustrated in Fig. 3 in which the points obtained in this work are denoted by dots, and the experimental data of Franklin, by crosses.

The reason that all points obtained in this work lie below the points indicated by crosses might be found in the difference in the substances from which the artificial graphites were prepared and the method of heat treatment.

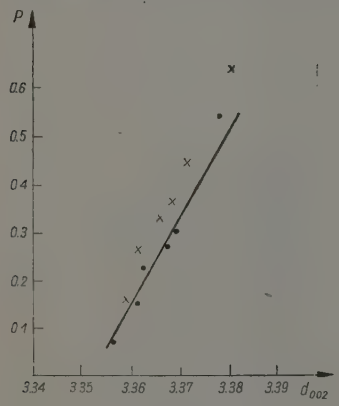

Fig. 3

TABLE I

No. of sample	p	d_{002}
I	0.05	3.355
II	0.15	3.361
III	0.21	3.362
IV	0.26	3.367
V	0.30	3.369
VI	0.52	3.378

Perhaps this may in some degree, be explained by the fact that the present author took into account geometrical line breadths for all samples, while Franklin, in the majority of cases (except for two of the best graphitised samples) did not take the breadths into account.

I would like to express my appreciation to Professor L. Sosnowski and to J. Auleytner for their valuable critical remarks and discussion. I also wish to thank Professor A. Grossman for supplying the samples of artificial graphites and Mrs. Z. Wójcik for help in the analysis of the experimental material.

INSTITUTE OF PHYSICS, POLISH ACADEMY OF SCIENCES

REFERENCES

[1] R. E. Franklin, Acta Cryst. **4** (1951), 253.
[2] J. Biscoe, B. E. Warren, J. Appl. Phys. **13** (1943), 364.
[3] B. E. Warren, Phys. Rev. **9** (1941), 693.
[4] G. W. Brindley, J. Mering, Acta Cryst. **4** (1951), 441.
[5] G. E. Bacon, Acta Cryst. **4** (1951), 558.

BULLETIN DE L'ACADÉMIE
POLONAISE DES SCIENCES
Cl. III — Vol. V, No. 5, 1957

EXPERIMENTAL PHYSICS

Investigation of the Pyridine-Sulphur Dioxide System by Raman Spectroscopy. II. Investigation of the Contours of the Lines and Their Dependence on Temperature

by

A. TRAMER

Presented by A. JABŁOŃSKI on February 19, 1957

The close analogy between acids in the classical concept of this term and the so-called generalised Lewis acids, of which sulphur dioxide is a representative, appears, in part, in the similar nature of complexes formed with compounds of a basic character (e. g., the analogy in the electron absorption spectra [1]—[3]). In a previous paper [4] the author showed that there was a similarity between the changes arising in the vibration spectrum of pyridine as a result of the formation of the sulphur dioxide complex $C_5H_5N.SO_2$ and complexes with organic acids $C_5H_5N..H{-}OOC{-}R$.

In this paper, we examine in closer detail the changes in the spectrum of SO_2 molecules which accompany the formation of the complex, such changes being similar to changes in the valence frequency of the O—H bond in the case of the hydrogen bond. The results are given of the investigation of the dependence of the intensity and width of the SO_2 lines and the strongest pyridine lines on the composition and temperature of the solutions and attempts to interpret them.

Experimental part

A fully anhydrous mixture, of a pale green-yellow colour, of SO_2 and C_5H_5N was prepared and analysed by a method already described [4]. The Raman spectra were investigated by a photographic method; use was made of: a "Huet B" spectrograph with its dispersion increased to 9 Å/mm. at about 4500 Å by bringing the prisms out of the minimum deviation [5], high pressure PRK-2 lamps, and "Agfa" "Ramanplatten ortho" photographic plates. Solutions liable to gradual decomposition were redistilled after several hours of exposure. The temperature of the solutions was changed within the range of 5 to 80°C. by means of a water

jacket. The temperature during long exposures was maintained constant within $\pm 2°C$.

The integral intensities I were determined by integrating along the intensity contour of the lines photographed with a narrow setting of the spectrograph slits. The half-width of the lines σ was determined by the Bazhulin method [6] by substracting from the observed half-width the width of the excitation line photographed under similar conditions.

The determination was carried out of the half-width and intensity of the free SO_2 line $\nu_1 = 1145.5$ cm.$^{-1}$, of the free pyridine lines, $\nu_1 = 990$, $\nu_{12} = 1030$ and $\nu_2 = 3056$ cm.$^{-1}$, and of the corresponding lines of the bound SO_2 molecules, $\nu_1^* = 1130$, and bound pyridine molecules $\nu_1^* = 1006$, $\nu_{12}^* = 1030$ and $\nu_2^* = 3072$ cm.$^{-1}$. Because of the instability of the solutions, the presence of background, random differences of the absorption coefficient, no attempt was made to compare the absolute intensities with different photographs. No substances were introduced into the solutions to serve as a standard; the 1030 cm.$^{-1}$ of pyridine was used as an internal standard; the position and half-width of this line depends least on the concentration and temperature of the solution. The line intensities are given everywhere relative to $I_{1030} = 100$, for SO_2 computed on the basis of a quantity of 1 mole. The half-width of the ν_1^* band of SO_2 was determined by substracting from the observed contour the contour of the line observed in pure sulphur dioxide.

Tabulation of results

In Tables I and II and in Figs. 1, 2 and 3 the contours and the main parameters of the lines are shown as a function of the composition of the mixture at a temperature of 20°C.

TABLE I

Variation of the main parameters of the pyridine lines with the composition of the solution at the temperature of 20°C

SO_2 content % mole	Line										
	ν_1			ν_1^*			ν_{12}			ν_2	
	ν	σ	I	ν	σ	I	ν	σ	I*)	ν	σ
100.0	990	2.7±0.2	125±5	–	–	–	1030	3.0±0.2	100	3056	11.5±0.5
67.2	991	2.7±0.3	62±5	1004	~7	~15	1030	3.0±0.3	100	3061	~14.5
53.2	992	~3	~9	1006	6.6±0.4	31±5	1030	3.2±0.3	100	3067	16.0±2.0
49.1	993	~4	~2	1008	6.5±0.5	29±3	1030	3.0±0.2	100	3072	18.0±2.0
45.1	993	~3	~1	1008	6.7±0.5	34±5	1030	3.0±0.2	100	3075	21.0±2.0
24.3	–	–	–	1008.5	~7	30±5	1030	3.2±0.3	100	–	–

*) standard intensity.

TABLE II

Variation of the main parameters of the sulphur dioxide lines with the composition of the solutions at a temperature of 20°C

SO_2 content % mole	Line						$\frac{\sum I_{SO_2} \cdot n_{C_5H_5N}}{I_{1030} \cdot n_{SO_2}}$
	ν_1			ν_1^*			
	ν	σ	I	ν	σ	I**)	
100.0	1145.5	2.55±0.2	—	—	—	—	—
75.7	1145.5	2.5 ±0.2	210±30	1129	~25	100	~135
54.9	1145	2.5 *)	19±3	1131	24.6±1.2	100	155±15
50.9	1145	2.5 *)	8±2	1130	23.3±1.2	100	155±10
46.8	—	—	—	1131	18.4±0.8	—	152±10
32.8	—	—	—	1136	13.5±1.5	—	140±20

*) assumed width.
**) standard intensity.

The influence of the temperature was investigated more closely for solutions containing 46.8, 50.9, and 54.9 mole % SO_2. The results are

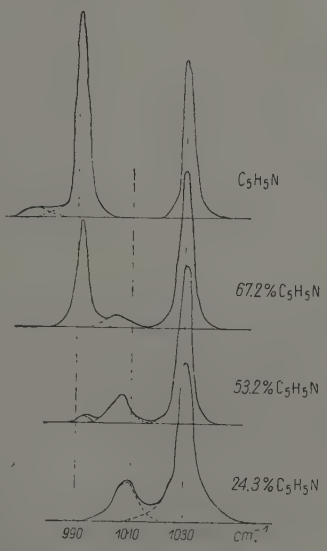

Fig. 1

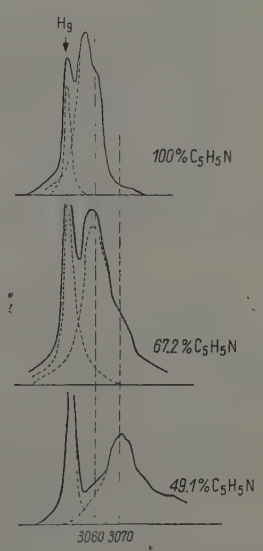

Fig 2

Fig. 1. Variation of the contour of the ν_1, ν_1^* and ν_{12} lines of pyridine with solution composition

Fig. 2. Variation of the contour of the ν_2 line of pyridine with solution composition

shown in Table III, and sample-line contours in a solution consisting of 50.9 mole % at $t = 10°C$. and 80°C. are shown in Fig. 4.

Changes of frequency, half-width and relative line intensity due to temperature changes in pure liquids lie within the limit of error of the measurement. The same holds true for the dependence of the lines of free molecules in solution on the concentration and temperature.

The line $\nu_{12} = 1030$ cm.$^{-1}$ of pyridine shows nearly the same position and width

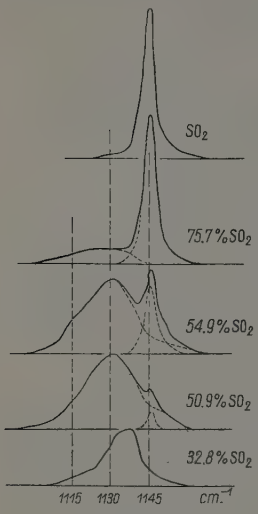

Fig. 3

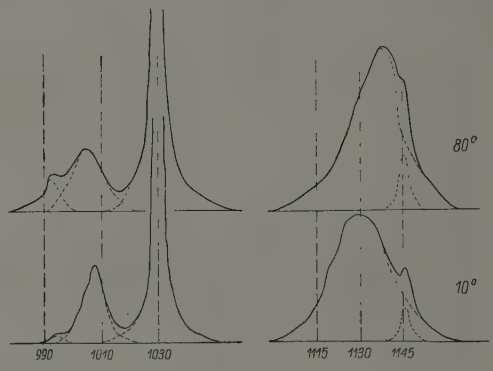

Fig. 4

Fig. 3. Variation of the contour of the ν_1 and ν_1^* lines of SO_2 with solution composition
Fig. 4. Variation of the contour of the ν_1, ν_1^* and ν_{12} lines of pyridine and ν_1^* of SO_2 with temperature

in the spectra of the free and complex molecules. The effect of temperature is insignificant in both cases.

TABLE III

Variation of the line width and frequency with temperature

SO_2 content % mole	Temperature	Line					
		$\nu_1^* C_5H_5N$		$\nu_{12} C_5H_5N$		$\nu_1^* SO_2$	
		ν	σ	ν	σ	ν	σ
54.9	10°	1008	6.7±0.5	1030	3.0±0.2	1131	24.6±1.2
	50°	1006.5	8.1±0.8	1030	3.0±0.3	1135	19.8±0.5
	80°	1005	~10	1030	3.5±0.3	1137	15.2±1.2
50.9	10°	1008	6.5±0.5	1030	3.0±0.2	1130	23.2±1.2
	50°	1006	8.5±1.0	1030	3.0±0.3	1135	17.5±0.6
	80°	1005	8.5±1.0	1030	3.3±0.2	1138.5	14.8±1.5
46.9	10°	1006.5	6.6±0.4	1030	3.05±0.25	1131	18.4±0.8
	50°	1004	7.6±0.6	1030	3.3±0.2	1135.5	16.2±1.0
	80°	~1004	?	1030	3.0±0.5	1137.5	~14.0

To the pyridine line ν_1, of a frequency of 990 cm.$^{-1}$, there corresponds in the case of the complex, the line $\nu_1^* = 1006$ cm.$^{-1}$, whose width is over twice as great and the intensity about 4 times as small as in the case of free pyridine. This is surprising, since in the complexes with organic acids [7] the intensity of this line increases. With an increase in the SO_2 content of the mixture, the line maximum shifts towards the higher frequencies, the increase in temperature producing a shift in the opposite direction, and, in addition, a marked broadening of the line.

To the pyridine line $\nu_2 = 3056$ cm.$^{-1}$ there corresponds, in the complex, a strongly shifted and broadened line $\nu_2^* = 3072$ cm.$^{-1}$ with a markedly diminished intensity. The contour of the line in some solutions (Fig. 2) suggests that the 3072 line arises to the same extent as the 3056 line vanishes; on the other hand, the quasi-continuous change in position and width seems to indicate a more complicated mechanism.

The increase in frequency of the valence vibrations of the C-H bond in the aromatic ring — as Josien showed for monosubstituted benzenes [8] — is caused by a drop in the polarity of the C-H bond (decreased electron density in the carbon atoms) resulting from the introduction of electron-attracting substituents into the ring. An effect similar to this substitution can be caused by the addition of SO_2 to a lone electron pair of pyridine nitrogen. The electric charge distribution for different carbon atoms is not uniform already in the pyridine molecule, and all the more so in the case of the complex. It is supposed that the 3056 line is the result of the superposition of three normal vibrations of C-H with frequencies that are close to each other [9] and the shift of the various components may be different. This might explain the broadening of the lines in the transition from benzene ($\sigma = 7.5$ cm.$^{-1}$ [10]) to pyridine, (11.5 cm.$^{-1}$) and the complex ($\sim$20 cm.$^{-1}$).

The line of the fully symmetric valence vibrations of SO_2, $\nu_1 = 1145.5$ cm.$^{-1}$, undergoes the most characteristic changes. This picture is fully analogous to changes in the O-H band in systems forming hydrogen bonds; but the shifting and broadening of the line is smaller by 1 to 2 orders of magnitude and does not exceed about 25 cm.$^{-1}$. The broad ν_1^* band does not show any distinct structure. Comparison of the sum of the integral intensities of the ν_1 and ν_1^* lines with the 1030 line of pyridine (calculated for a quantity of 1 mole) (see Table II) shows that the change of the line intensity during the formation of the complex is slight, if it changes at all.

A very distinct change in the contour of the band is caused by raising the temperature of the solution. Then there is observed:

(1) a shift of the ν_1^* band as a whole towards the higher frequencies;
(2) a narrowing of the band with a simultaneous increase in the intensity at the maximum such that the integral intensity undergoes practically no change;

(3) the occurrence of an asymmetry in the band, with the maximum distinctly shifted in the direction of the higher frequencies.

Similar changes, though less distinct, also arise with an increase in the pyridine content of the mixture.

In the spectra of solutions the lines of free and bound molecules appear alongside each other. The accuracy of the measurements of the relative intensities is unfortunatelly not very great because of the large differences of intensities and the superposition of the lines on one another. This latter effect occurs particularly strongly for SO_2 lines and renders impossible even an approximate comparison of the intensities. Quantitative conclusions (see below) are therefore based exclusively on the ratios of the intensities of the ν_1, ν_1^*, and ν_{12} lines of pyridine in solutions containing 46.8, 50.9, and 54.9 mole % SO_2.

An increase in the temperature is accompanied, as should be expected, by an increase in the intensities of the lines of free molecules as a result of the thermal dissociation of the complex.

Discussion

A uniform interpretation of the changes of the spectrum of the complex as a result of changes in temperature and intensity seems difficult.

These changes, in contradistinction to changes accompanying the formation of the complex (disappearance of some lines and the appearance of modified frequencies) arise in a continuous manner and cannot be explained by the formation of complexes of a different composition.

Also, interactions of the van-de-Waals type between the molecules of the complex do not completely explain this effect. These interactions are fairly important; the orientation effect plays an especially notable role because of the high dipole moment of the complex ($\mu = 6.2$ D) [3]. The narrowing and increase of frequency of the ν_1^* band of SO_2 in the transition from equimolar solutions to mixtures containing a considerable excess of pyridine can be explained by the fact that in the latter case the molecule of the complex interacts primarily with molecules of pyridine, which have a considerably lower dipole moment [4]. This does not, however, explain why a similar effect is not observed in solutions with an excess of sulphur dioxide. The same concerns changes of the position of the ν_1^* lines of pyridine.

Changes of width and frequency of the ν_1^* band of SO_2 with temperature are in agreement, as regards direction, with the predictions from the theory of Buchheim [11] for the dipole orientation interaction. However, the changes are considerably greater than those resulting from the theory, according to which the drop is inversely proportional to the absolute temperature. In Fig. 5 the dotted lines represent the maximum drop

in the value of the shift $\Delta\nu$ and the width σ which may be assumed on the basis of this theory. Nor does the theory of Buchheim explain the occurrence of an asymmetry in the band at higher temperatures. Most important, however, the theory predicting similar changes of all frequencies completely fails for the ν_1^* and ν_{12} lines of pyridine. The frequency of the ν_1^* lines, higher than the frequency of the lines of the free molecule, decrease with an increase in temperature, and the ν_{12} line, with the same position in the free and bound molecule, undergoes no change with a change in temperature.

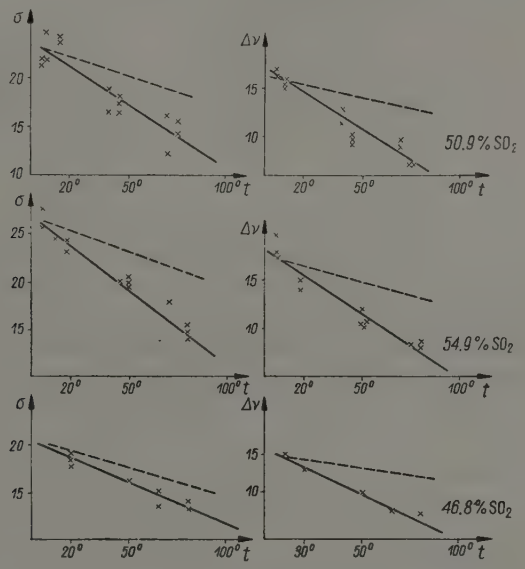

Fig. 5. Variation of the shift $\Delta\nu$ and width σ of the ν_1^* band of SO_2 with temperature for different solutions

The fact that at higher temperature the lines of the bound molecules "converge" as regards the position (and width, in the case of SO_2) to the lines of the free molecules suggests an intra-complex mechanism for the changes, i. e., the weakening at higher temperatures of the intermolecular bond in the complex.

An attempt to interpret these changes as well as the fact of the occurrence of the band in the SO_2 spectrum is the use of a modification of Stepanov's model of the hydrogen bond for the complex under investigation [12].

Comparison of the intensities of the lines of free and bound molecules under these same conditions permits the determination of the dissociation constants of the complex at different temperatures and, in

turn, the heat of formation of the complex and therefore also the approximate value of the energy of the intermolecular bond. Because of the above mentioned errors in measurement of the intensities and because of the limited applicability of the thermodynamic constant of equilibrium, expressed in mol fractions for concentrated solutions these values are only approximate.

The value of the constant of dissociation (instability constant) $K_n = \frac{n_{C_5H_5N} \cdot n_{SO_2}}{n_{C_5H_5N.SO_2}}$ $\sum n = 1$ determined from several measurements for three different solutions lie in the limits:

$$K_{10^\circ} = 0.7 - 1.3 \times 10^{-3}, \quad K_{50^\circ} = 2.1 - 3.8 \times 10^{-3}, \quad K_{80^\circ} = 4.0 - 5.9 \times 10^{-3}.$$

These values differ basically from the values of the constant of dissociation given by Moede for strongly diluted solutions ($K_c \cong 4$) [3].

The thermodynamic relation between the equilibrium constant and the temperature, employed in the form $\Delta H = \frac{\Delta \ln K_n . RT(T+\Delta T)}{\Delta T}$, permits the evaluation of the heat of formation as $\Delta H = 6 \pm 2.5$ kcal./mole, which is comparable to the heat of formation of other complexes of SO_2 with amines determined by other methods [13].

This value is close to the energy of strong hydrogen bonds.

All the results described confirm the view that the specific effect for the hydrogen bond appears also, though in modified form, in other systems of the donor-acceptor type, of which the hydrogen bond is a special case.

The author would like to thank Professor A. Jabłoński for numerous discussions and valuable comments.

INSTITUTE OF PHYSICS, POLISH ACADEMY OF SCIENCES

REFERENCES

[1] J. Collin, Bull. Soc. Roy. Sci. Liège **23** (1954), 395.
[2] G. W. Lewis, J. Bigeleisen, J. Amer. Chem. Soc. **65** (1943), 1144.
[3] J. Moede, C. Curran, ibid. **71** (1949), 852.
[4] A. Tramer, *Raman spectra of sulphur dioxide solutions*, Bull. Acad. Polon. Sci. Cl. III, **4** (1956), 355.
[5] B. I. Malishev, Izv. A. N. SSSR **16** (1950), 6.
[6] P. A. Bazhulin et al., ibid. **18** (1954), 678.
[7] R. Mierzecki, Curr. Sci. **25** (1956), 200.
[8] M. L. Josien, J. M. Lebas, C. R. Acad. Sci. **240** (1955), 181.
[9] L. Corrsin, B. J. Fax, R. C. Lord, J. Chem. Phys. **21** (1953), 1170.
[10] P. A. Bazhulin, A. V. Rakov, D. A. N. SSSR **105** (1955), 54.
[11] W. Buchheim, Phys. Zs. **36** (1935), 634.
[12] A. Tramer, *Investigation of the pyridine-sulphur dioxide system by Raman spectroscopy, III*, Bull. Acad. Polon. Sci., Cl. III, in this issue p. 509.
[13] A. E. Hill, T. B. Fitzgerald, J. Amer. Chem. Soc. **57** (1935), 250.

BULLETIN DE L'ACADÉMIE
POLONAISE DES SCIENCES
Cl. III — Vol. V, No. 5, 1957

EXPERIMENTAL PHYSICS

Investigation of the Pyridine-Sulphur Dioxide System by Raman Spectroscopy. III. Application of the Hydrogen Bond Model

by

A. TRAMER

Presented by A. JABŁOŃSKI on February 19, 1957

The similarity between the changes in the vibration spectra in the pyridine-sulphur dioxide system and the phenomena known from the spectroscopy of the hydrogen bond, as well as the fact that the nature of the chemical intermolecular bonds in both cases is quite the similar, suggests that the hydrogen bond model of Stepanov [1] may be used to investigate the system. This model, however, requires a rather basic modification. Above all, the assumption of the predissociation character of the excited vibration level and other consequences resulting from it cannot be used in our case.

We shall examine the relation between the energy of the two-molecule system of $C_5H_5N + SO_2$ and the intermolecular distance. The potential curve has a minimum corresponding to the complex with a binding energy of $\sim$6.0 kcal./mole, that is, $\sim$1900 cm.$^{-1}$ [2], the distance R_e doubtlessly being relatively large. To the six additional degrees of freedom of the complex there correspond a valence vibration ν_m of the N..S bond with a frequency of the order of 100 cm.$^{-1}$, that is, the order of the typical lattice frequencies in molecular crystals, and five deformation vibrations. The deformation vibrations correspond to the torsional oscillations and hindered rotations of the components of the complex about the intermolecular bond; they may therefore be ascribed to frequencies not much higher than the frequencies of rotation. The superposition of these vibrations on the valence vibrations ν_m would therefore lead to a considerable increase in the breadth of the ν_m level.

The shape of the potential curve of the $C_5H_5N.SO_2^{\nu_1}$ system (where by $SO_2^{\nu_1}$ we denote the sulphur dioxide molecule in which symmetrical valence vibrations are excited) should differ only slightly from the curve

of the fundamental state. It may be expected that in the excited state, as a result of the anharmonicity of the vibrations of the S—O bond, the polarity of this bond increases, which, in turn, should be reflected by a very small increase in the intermolecular interaction. The curve of the excited state would thus possess a somewhat deeper minimum. This hypothesis is in agreement with the observed lowering of the ν_1 vibration frequency of SO_2; to provide agreement with the experiment we assume that the energy difference is about 20 cm.$^{-1}$, while the total depth of the minimum is about 2000 cm.$^{-1}$. It should be expected that

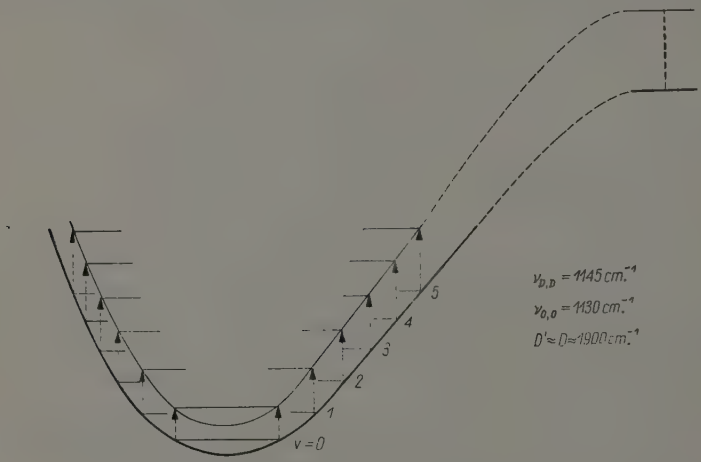

Fig. 1. Potential curves of the $C_5H_5N + SO_2$ system

the differences in the shape of the curves occur principally in the vicinity of the minimum, and that the shapes of the curves at a considerable distance from it approach each other until they entirely coincide for sufficiently high values of R. Because of the relatively flat shape of the curves, the slight change in the value of R_e may be neglected. An approximate picture of the potential curves is shown in Fig. 1, the differences in the shape of the curves being considerably exaggerated.

The observed vibrational transition of the SO_2 molecule bound in the complex corresponds to the superposition of the transition lines between the different v_m levels of both states. The transitions with $v'_m - v''_m \neq 0$ can be neglected on the basis of the Frank-Condon rule, because of the relatively flat shape of the curves, only the $0 \rightarrow 0$, $1 \rightarrow 1$, etc. transitions being taken into account. Under the assumption that the width of the levels is sufficiently large (which seems justified because of the superposition of the torsional oscillation and hindered rotations) the resultant structure of the band is completely diffuse.

In accordance with the assumed shape of the potential curves, the series of frequencies corresponding to the successive transitions with $v''_m = 0, 1, 2, \ldots$ is rapidly convergent. By way of simplification, we assume that the probability of the transition is the same in all cases. This assumption does not have any basic justification and the differences of probability of the transition may seriously affect the band envelope. Because of the simplification which has been made, the relative intensities of the individual lines depend only on the population of the individual levels of the fundamental state as determined by the Boltzmann factor.

Shown in Fig. 2 as an illustration is the resultant envelope of the band at temperatures of 10° and 80°C. obtained by superimposing the lines, the states $v''_m \leqslant 7$ being taken into account. The parameters of the

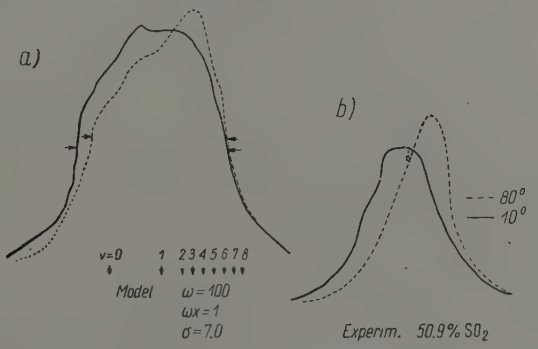

Fig. 2. Calculated and observed envelopes of the ν_1^* band of SO_2

potential curves and the width of the lines of the components were chosen arbitrarily; it was assumed that the contour of the lines of the components was Gaussian. The approximate normalisation of the resultant envelope was carried out by using the vibrational partition function, the states with $v''_m \leqslant 12$ being taken into account.

Comparison with the experimental envelope of the ν_1^* band of SO_2 shows a qualitative similarity between the shapes of the bands and their temperature dependence; at higher temperatures there takes place a shifting of the band towards the higher frequencies, an increase in the asymmetry and a shifting of the maximum, a decrease in the half-width and, at the same time, an increase in the intensity of the maximum.

From the model adopted, it further results that the maximum of the band shifts towards the lower frequencies, but with a simultaneous narrowing of the band at a considerable lowering of the temperature as a result of a weaker population of the higher v''_m levels. Perhaps it should also be expected that in face of the changes of population of the levels of the intermolecular deformation vibrations, there occurs a nar-

rowing of the individual lines of the components and the splitting of the band structure. An experimental check of these suggestions for the $C_5H_5N.SO_2$ complex does not, however, seem possible because of the high melting temperature.

The explanation of the changes of the parameters of the ν_1^* lines of the bound pyridine molecules by means of this same model seems, in principle, possible; however, another shape of the potential curve is assumed for the excited level $C_5H_5N^{\nu_1}.SO$. Experimental observations disclose an increase of the ν_1 frequency of pyridine during the formation of the complex; the minimum of the energy in the excited state would therefore be flatter. Hence it should be assumed that the excitation of the ν_1 vibrations (ring pulsation) of pyridine weakens the intermolecular binding. This hypothesis is not in contradiction with our knowledge of the electron structure of pyridine. Such a curve shape would explain the lowering of the frequency of the ν_1^* lines at a higher temperature. Too scanty experimental data do not permit the suggestion of more far-going hypotheses *).

The model does not explain the changes of frequency and line width by changes in the composition of the solution.

No doubt, besides the discussed intra-complex effects, a considerable role is also played by the mutual interactions of the complex molecules.

A check of the suitablity of the model is provided by comparison of the predictions of effects on its basis with the spectra of other complexes of the donor-acceptor type. Investigation of the appropriate systems is in progress.

The author would like to thank Professor A. Jabłoński for his valuable discussions and critical remarks.

INSTITUTE OF PHYSICS, POLISH ACADEMY OF SCIENCES

REFERENCES

[1] B. L. Stepanov, Zh. eksp. theor. fiz. **15** (1945), 435.

[2] A. Tramer, *Investigation of the pyridine-sulphur dioxide system by Raman spectroscopy. II. Investigation of the contours of the lines and their dependence on temperature*, Bull. Acad. Polon. Sci., Cl. III, in this issue p. 501.

[3] G. S. Kastha, Ind. J. Phys. **39** (1956), 519.

*) Quite recently Kastha [3] has observed too the increase of the ν_1^* frequency in partially analogical pyridine-alcohol complex, when cooled to the liquid air temperature. No information concerning the line width is given.

BULLETIN DE L'ACADÉMIE
POLONAISE DES SCIENCES
Cl. III — Vol. V, No. 5, 1957

Yield of Photoluminescence of Solutions

by

A. JABŁOŃSKI

Presented on March 6, 1957

Several theories on quenching the photoluminescence of solutions were put forward by different writers, who obtained various expressions for the yield of photoluminescence as a function of the concentration of quenchers *). A simplified version of the present writer's expression [3] is obtained here by the use of a general result established below, concerning solutions containing centres of different kind.

Consider a solution containing n different kinds of luminescent centres (n groups of centres). Let A be the energy absorbed by all groups together per unit time, and let $A_i = P_i A$ be that absorbed by centres of group i, P_i thus denoting the distribution of the absorbed energy between different groups fulfilling the condition:

$$\sum_{i=1}^{n} P_i = 1. \tag{1}$$

If the luminescent energy emitted per unit time by centres of the group i is J_i, then the yield of that group is

$$\eta_i = \frac{J_i}{A_i}. \tag{2}$$

The yield of the whole solution is obviously

$$\eta = \frac{\sum_{i=1}^{n} J_i}{A}. \tag{3}$$

*) Papers published before 1949 are discussed in Pringsheim's well known monograph [4]. Since 1949 further theories appeared, viz. that of Förster [2], and that of the present writer [3]. Förster's paper was unfortunately not quoted in [3], since it was neither accessible, nor even known to the author before the end of 1956.

We shall now prove a result, which may be stated as follows: *If in a luminescent solution the distribution of absorbed energy between different groups of centres is given by* $P_i (i = 1, 2, ..., n)$, *fulfilling the condition* (1), *and* η_i *are the yields of luminescence of particular groups, then the yield of the whole solution is*

$$\eta = \sum_{i=1}^{n} P_i \eta_i , \tag{4}$$

since, by means of Eqs. (2) and (3), we have

$$\eta = \sum_{i=1}^{n} \frac{J_i}{A} = \sum_{i=1}^{n} \frac{P_i J_i}{P_i A} = \sum_{i=1}^{n} P_i \frac{J_i}{A_i} = \sum_{i=1}^{n} P_i \eta_i .$$

If the probability of excitation of a centre per unit time is the same for centres of all groups, then P_i is simply the relative abundance of unexcited centres belonging to the group i in a given solution.

We now consider a solution in which quenchers are present, and assume that the excitation probability of a luminescent molecule is not influenced by the proximity of quenchers, thus being the same for centres of all groups.

For the simplified model of the centre [3], consisting of a luminescent molecule with an active sphere, in which there may be $i = 0, 1, 2, ...$ quenchers present, the Smoluchowski distribution (5), (6)

$$P_i = e^{-\nu} \frac{\nu^i}{i!} \qquad (i = 0, 1, 2, ...) \tag{5}$$

may be applied, where $\nu = Nv$, v cm^3. being the volume of the active sphere and N cm^{-3}. the concentration of quenchers in the solution. Eq. (4) thus becomes:

$$\eta = e^{-\nu} \sum_{i}^{\infty} \frac{\nu^i}{i!} \eta_i . \tag{6}$$

For the case of optical excitation of a solution, in which the molar absorption coefficient is the same for centres of all groups, and, besides, in which the influence of diffusion on the yield may be neglected, η_i may be assumed to be [2]:

$$\eta_i = \frac{Q\gamma}{\gamma + W_0 + W_i} = \frac{\eta_0}{1 + W_i \tau_0} , \tag{7}$$

γ denoting the probability per unit time of electronic transition connected with the emission of photoluminescence, and W_0 that of inner quenching, W_i is the probability per unit time of external quenching of centres of group i, and Q the yield which would be observed, if no

quenching would occur, except that due to the energy loss occurring in the moment of excitation. $\tau_0 = \frac{1}{\gamma + W_0}$ is the duration of photoluminescence for $i = 0$.

In our simplified model of centre the volume of the active sphere is to a certain extent arbitrary [3] – it depends on the value adopted for W_i*). If we assume that $W_i = iW_1$ (W_i proportional to the number of quenchers in the centre), and (arbitrarily!) $W_1 = \frac{1}{\tau_0}$ (probability of quenching by one quencher equal to the reciprocal value of τ_0), then Eq. (6) becomes

$$\frac{\eta}{\eta_0} = e^{-\nu} \sum_{i=0}^{\infty} \frac{\nu^i}{(1+i)!}. \tag{8}$$

In spite of the arbitrariness of the above assumptions Eq. (8) agrees surprisingly well with experimental curves, published by different writers. It is worth stressing that there is in (8) only one constant to be fitted to the experimental results, viz. the volume $v = \frac{\nu}{N}$ of the active sphere.

Let us now compare expression (8) with the available experimental results. The most suitable for this purpose seem to be the results of measurements obtained by Förster [2] on quenching fluorescence of trypaflavine in methanol by rhodamine *B*, and those by Bowen and Brocklehurst [1] on quenching fluorescence of 9-phenyl anthracene in benzene by 9:10-dichloroanthracene. The experimental points marked on the curves published by the above writers were carefully measured and reproduced in Fig. 1, together with the theoretical points, calculated by means of Eq. (8). The abscissa of our graph is chosen to be $\log \nu = \log N + \log v$, differing merely by an additive constant $\log v$ from that used by Förster. The ordinate is $\frac{\eta}{\eta_0}$ as in Förster's paper. $\frac{\eta}{\eta_0}$ calculated from the results of Bowen and Brocklehurst, as well as those given by Förster, was first drawn as function of the logarithm of concentration of quenchers. These curves had to be shifted along the abscissa-axis ($\log \nu$-axis) of our graph to obtain their best fit to the theoretical curve. As already pointed out, the logarithm of concentration differs by an additive constant from $\log \nu$, this constant being the logarithm of the volume of the active sphere v, which thus can be evaluated for every particular case on the ground of experimental results. For trypaflavine in methanol,

*) The refined model of a luminescent centre [3] does not allow such arbitrariness, and is believed to describe adequately not only the yield as a function of concentration of quenchers, but also the decay of photoluminescence (intensity of photoluminescence as a function of the decay time).

quenched by rhodamine B, there results from Förster's experimental data $v = 2 \cdot 10^{-18}$ cm.^{3}, the radius of this sphere ("the range of quenching") ~ 78 Å. This estimate is made without taking into account the influence of the diffusion of luminescent molecules and that of quenchers (as it is also done in Förster's paper). Let Förster's estimate be quoted here for comparison. According to him the experimental value of the distance of a rhodamine B molecule from the excited trypaflavine molecule, for which the quenching probability is just equal to the tran-

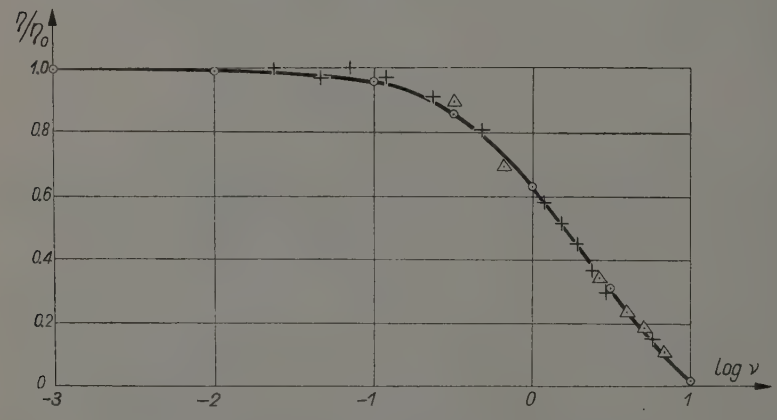

Fig. 1. Relative yield $\frac{\eta}{\eta_0}$ versus $\log \nu = \log N + \log v$ (N the concentration of quenchers, v the volume of the active sphere)

⊙ points calculated by means of Eq. (8)
\+ experimental points for trypaflavine + rhodamine B in methanol (Förster)
△ experimental points for 9-phenyl anthracene + 9:10-dichloro anthracene in benzene (Bowen and Brocklehurst)

sition probability of fluorescence emission, is 58 Å, the same distance estimated on ground of certain theoretical considerations is 68 Å.

Förster's experimental points fit very well to the theoretical curve, following from his own theory [2]:

$$\frac{\eta}{\eta_0} = 1 - \sqrt{\pi}\left(\frac{N}{N_0}\right) e^{(N/N_0)^2}\left[1 - \Phi\left(\frac{N}{N_0}\right)\right], \tag{9}$$

where

$$\Phi\left(\frac{N}{N_0}\right) = \frac{2}{\sqrt{\pi}} \int_{N/N_0}^{\infty} e^{-x^2} dx .$$

The slope of this curve is very similar to that of Eq. (4), except, perhaps, in the region of highest concentrations of quenchers, where, however, there are no experimental points.

Eq. (9) is derived on the following assumptions. The probability of quenching (excitation energy transfer to a quencher) is assumed to be $\frac{1}{\tau}\left(\frac{R_0}{R}\right)^6$, where τ is the mean life of the excited state of luminescent molecules in a solution with no quenchers, and R_0 the distance, for which the quenching probability is just equal to $1/\tau$. If in the volume $V=\frac{4}{3}\pi R_g^3$ there are N quenchers, the decay of fluorescence of those luminescent molecules, from which the distance of quenchers are $R_1, R_2, \ldots R_n$, is given by

$$J(t)=J_0 \exp\left[-\frac{t}{\tau}-\frac{t}{\tau}\sum_{k=1}^{N}\left(\frac{R_0}{R_k}\right)^6\right], \tag{10}$$

where t is the decay time.

Assuming that the probability distribution of R is given by

$$w(R)\,dR=\frac{4\pi R^2 dR}{V}. \tag{11}$$

Förster obtains the following expression for the decay averaged over different configurations of quenchers

$$\overline{J(t)}\approx J_0 \exp\left[-\frac{t}{\tau}-\frac{\sqrt{\pi}\,N R_0^3}{R_g^3}\sqrt{\frac{t}{\tau}}\right], \tag{12}$$

By means of Eq. (12) the relative yield

$$\frac{\eta}{\eta_0}=\frac{1}{\tau J_0}\int_0^\infty \overline{J(t)}\,dt \tag{13}$$

is approximately calculated and the expression (9) obtained.

Eqs. (8) and (9) are derived on the ground of very different assumptions, nevertheless, both expressions describe equally well the experimental results so far available, and for the time being there seems to be no need for better approximations. A better approximation may be obtained by means of a more refined model of a luminescent centre, as e. g. described in an earlier paper [3] of the present writer.

PHYSICS DEPARTMENT, NICHOLAS COPERNICUS UNIVERSITY, TORUŃ

REFERENCES

[1] E. J. Bowen and B. Brocklehurst, Trans. Farad. Soc. **49** (1953), 1131.
[2] T. Förster, Z. f. Naturforsch. **4a** (1949), 321.
[3] A. Jabłoński, Acta Phys. Pol. **13** (1954), 175.
[4] P. Pringsheim, *Fluorescence and Phosphorescence*, Interscience Publishers, Inc. New York (1949).
[5] M. Smoluchowski, Boltzmann-Festschrift (1904), 626.
[6] — Bull. Intern. Acad. Pol. (1907), 1057.

BULLETIN DE L'ACADÉMIE
POLONAISE DES SCIENCES
Cl. III — Vol. V, No. 5, 1957

The Effect of Cathodic Hydrogen on the Magnetic Properties of Chrome-Nickel Austenitic Steel

by

L. KOZŁOWSKI

Presented by M. ŚMIAŁOWSKI on February 12, 1957

An analysis made by Krupkowski and Śmiałowski of the deformations of soft steel samples subjected to the action of cathodic polarisation [1] showed that in rods with a radius of from 0.8 to 2.4 mm. the mean stress related to the active layer changes within the limits of from 18 to 2 kG/mm².

For low carbon steel rods, silicon steel and nickel sheets and strips, the author [2] found that the coercive force increases with cathodic charging. These changes also indicate that the cathodic hydrogen creates inside the metal local variable stresses of large amplitude.

Eisenkolb and Ehrlich [3] investigated the process of the penetration of cathodic hydrogen into austenitic steel containing 16—17.4 per cent Cr and 7.7—8.5 per cent Ni. These investigations concerned the quantity of absorbed hydrogen in the cathodic charging process and its influence on the mechanical brittleness of the steel. Eisenkolb and Ehrlich showed that in the cathodic charging process a gram of austenitic steel dissolves more than twice the amount of hydrogen dissolved by low-carbon steel. At the same time, there occurred a very small increase in brittleness (the number of bends decreases from 35 to 28). Metallographic investigations showed that hydrogen does not cause in austenitic steel any cracks, microfractures or other damages.

In the course of 24 hours after electrolysis about 90 per cent of the hydrogen escaped from thin sheets at room temperature; at a temperature of 140°C. this time was reduced to 2 hours. On the basis of these investigations the authors concluded that in austenitic steels, the hydrogen penetrates only into a thin surface layer in which a large drop in concentration occurs.

The results of the work of S. Nosireva [4] on the influence of the structure on the diffusion of hydrogen in steel also showed that austenitic steel dissolves a greater quantity of hydrogen than armco iron or

carbon steel. At the same time it was found that the diffusion of the hydrogen through a sheet 0.5 mm. thick takes place very slowly in austenitic steel in comparison to carbon or transformer steel. The atomic hydrogen therefore penetrates with relative ease in a regular body-centered α-Fe lattice, but with difficulty in a regular face-centered lattice.

It thus seemed worth-while to investigate effect of cathodic polarisation on the intrinsic saturation induction of austenitic steel. Tests were made with samples in the form of wire 3 mm. in diameter and strip 0.6 and 0.3 mm. in thickness. The chemical composition of the steel investigated is given in Table 1.

TABLE I

Chemical composition of austenitic steel in %

	C	Mn	Si	P	S	Cr	Ni
rod	0.08	0.77	0.49	0.03	0.023	16.85	9.13
strip	0.25	—	—	—	—	16.80	9.50

Samples in the same state as delivered were annealed at a temperature of 1150°C. for 15 minutes and quenched in water. To avoid excessive oxidation the samples were wrapped in a thin iron sheet. After this treatment the surface layer of the samples contained a considerable amount of the ferromagnetic phase. This was removed with emery paper and by anodic treatment. Wires 100 mm. long and strips $0.6 \times 12 \times 100$ mm^3. and $0.3 \times 12 \times 100$ mm^3. were saturated with cathodic hydrogen in a normal solution of H_2SO_4 with an addition of 0.25 g. As_2O_3 per litre, the current density being 0.1 A/cm^2. and the temperature 25°C.

Cathodic charged samples were placed in the gap of an electromagnet in a field of 4000 oersteds. The central part of the sample was surrounded by a measuring coil of 2000 turns of copper wire connected to a ballistic galvanometer of high sensitivity. From the deflection of the galvanometer resulting from the removal of the sample from the field, the value of 4πIs was calculated. The sensitivity of the measurements was ± 1 gauss.

Numerous tests showed that for austenitic steel both in the wire sample and in the case of the strip the value 4πIs changed only slightly. A typical curve showing the changes with the increase in the electrolysis time is given in Fig. 1. Although the values of 4πIs before and after cathodic charging depend on the state of surface oxidation and the rate of cooling, the curve form is always similar. It is worth-while noting that the samples heated at 1150°C. in an atmosphere of hydrogen had a low value of 4πIs; this value showed practically no change during a two-hour cathodic charging.

It was shown that after the electrolysis was interrupted, a large amount of hydrogen was given off, and, simultaneously, the value of $4\pi Is$ decreased according to Fig. 2. During a period of about 30 min.

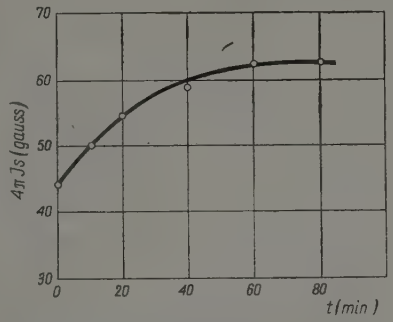

Fig. 1. Variation of $4\pi Is$ of austenitic steels with the time of cathodic charging

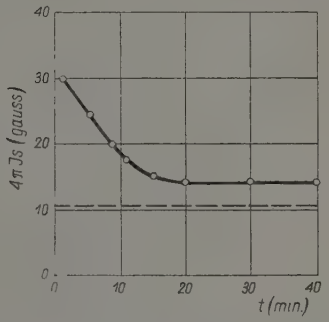

Fig. 2. Dependence of $4\pi Is$ of charged samples of austenitic steel on the time after electrolysis; – – – $4\pi Is$ before electrolysis

the intrinsic saturation induction reached a steady value higher than the value immediately before the cathodic charging.

By means of anodic treatment it was found that the change in induction occurs in the surface layers to a thickness of the order of several microns.

Some charged samples showed a greater constancy of the value of $4\pi Is$. In this case the surface layer of the sample was anodic treated

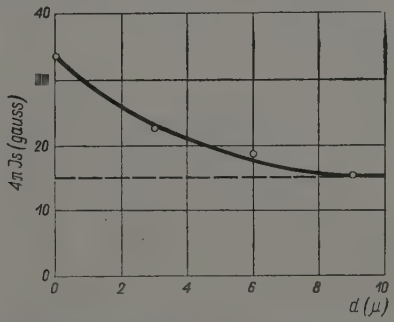

Fig. 3. $4\pi Is$ of cathodic charged samples of austenitic steel as a function of the thickness of the removed surface layer; – – – – $4\pi Is$ before electrolysis

in steps and the value of $4\pi Is$ was measured each time. Fig. 3 shows the changes in $4\pi Is$ as a function of the thickness of the removed surface layer.

The results obtained seem to confirm the conclusions of Eisenkolb and Ehrlich that cathodic hydrogen in austenitic steels penetrates ra-

pidly only through a thin surface layer. It is difficult, however, on the basis of these results to state that this layer has a thickness of the order of several microns. The removal of a layer of this thickness restores the initial magnetic properties of the steel, but perhaps this layer merely obstructs the free penetration of hydrogen from inside the sample to the outside.

When it is assumed, however, that the change in the intrinsic saturation induction occurs only in this thin layer and that the values measured ballistically give a mean for the entire sample cross-section, then it turns out that the value $4\pi I_s$ calculated for this thin layer is very high. It varies between 1100 and 4400 gausses after cathodic charging and between 15 and 110 gausses before charging. The same changes in entire strip are obtained in austenitic steels after 35–50 per cent cold working. Within a layer several microns thick there thus occurs a rapid change in $4\pi I_s$ of from several thousand gausses to 10–100 gausses. This last hypothesis is supported also by a fact observed during the anodic treatment of a layer hardened by cleaning with emery. The mean values of $4\pi I_s$ of cleaned strips were increased by about 40 gausses and the thicknesses of the cold-worked layers were about 5 μ. The actual intrinsic induction in those layers was therefore about 2000 gausses.

INSTITUTE OF PHYSICAL CHEMISTRY, POLISH ACADEMY OF SCIENCES

REFERENCES

[1] A. Krupkowski, M. Śmiałowski, Arch. Hutnictwa, **1** (1956), 101.
[2] L. Kozłowski, Arch. Hutnictwa (in press).
[3] F. Eisenkolb, G. Ehrlich, Arch. f. d. Eisenhüttenwesen, **25** (1954), 187.
[4] S. Nosirêva, Stal, **6** (1948), 542.

BULLETIN DE L'ACADÉMIE
POLONAISE DES SCIENCES
Cl. III — Vol. V, No. 5, 1957

CHEMISTRY

On the Preparation of Pure Hydrofluoric Acid

by

A. OSTASZYŃSKI and Z. PIASEK

Presented by T. URBAŃSKI on February 11, 1957

Technical hydrofluoric acid is usually made by acting with sulphuric acid on calcium fluoride.

Technical fluorspar contains aluminium, calcite, quartz, calcium sulphate, sulphides, as well as small amounts of pyrites, galena and chalcopyrite (even in purified state, fluorspar contains up to 1 per cent of SiO_2 and 0.05 S). Consequently, the hydrofluoric acid obtained is usually contaminated with silicofluoric acid, sulphuric acid, SO_2 and S; depending on the vessels used for the reaction, impurities include also iron, lead, etc.

Volatile impurities of hydrofluoric acid — SiF_4, SO_2, H_2S — are most difficult to eliminate.

In purification of hydrofluoric acid, various methods are employed. I. G. Farbenindustrie A. G. [1], Duzzi [2], Verein für Chemische und Metallurgische Produktion [3], and others [4], use the method of distillation. Howard [5], Chemische Werke Albert und Hesse [6], Tartakowski [7], Jatlow [8], Kachulkov [9], Müller [10], Söll [11], the Meyerhofer Firm [12], Bachman [13], Catlin [14], Dixon and Scott [15], precipitate SiF_4 in the form of hydrosilicofluoric acid salts of alkaline metals. Preisman [16], and Jones [17], on the other hand, use prior purification of calcium fluoride, whereas Allied Chemical Corporation [18] and Pensylvania Salt Manufacturing Co. [19] obtain pure hydrofluoric acid by decomposition of fluorosulphonic acid.

Sulphur dioxide is removed by distillation [20] or sometimes by contacting with olefines [21] or with silver and cobalt fluorides [22].

The fundamental inadequacy of distillation methods is the fact that the silicofluoric acid content cannot be brought to less than 0.1 per cent. Purification of hydrofluoric acid by decomposition of fluorosulphonic acid, or by passing HF through concentrated H_2SO_4, usually causes contamination of the acid with sulphuric acid which resists complete elimination.

Precipitation of hydrosilicofluoric acid with salts of alkaline metals yields in some cases better results, but the technical process is more complicated, particularly since decomposition of fluorsilicates requires high temperatures. It has also to be considered, that technical (40 per cent) hydrofluoric acid causes notable corrosion of the distillation apparatus and, consequently, the acid is as a rule contaminated with iron, lead, copper, etc.

Distillation from platinum vessels, used in laboratory practice, is too expensive to be applied on a technical scale.

The purpose of this work was to develop a technical method of producing 40 per cent hydrofluoric acid of a high degree of purity.

While the non-volatile fluorides, those of iron, lead, cadmium and copper, may be removed by distillation, the volatile fluorides of boron, silicium or sulphur required a simple method of precipitation in the form of insoluble salts of hydrosilicofluoric, sulphuric and other acids.

Of the salts of hydrofluorosilicic acid, potassium fluorosilicate is but sparingly soluble in acid; however, it is difficult to be filtered off, and is not suitable for precipitation of sulphuric acid. Consequently, attention was turned to barium salt which is the least soluble of all fluorosilicates, as is shown by solubility data quoted by Carter [23]. According to the latter, solubility of $BaSiF_6$, at a temperature between 0 and 100°C., is on the average ten times less than that of potassium fluorosilicate. In addition, barium salt has the advantage of precipitating also sulphuric acid and barium sulphate occludes other compounds thus favouring purification.

We used in our experiments technical carbonate of barium, which was added to hydrofluoric acid in stoichiometrical quantities according to the contents of H_2SO_4 and H_2SiF_6. The amounts added were between 10 and 15 per cent in excess of the calculated proportion. Precipitation was improved by stirring for half an hour. The hydrofluoric acid was distilled from a copper vessel. Results of distillation from acid resistant steel vessels proved negative. Since copper proved less resistant to the acid than was expected, we used a silver pipe in the condenser with very good result.

Distillation of the acid began at a temperature below 110°C., but most of the acid passed between 111° and 112°C. Most of the experiments were carried out with technical, 45—47 per cent, acid, but also 30 and 53 per cent acid was distilled. The yield of pure acid was 92 per cent of the starting product.

The purity of the end product was as follows: Si $<2\gamma$, H_2SO_4, SO_2, S, B — absent, Cl $<100\,\gamma$. Dry residue was 0.002 per cent.

In order to determine the degree in which the method eliminates the presence of boron, we distilled hydrofluoric acid to which a quantity of boric acid had been added. Boron could not be detected in the distil-

late, but it was found in the dry residue of barium salts in the still, after distillation of the acid. Probably a barium salt of borofluoric acid is produced *).

We also investigated the efficiency of the method with regard to elimination from the acid of sulphides, SO_2, and chlorides. For this purpose, we added to the technical acid chlorides, sulphites and sulphides. The latter two could not be detected in the distillate, but chlorides were found to be present in small amounts (0.022 per cent).

As was shown by results of analyses, purification of hydrofluoric acid by distillation from over barium carbonate represents a simple and inexpensive method of obtaining hydrofluoric acid of a high degree of purity.

Instead of barium carbonate also barium hydroxide may be used. In order to remove chlorides altogether, small amounts of silver carbonate may be added to hydrofluoric acid prior to distillation.

The experimental part will be described in detail in Roczniki Chemii.

Patent rights relating to the method have been secured by the Institute of Nuclear Research [24] which sponsored the research work.

DEPARTMENT OF ORGANIC TECHNOLOGY, II, WARSAW TECHNICAL UNIVERSITY
INSTITUTE OF ORGANIC SYNTHESIS, POLISH ACADEMY OF SCIENCES

REFERENCES

[1] I. G. Farbenindustrie A. G., German Patents 558,132 (1930), 580.633 (1933), 581,714 (1933); US Patents 1,903,408 (1933), 1,851,652 (1932); French Patents 708,139 (1930), 741,966, (1933).

[2] A. Duzzi, Italian Patent 465.066 (1951).

[3] Verein für Chemische und Metallurgische Production, British Patent 289,383 (1927).

[4] N. S. Nikolajev and N. A. Ivanov, Zhurnal Khemicheskoi Promyshlennosti **13** (1936), 606.

[5] H. Howard, British Patent 186,606 (1922); German Patent 442,827.

[6] Chemische Werke vorm H., E. Albert u. E. Hesse. French Patent 698,921 (1930).

[7] V. J. Tartakowski, Mineral Suire **6** (1931), 853.

[8] V. S. Yatlov, Russian Patent 30,268 (1933); I. G. Ryss, V. S. Yatlov, Russian Patent 36,392 (1934).

[9] A. N. Kachulkov, Trans. Sci. Fertilizers and Insectofungicides USSR No. 123 (1935), 174.

[10] R. Müller, Yugoslav Patent 6,917 (1930).

[11] J. Söll, I. G. Farbenind. A. G., German Patent 580,062 (1933).

[12] M. Buchner, British Patent 234,852 and 255,464 (1924); M. Buchner, Fr. Meyerhofer Firm, U. S. Patent 1,701,225 (1929).

[13] W. Bachman, Austrian Patent 117,010 (1930).

[14] R. M. Catlin, U. S. Patent 1,293,703 (1919).

*) Further quantitative research relating to precipitation of boron in barium salts is in progress.

[15] P. Dixon, T. R. Scott, Australia, Council Sci. Ind. Research, Bull. No. 214 (1947), 5.

[16] L. Preisman, General Chemical Co. U. S. Patent 2,296,118 (1943).

[17] A. G. Jones, Imperial Chemical Ind. Ltd., British Patent 620,745 (1949).

[18] A. C. Hopkins, Jr. R. M. Stephenson, W. E. Watson, Allied Chemical and Dye Corp., U. S. Patent 2,456,509 (1948).

[19] W. F. Mitchell, J. A. G. Mackay, Pensylvania Salt. Manuf. Co., U. S. Patent 2,702,233 (1955).

[20] H. C. Kremers, I. E. Johnson, Harshaw Chemical Co., U. S. Patent 2,459,438 (1949).

[21] R. C. Cole, Philips Petroleum Co., U. S. Patent 2,376,328 (1945) and 2,415,003 (1947).

[22] W. J. Shenk, Jr. G. R. Pellon, Harshaw Chemical Co., U. S. Patent. 2,526,585 (1950).

[23] R. H. Carter, Ind. Eng. Chem. 22 (1930), 886.

[24] Polish Patent No. 39,945.

BULLETIN DE L'ACADÉMIE
POLONAISE DES SCIENCES
Cl. III — Vol. V, No. 5, 1957

CHIMIE

L'autorédoxydation du métabisulfite de sodium ($Na_2S_2O_5$) en phase solide

par

T. MIŁOBĘDZKI et R. RUDNICKI

Présenté par T. MIŁOBĘDZKI le 19 Février 1957

Dans le cadre des recherches des sources d'origine de l'acide hypophosporique ($H_4P_2O_6$) ainsi que des hypophosphates, recherches entreprises par l'Institut de Chimie Inorganique de l'École Polytechnique à Varsovie de par l'initiative de T. Miłobędzki [1], [2], une expérience d'autorédoxydation à sec du phosphite bisodique fut réalisée par Mme. B. Fulde-Krukowska [3] et du hypophosphite monosodique — par K. Wieczffiński [4]. Cette expérience démontra que l'effet de la désélectronisation du P^{+3} dans le premier cas et du P^{+1} dans le deuxième, est dû à l'action des protons qui font partie de ces compositions et qui, en s'enrichissant chacun d'un électron, se transforment en hydrogène libre qui s'évapore sous forme de gaz H_2:

$$2\overset{+1}{Na_2}\overset{+3}{H}PO_3 = H_2^0 + \overset{+5}{Na_3}PO_4 + \overset{+3}{Na}PO_2,$$

$$\overset{+1}{Na}H_2PO_2 = H_2^0 + \overset{+3}{Na}PO_2$$

Les réactions à sec, au cours desquelles l'hydrogène libre se forme et se dégage, sont connues de longue date, mais la nouveauté consiste dans la constatation que c'est le proton qui joue dans ces transformations le rôle de facteur oxydant, en se desoxydant lui-même de H^+ en H^0 et servant par cela-même le procès d'oxydation; cette nouvelle constatation n'avait pas trouvé jusqu'alors son propre terme généralisant dans le domaine de la chimie.

Cette étude [5] devait avoir pour objet initialement le sulfite monosodique $NaHSO_3$ — analogue au Na_2HPO_3 dont la structure et le caractère de similitude aux phosphites et aux nitrites fut le sujet des travaux antérieurs du premier des auteurs de ce compte-rendu [6], [7]. Pourtant, après avoir revu la littérature concernant ce sujet, nous avons dû nous rendre à l'évidence [8], [9] que contrairement à ce que citent

certains manuels de chimie inorganique et même en discordance avec les tarifs des produits chimiques, ce composé n'existe point à l'état cristallique et l'on considère, par erreur, comme tel un tout autre produit, notamment le métabisulfite de sodium (Na_2S_2O) qui se transforme en $NaHSO_3$ du moment seulement où il est dissous dans l'eau:

$$Na_2S_2O_5 + H_2O = 2NaHSO_3.$$

Comme il ne nous a pas été possible d'analyser efficacement les transformations à sec du sulfite monosodique, nous avons entrepris dans le travail retracé ici l'étude de la décomposition du bisulfite sodique pur, afin de pouvoir par la suite entreprendre l'étude de la décomposition du métabisulfite de sodium en présence du NaOH à l'état solide.

G. A. Barbaglia et P. Gucci [10] firent l'observation que le sulfite monosodique à l'état de solution saturée se transforme, dans une éprouvette hérmétiquement close et chauffée à 150°C, en sulfate de sodium, en soufre et en acide sulfurique.

La décomposition de l'acide sulfureux et des sulfites dans des solutions hydriques fut étudiée par F. Foerster [11].

Zachariasen [12], [13] et Simon [9] affirment que l'ion $S_2O_5^{2-}$ n'est point un ion pyro, dans lequel les soufres sont raccordés par l'oxygène, mais qu'il représente bien une sorte d'ion, dans lequel les soufres sont reliés directement les uns aux autres $(O_3S.SO_2)^{2-}$.

Le $Na_2S_2O_5$ fut obtenu pour la première fois par H. Endemann [14] qui constata que ce sel est assez résistant à la température normale, qu'il dégage, après avoir été chauffé à 80°C, le SO_2 et qu'il se transforme, par redoxydation, en sulfate.

A. H. Röhrig et M. Berthelot présentèrent la décomposition du métabisulfite au moyen de l'expression suivante:

$$2M_2\overset{+4}{S}_2O_5 = 2M_2\overset{+6}{S}O_4 + S^0 + \overset{+4}{S}O_2,$$

A. Geuther observa qu'une petite quantité de thiosulfate se forme comme produit intermédiaire, mais E. Divers n'est pas d'accord avec lui sur ce point [18].

E. Foerster et G. Hamprecht [15] étudièrent la façon de réagir du métabisulfite de sodium chauffé dans une atmosphère d'azote à circulation lente.

Description des expériences

Pour toutes les analyses nous avons procédé de la façon suivante: dans une fiole jaugée, à capacité de 250 ml, remplie d'eau distillée et bouillie, ainsi que de 20 ml 0,1 N de NaOH, nous avons délayé du métabisulfite de sodium et les produits solides de sa décomposition.

Cette solution fut analysée pour le contenu de S^{-2} en appliquant la méthode indiquée par W. Feld [16] et pratiquée par F. Foerster et K. Kubel [17].

Le S^{+4} fut défini par titration et le S^{+6} — par gravimétrie. Le $Na_2S_2O_5$ fut obtenu par la méthode de Foerster [8].

L'analyse de cette préparation démontra ce qui suit:

1. S^{-2} — absent,
2. S^{+4} — 33,13 %,
3. contenu global de soufre — 33,40 %,
4. S^{+6} (obtenu de la soustraction $S_{glob} - S^{+4}$) — 0,27 %.

La réaction de décomposition du métabisulfite de sodium a été entreprise dans une nacelle en porcelaine dans une atmosphère d'azote

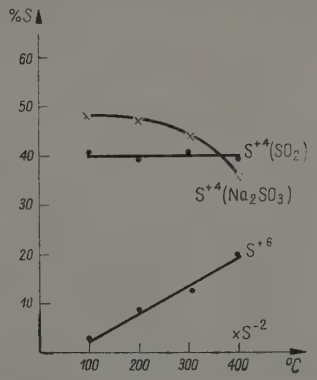

Fig. 1. Parcours du chauffage du $Na_2S_2O_5$ en atmosphère d'azote durant 4 heures

à circulation lente. La nacelle fut placée dans une tube en verre d'Iéna. Nous nous sommes servis d'un four de fabrication Siemens-Plania, type CSBO 0-1.

Pour le disproportionnement, nous avons introduit dans la nacelle environ 0,2000 g de métabisulfite défini par pesage. La nacelle fut introduite dans le tube en verre, fixé dans le four, et par lequel l'azote s'écoulait lentement.

Par analogie avec les opérations précédentes [1]—[5], la durée de la réaction propre fut fixée à une période de 4 heures.

A partir du moment où la température convenable avait été obtenue, la réaction fut soutenue durant 4 heures. Ensuite, on laissa le four se refroidir durant 2 à 3 heures jusqu'à 100°C, après quoi la nacelle fut retirée du four et introduite dans une fiole jaugée remplie d'eau, où les produits de la réaction se dissolvèrent.

Le soufre qui se dégageait au cours de la réaction, apparaissait sous forme de flocons blancs et fréquemment comme dépôt sur la partie froide du corps du four.

Les résultats obtenus sont présentés au tableau I ainsi que dans le diagramme (Fig. 1).

TABLEAU I

Le chauffage du $Na_2S_2O_5$ dans une atmosphère d'azote à circulation lente

Température °C	Durée de la réaction h	S^{-2}	S^0	S_s^{+4} (Na_2SO_3)	S_g^{+4} (SO_2)	S^{+6}
		en pourcents par rapport à la quantité globale de soufre (S^{+4}) après le disproportionnement de celui-ci				
100	4	–	présent	48,88	40,50	2,65
200	4	–		47,87	38,98	8,16
300	4	–		44,99	40,80	12,87
400	4	1,5		35,05	39,90	18,09

Conclusions

Les résultats que nous avons réussi à obtenir confirment le point de vue de Foerster que la réaction de décomposition du métabisulfite de sodium seul,

$$\overset{+4}{Na_2S_2O_5} = Na_2SO_3 + SO_2\,,$$

placé dans une nacelle en porcelaine, placée elle-même dans une atmosphère d'azote à circulation lente, constitue l'opération principale. Comme il résulte de cette réaction, on devrait obtenir 50% de $S^{+4/g}$ sous forme de SO_2. Pourtant nous avons toujours obtenu des valeurs de 40% de $S^{+4/g}$. Le dégagement du soufre et l'apparition du S^{+6} prouvent que déjà – même à 100°C – se produit, d'ailleurs comme phénomène secondaire, la réaction de disproportionnement:

(1) $$2\overset{+4}{Na_2S_2O_5} = 2\overset{+6}{Na_2SO_4} + S^0 + \overset{+4}{SO_2}$$

ou peut-être

(2) $$3\overset{+4}{Na_2S_2O_5} = 3\overset{+6}{Na_2SO_4} + 2S^0 + \overset{+6}{SO_3}\,.$$

La preuve que le cours du disproportionnement est conforme au schéma final de la réaction, est donnée par la quantité immuable du SO_2 dégagé, chiffre qui devrait subir des variations dans le cas d'une réaction d'après l'équation (1).

Le sulfite qui se forme par suite de la décomposition du métabisulfite, se trouve disproportionné en sulfite et sulfate dans le cas extrême suivant le schéma:

$$4Na_2SO_3 = 3Na_2SO_4 + Na_2S\,.$$

Le fait qu'une telle réaction commence à se produire déjà à 400°C, a trouvé sa preuve dans l'apparition de sulfures à cette température.

Résumé

On a réalisé l'étude de la décomposition du métabisulfite de sodium ($Na_2S_2O_5$) à l'état solide dans une atmosphère d'azote à circulation lente, dans les limites de 100° à 400°C.

Il fut constaté que la décomposition du métabisulfite de sodium à l'état sec se manifeste déjà à la température de 100°C et la réaction principale se produit sous sa forme extrême comme suit:

$$Na_2S_2O_5 = Na_2SO_3 + SO_2 .$$

Comme réactions auxiliaires, se produisant à cette-même température ainsi qu'à des températures plus élevées, nous avons les transformations présentées sous leur forme extrême comme des actes de disproportionnement:

$$2Na_2\overset{+4}{S}_2O_5 = 2Na_2\overset{+6}{S}O_4 + S^0 + \overset{+4}{S}O_2 ,$$

$$3Na_2\overset{+4}{S}_2O_5 = 3Na_2\overset{+6}{S}O_4 + 2S^0 + SO_3 .$$

A 400°C, le sulfite — produit de décomposition du métabisulfite — est sujet au disproportionnement et on présente cette transformation dans son aspect extrême par la formule suivante:

$$4Na_2\overset{+4}{S}O_3 = 3Na_2\overset{+6}{S}O_4 + Na_2\overset{-2}{S} .$$

FACULTÉ DE CHIMIE INORGANIQUE, ÉCOLE POLYTECHNIQUE, VARSOVIE
ACADÉMIE POLONAISE DES SCIENCES

OUVRAGES CITÉS

[1] T. Miłobędzki, Annales de chimie, **24** (1950), 48.

[2] T. Miłobędzki, B. Fulde-Krukowska i K. Wieczffinski, C. R. de l'Acad. Polon. Sci. et Lettres, **52** (1951), 344.

[3] B. Fulde-Krukowska, Dissertation doctorale, 1951.

[4] K. Wieczffinski, Dissertation doctorale, 1951.

[5] R. Rudnicki, Travail de diplôme, 1951.

[6] T. Miłobędzki, Kosmos, **38** (1913), 952.

[7] — Chemik Polski, **14** (1914), 1.

[8] F. Foerster, A. Brosche u. Chr. Norberg-Schulz, Zeit. phys. Chem. **110** (1924), 435.

[9] A. Simon et K. Waldmann, Zeit. anorg. u. allg. Chem. **281** (1955), 113; **281** (1955), 135; **284** (1956), 36; **284** (1956), 47; **288** (1956), 131.

[10] G. A. Barbaglina et P. Gucci, Ber. **13** (1886), 2325.

[11] F. Foerster, F. Lange, O. Droschbach et W. Seidel, Zeit. anorg. Chem. **128** (1923), 245.

[12] W. H. Zachariasen, Phys. Rev. **40** (1932), 923.

[13] Strukturbericht, **2** (1937), 104, 505.

[14] H. Endemann, Lieb. Ann. **140** (1866), 337.

[15] F. Foerster et G. Hamprecht, Zeit. anorg. Chem. **158** (1926), 227.

[16] W. Feld, Chem. Zentralbl. **11** (1889), 868.

[17] E. Foerster u. K. Kubel, Zeit. anorg. Chem. **139** (1924), 261.

[18] M. Mellor, Inorganic and theoretical chemistry, **10** (1947), 327.

POLONAISE DES SCIENCES
BULLETIN DE L'ACADÉMIE
Cl. III — Vol. V, No. 5, 1957

CHEMISTRY

On Infra-Red Absorption Spectra of Aminonitrocompounds Deriving from Nitroparaffins

by

T. URBAŃSKI

Presented on March 13, 1957

The author formerly examined infra-red absorption spectra of nitroalcohols, obtained by aldolic addition of formaldehyde to nitroparaffins [1]. This led to confirmation of the hypothesis previously postulated [2]—[4]. that hydrogen bonds can exist between alcoholic and nitro groups. To extend these experiments, infra-red absorption spectra of five compounds deriving from 1- and 2-nitropropane and containing the secondary or tertiary amino group were now investigated. Some of the compounds also contain the alcoholic group (or groups) and some of them — the tetrahydro-1,3-oxazine or homologous ring. The formulae of the compounds are given below (I—V).

The infra-red absorption spectra were measured with a Hilger H-668 single-beam spectrophotometer, using optics of sodium chloride for the range from 1μ to 10μ.

Solid specimens were used as mulls in paraffin oil, the ratio of the substance to the oil being 1:8. The thickness of the layer was 0.1 mm. or 0.02 mm.

The results obtained are summarised in Table I, and the curves are reproduced in Figs. 1—5.

Strong bands 1481—1460 cm.$^{-1}$ and 1395—1374 cm.$^{-1}$ (marked on the diagrams with broken lines) have also been found. They belong to CH_2 and CH_3 vibrations mainly of the paraffin oil.

Discussion

The following assignments are being suggested.

1. Amino groups. Strong bands in the 3μ region of the amino group stretching vibrations exist in all the examined compounds, both hydrochlorides of secondary amines (I, IV, V) and free tertiary bases (II), (III).

TABLE I

Compound and Figure	Absorption frequencies (*s*)-strong, (*m*)-medium, (*sh*)-shoulder
I/Fig. 1	9524, 9091, 8197, 7407, 6803, 6452, 6061, 5556, 5128, 4651, 4444 (m), 4167, 4000, 3636, 3509, 3333, 3030 (s), 2899 (s), 2469, 2247, 2198, 2062, 2000, 1942, 1887, 1845, 1795 (m), 1689, 1613, 1558 (m), 1328 (m), 1220, 1209 (m), 1188 (m), 1179, 1136 (m), 1111, 1087 (m), 1031 (m).
II/Fig. 2	9524, 8696, 8000, 7576, 6897, 6061, 5556, 5128, 5000, 4651, 4348, 4167, 3846, 3636, 3448 (s), 3077 (s), 2857, 2703, 2457, 2326, 2198, 1953 (m), 1862, 1681, 1543 (s), 1511, 1348 (m), 1242 (s), 1222, 1195, 1176, 1166 (m), 1111 (m), 1075 (m), 1036 (m), 1015 (m), 1005.
III/Fig. 3	9524, 8547, 8000, 7407, 7143, 6061, 5405, 5128, 4444, 4255, 3922, 3509 (s), 3247, 3030 (s), 2941 (s), 2532, 2247, 2041, 1934, 1880, 1764, 1546 (s), 1342 (m), 1247 (s), 1224 (m), 1195, 1163 (m), 1111 (m), 1073 (m), 1036 (m), 1015 (m).
IV/Fig. 4	9524, 9091, 8696, 8197, 7692, 7092, 6803, 5988, 5556, 5128, 4878, 4444 (s), 3175, 3077 (s), 2941 (s), 2500, 2273, 2083, 1905, 1621 (m), 1563 (s), 1481 (s), 1342 (m), 1250 (m), 1217, 1190, 1176, 1143, 1075 (m), 1047 (m), 1015 (m).
V/Fig. 5	9524, 9091, 8696, 8000, 7299, 6061 (m), 4831, 4405 (m), 3509, 3058 (s), 2941 (s), 2703 (s), 2410, 2141, 2075, 1880, 1779, 1701, 1567 (s), 1355 (m), 1215 (s), 1183 (s), 1130 (sh), 1058 (m), 1042 (m).

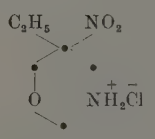

(I)

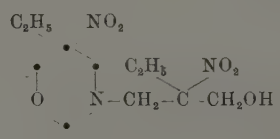

(II)

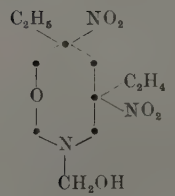

(III)

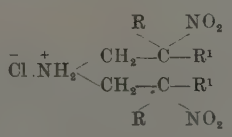

(IV) R = C_2H_5, R^1 = CH_2OH

(V) R = R^1 = CH_3

In the hydrochloride (I), three bands are probably produced by the amino group: 3509 and 3333 cm.$^{-1}$ (free NH group vibrations) and a very strong 3030 cm.$^{-1}$ band. The latter would appear to correspond

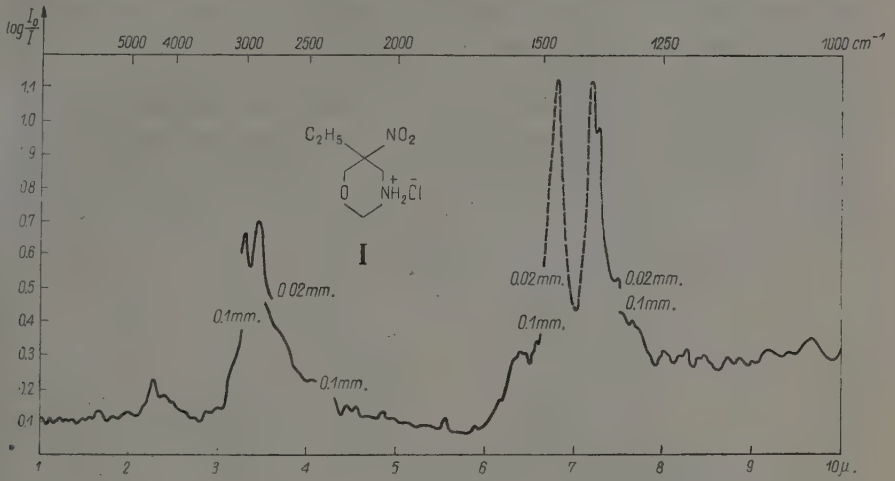

Fig. 1

to NH groups bonded with intermolecular hydrogen bonds, existing in the solid state.

The same strong 3077 and 3058 cm.$^{-1}$ bands, probably characterising NH groups, bridged with inter- and intramolecular hydrogen bonds,

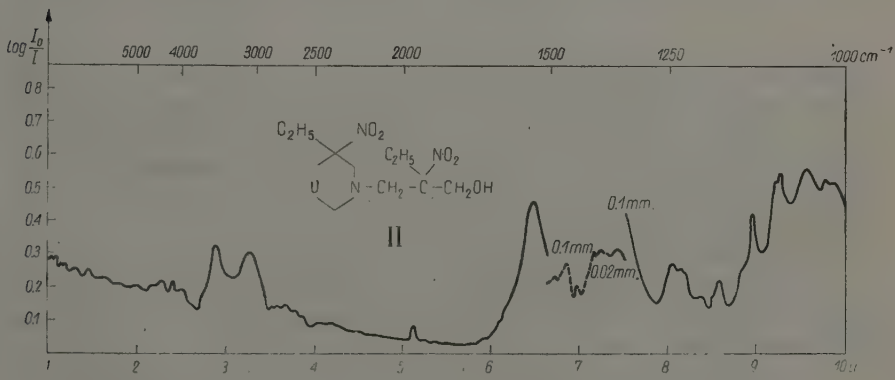

Fig. 2

exist in the spectra of two other hydrochlorides of secondary amines, (IV) and (V) respectively. There is no free NH group band in the spectrum of the compounds (IV) and (V). This corresponds to the hypothesis

expressed previously, as to existence of hydrogen bonds between NH and NO_2 groups [2]—[4].

The spectra of tertiary amines (II) and (III) contain very strong 3077 and 3030 cm.$^{-1}$ bands, respectively, which are most likely produced by the tertiary amino groups.

In the region of amino group deformation vibrations near 6 μ, the following bands are present: 1689 and 1613 cm.$^{-1}$ in the compound (I). The latter probably corresponds to the amino group attached to intermolecular hydrogen bonds. In the compounds (II), (III), (IV) and (V), the frequencies are 1681, 1764, 1621 and 1701 cm.$^{-1}$ respectively. The

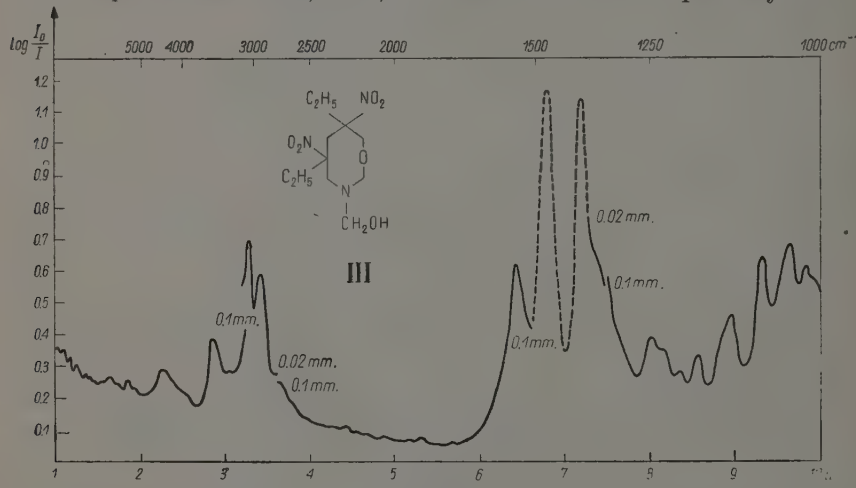

Fig. 3

six-member 1.3-oxazine ring compounds (I) and (II) show much the same frequencies: 1689 and 1681 cm.$^{-1}$. The eight-member ring of 1-oxa-3-azacycloöctane compound (III) probably gives a higher frequency band — 1764 cm.$^{-1}$. A low value (1621 cm.$^{-1}$) in the compound (IV) is presumably produced by intra- and intermolecular hydrogen bonds between the amino and nitro groups.

C—N stretching vibrations give a number of bands. They seem to be placed in the region of frequencies 1224—1215 cm.$^{-1}$ (all compounds), 1209—1190 cm.$^{-1}$ (compounds (I), (II) and (IV)) 1195—1176 cm.$^{-1}$ (all compounds), 1047—1031 cm.$^{-1}$ (all compounds).

2. Hydroxyl groups. The assignement of hydroxyl groups is somewhat complicated, because of overlapping between the stretching frequencies of hydrogen-bonded hydroxyl groups and those of free and bonded amino groups.

The author suggests that strong 3448 and 3509 cm.$^{-1}$ bands in the compounds (II) and (III) respectively be assigned to hydroxyl groups.

In the compound (II) the hydroxyl group is bonded with the nitro group. The shape of the band and its frequency are in good agreement with the spectra of nitroalcohols described formerly [1].

Frequency in the compounds (III) is higher due to the lack of an internal bond between hydroxyl and nitro group.

A weak band with frequency 3175 cm.$^{-1}$ would correspond to the bonded hydroxyl group in the spectrum of the compound (IV). This band obviously cannot exist in the spectrum of the amine (V) similar to (IV)

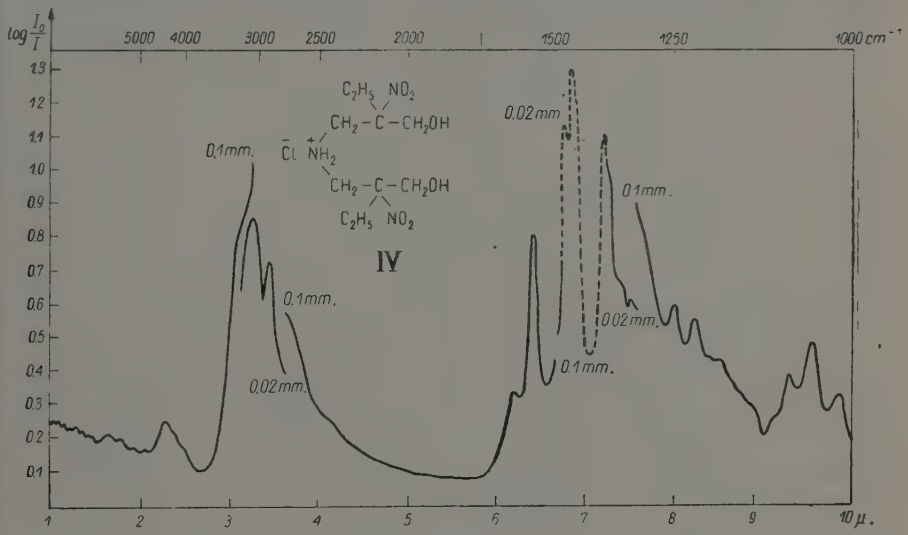

Fig. 4

from the point of view of the structure, but differing by the lack of a hydroxyl group.

In the overtone region the hydroxyl frequencies are 6897, 7143 and 6803 cm.$^{-1}$ in the spectra of compounds (II), (III) and (IV), respectively. The highest frequency is in the compound (III), where no intramolecular hydrogen bonds are present.

In the C—O stretching or O—H deformation region, near 10 μ, a frequency of 1015 cm.$^{-1}$ in the spectra of all hydroxyl-containing compounds (II), (III), and (IV) is present.

3. Cyclic C—O—C bond. It is know, that the C—O—C stretching frequency in cyclic ethers with larger rings is 1140—1070 cm.$^{-1}$.

In the spectra of cyclic compounds (I), (II) and (III) the corresponding frequency is 1111 cm.$^{-1}$. In addition, a band with a frequency of 1942, 1953 and 1934 cm.$^{-1}$ respectively should also be assigned to the ether bond. It does not exist in open chain compounds (IV) and (V).

The same observation applies to the 4000, 3846 and 3922 cm.$^{-1}$ bands, respectively, which can probably be assigned as overtone frequencies of the same group C—O—C.

4. Nitro group. In the region of 6.4 μ corresponding to asymmetric stretching valence vibrations of the nitro group, the following are strong bands recorded in the examined absorption spectra:

1558 cm.$^{-1}$ (I), 1543 cm.$^{-1}$ (II), 1546 cm.$^{-1}$ (III), 1563 cm.$^{-1}$ (IV), 1567 cm.$^{-1}$ (V). Their frequencies correspond to the free nitro group or to the nitro group bounded through a hydrogen bridge with only one hydroxyl group and one amino group (compound IV). The frequency is not very much affected by hydrogen bonds and this is in agreement with the facts previously observed for nitro alcohols [1].

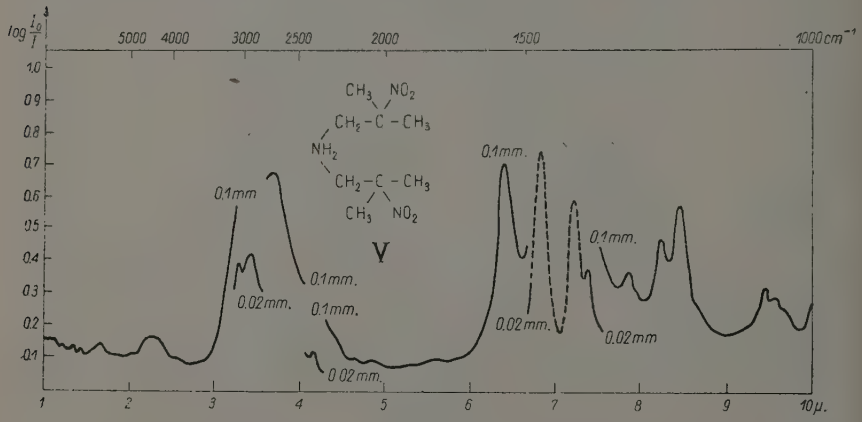

Fig. 5

Only in the instance of the compound (II) the spectrum shows the existence of a weak band of low frequency, 1511 cm.$^{-1}$, which may be assigned to one of the nitro groups, which is bonded with a hydroxyl group.

In the region of 7—7.5 μ corresponding to symmetric stretching valence vibrations of the nitro group, the following moderately strong bands were recorded: 1328 cm.$^{-1}$ (I), 1348 cm.$^{-1}$ (II), 1342 cm.$^{-1}$ (III) and (IV), 1355 cm.$^{-1}$ (V). Relatively low frequencies in the instance of the compounds (I—III) may be due to a steric influence on the nitro group of rings. The frequency in the compound (IV) is probably lowered by hydrogen bonds between the hydroxyl and amino groups and the nitro group. One amino group (without hydroxyl groups) in the compound (V) did not lower the frequency. The latter corresponds to that described in the literature [5], [6].

No definite influence of hydrogen bonds on the frequency of these bands could be detected.

Kornblum et al. [6] confirmed the existence of very weak nitro group bands in the 4.00—4.17 μ region, which, however, is unsuitable for diagnostic purposes. It seems that such bands are present in the spectra of all our compounds (I)—(V). They are 2469, 2457, 2532, 2500 and 2410 cm.$^{-1}$, respectively.

The stretching vibrations of the C—N bond between the carbon and nitrogen of the nitro group should probably be assigned to the following frequencies: 1087 cm.$^{-1}$ (I), 1075 cm.$^{-1}$ (II and IV), 1073 cm.$^{-1}$(III), and 1058 cm.$^{-1}$ (IV). This would be in agreement with the former assignment of this band [1].

Conclusions

1. The infra-red spectra of the compounds (I)—(V) agree with their structure. The presence of the oxygen-containing ring in the compounds (I)—(III) is confirmed by bands with a frequency of 1111 cm.$^{-1}$.

2. The secondary amino groups are bonded with intramolecular and, in some cases, with intermolecular hydrogen bonds. They exist presumably between amino and nitro groups. NH groups bonded with hydrogen bonds show frequencies of the order of 3030 cm.$^{-1}$ and 1610 cm.$^{-1}$. A slight lowering of nitro group frequencies under the influence of hydrogen bonds have been noticed.

3. The new bands, 1953—1934 cm.$^{-1}$ and 4000—3846 cm.$^{-1}$, were now assigned to the presence of the C—O—C ring bonds in 1,3-oxazine rings. The former are probably fundamentals, and the latter — the overtones.

The author is much indebted to Mrs. J. Świętosławska, Miss T. Kraczkiewicz and Miss B. Kontnik for measuring infra-red absorption spectra.

INSTITUTE OF ORGANIC SYNTHESIS, POLISH ACADEMY OF SCIENCES

REFERENCES

[1] T. Urbański, *On hydrogen bonds in some nitroalcohols (on the basis of infra-red absorption spectra)*, Bull. Acad. Polon. Sci. Cl. III, **4** (1956), 87, 381.

[2] — *On the structure of some aliphatic nitrocompounds*, Bull. Acad. Polon. Sci. Cl. III, **1** (1953), 239.

[3] T. Urbański, D. Ciecierska, Roczniki Chem. **29** (1955), 11.

[4] T. Urbański, Roczniki Chem. **29** (1955), 375.

[5] L. J. Bellamy, *The infra-red spectra of complex molecules*, London, Methuen & Co, 1956.

[6] N. Kornblum, H. E. Ungnade, R. A. Smiley, J. Org. Chem. **21** (1956), 377.

BULLETIN DE L'ACADÉMIE
POLONAISE DES SCIENCES
Cl. III — Vol. V, No. 5, 1957

CHEMISTRY

On the Preparation of Hydroxylamine Sulphate from 1,2-Dinitroethane

by

T. URBAŃSKI and T. DOBOSZ

Presented by T. URBAŃSKI on March 13, 1957

It is well known that primary nitroparaffins can isomerise to hydroxamic acids [1]—[5] and the latter can be subjected to further hydrolysis to hydroxylamine [5].

1,2-dinitroethane can be used as a primary nitroparaffin, readily available by preparation from ethylene and nitrogen dioxide [6]—[9]. Thus, Levy, Scaife and Wilder Smith [9] suggested hydrolysing small portions (0.30 g.) of 1,2-dinitroethane with hydrochloric acid at 150°C. for 13 minutes in a sealed tube. The yield was 90.8 per cent.

The authors of the present paper have, however, found that hydrolysis of slightly larger quantities of 1,2-dinitroethane (e. g., 2 g.) by this method is difficult; hydrolysis under pressure is often accompanied by decomposition, which can take a violent course.

It has now been found that hydrolysis of 1,2-dinitroethane with conc. sulphuric acid (molar ratio 1:2) is safer, since it does not require a temperature higher than 100° and can be carried out in an open vessel. The hydrolysis occurred almost immediately after portions of 1,2-dinitroethane were added to sulphuric acid warmed to 100° and stirred.

After the reaction mixture was cooled below room temperature, hydroxylamine sulphate in pure form was precipitated by adding ethyl alcohol.

A lower concentration of sulphuric acid reduced the yield of hydroxylamine and required a higher temperature (e. g., 120°) and a longer reaction-time.

The method seems to be more economic than the classical method of preparing hydroxylamine salts from sodium nitrite and sodium hydrogen sulphite. The cost of raw materials in the new method is c. 85 per cent of the costs in the classic method.

An application for the patent has been filed at the Polish Patent Office [10].

Experimental

2 g. of 1,2-dinitroethane (DNE) were added by small portions to 3.5 g. of conc. sulphuric acid (98 per cent) previously heated to 100°C. and stirred. The reaction was very vigorous with gas evolution produced by decomposition of oxalic acid formed during the reaction.

The reaction mixture was cooled below room temperature (5—10°C.) and 8—10 ml. of ethyl alcohol were added. A precipitate of hydroxylamine sulphate was filtered off, washed with alcohol and ether. The yield was 2.13 g. (79 per cent of theoretical).

A lower yield was obtained, when concentration of sulphuric acid was below 98 per cent. The rate of hydrolysis was also much lower, and it was necessary to raise the temperature of the reaction.

The comparative figures are shown in the Table.

TABLE

Concentration of sulphuric acid (% H_2SO_4)	98	85	85
Temperature (°C.)	100	100	120
Time (minutes)	2—3	180	15
Yield g. (from 2 g. DNE)	2.13	2.0	2.0
(per cent)	79	75	75

When 75% sulphuric acid was used, the yield dropped to 67%, at 65% — to 63% and at 55% — to 59%. Lower concentrations of sulphuric acid (e. g., 45%) did not allow hydroxylamine sulphate to be isolated by adding alcohol to the reaction mixture.

INSTITUTE OF ORGANIC SYNTHESIS, POLISH ACADEMY OF SCIENCES
DEPARTMENT OF CHEMISTRY, INSTITUTE OF TECHNOLOGY, WARSAW

REFERENCES

[1] E. Bamberger, E. Brüst, Chem. Ber., **35** (1902), 45.
[2] C. D. Nenitzescu, D. A. Isacenscu Bull. Soc. Chim. Roumanie, **14** (1932), 53.
[3] T. Urbański, J. Chem. Soc. (1949), 3374.
[4] T. Urbański, W. Gurzyńska, Rocz. Chem., **25** (1951), 213.
[5] S. B. Lippincott, H. B. Hass, Ind. Eng. Chem., **31** (1939), 118.
[6] Semenoff, Z. Chem. Pharm., **7** (1864), 129; Jahresber. (1864); 480.
[7] N. Y. Demianov, Thesis (in Russian), Moscow, 1899.
[8] N. Y. Demianov, K. Sidorenko, J. Russ. Chem. Soc., **41** (1909), 832 (in Russian).
[9] N. Levy, Ch. W. Scaife, A. E. Wilder Smith, J. Chem. Soc. (1946), 1096.
[10] T. Urbański, T. Dobosz, Polish Patent application, No. P 83,479 (1956).

BULLETIN DE L'ACADÉMIE
POLONAISE DES SCIENCES
Cl. III — Vol. V, No. 5, 1957

CHEMISTRY

On the Preparation of Caprolactam from Cyclohexanone and Dinitroethane

by

T. URBAŃSKI and A. PIOTROWSKI

Presented by T. URBAŃSKI on March 13, 1957

Caprolactam is usually prepared by acting on cyclohexanone with hydroxylamine, followed by a Beckmann rearrangement of cyclohexanone oxime.

Novotný [1] discovered that the oxime formation can occur in presence of conc. sulphuric acid or oleum at a high temperature. Simultaneously, the rearrangement takes place and caprolactam is formed. As a further development of this method Novotný suggests [2], [3] the use of primary nitroparaffins as a source of hydroxylamine. According to his invention a primary nitroparaffin is added to conc. sulphuric acid at 120-125°. Then cyclohexanone is added to the resulting solution, and the temperature kept near 120°. After the reaction is completed the reaction mixture is neutralised with ammonia and an upper layer of caprolactam is separated and then purified by distillation under reduced pressure. The yield of caprolactam is 80 per cent of theoretical, calculated on the basis of cyclohexanone.

The authors of the present paper suggest a further development of Novotný's method, which consists in using 1,2-dinitroethane as the cheapest of all primary nitroparaffins. The trend of the reaction is much the same as that described by Novotný. The modification of the original method consisted in dissolving 1,2-dinitroethane in acetic acid prior to reacting it. This facilitated the uniformity and control of the reaction.

The solution was introduced into hot concentrated (120°C.) sulphuric acid. Isomerisation of 1,2-dinitroethane to oxalhydroxamic acid was followed by hydrolysis to hydroxylamine and oxalic acid. The latter was decomposed into carbon oxide, carbon dioxide and water. Acetic acid was distilled off during the reaction and could be recovered.

The yield of caprolactam was, in laboratory conditions, 70—75 per cent calculated on the basis of cyclohexanone.

An application for the patent has been filed at the Polish Patent Office [4].

Experimental

10 g. of 1,2-dinitroethane were dissolved in an equal weight of acetic acid. The solution was introduced dropwise during 20 minutes to 35 g. of conc. sulphuric acid, the temperature being maintained within the limits 120—125°C. The reaction flask was kept in a bath with calcium chloride solution boiling at 120°.

Next, 12.5 mg. cyclohexanone were added dropwise during 25 minutes to the reaction mixture, the temperature being still kept near 120°.

Acetic acid, was distilled off through a condenser.

After the reaction was completed (this was marked by a fall of temperature in the reaction flask), the reaction mixture was carefully neutralised by introducing it into cold aqueous 25 per cent solution of ammonia. The temperature was kept by cooling below 50°.

The mixture was separated into two layers: the lower was formed by an aqueous solution of ammonium sulphate with crystals of the latter, the upper was formed of caprolactam. The upper layer was dissolved in ether and dried over anhydrous sodium sulphate.

The product was purified by distilling under reduced pressure at 138—9°C. by 11—12 mm. Hg.

The yield was 10.5 g. of caprolactam, i. e., c. 72 per cent (calculated on cyclohexanone).

INSTITUTE OF ORGANIC SYNTHESIS, POLISH ACADEMY OF SCIENCES

REFERENCES

[1] A. Novotný, Swiss Pat. 253,953 (1949).

[2] — US Pat. 2,569,114 (1952); Swiss Pat. 237,402 (1952).

[3] A. Stoy, A. Novotný, *Nová synthetická vlákna*, Statni Nakl. Techn. Liter. Praha, 1953.

[4] T. Urbański, A Piotrowski, Polish Patent application No. P 83,480 (1956).

BULLETIN DE L'ACADÉMIE
POLONAISE DES SCIENCES
Cl. III — Vol. V, No. 5, 1957

GEOCHEMISTRY

Critical Remarks on Some Geochemical Speculations Concerning Atmospheric Argon

by

A. POLAŃSKI

Presented by K. SMULIKOWSKI on March 2, 1957

Almost the whole amount of ^{40}A in the atmosphere is of radiogenic origin (^{40r}A). Such workers as K. F. Chackett [3], H. E. Tatel [9], A. Rostagni [7], F. Birch [2], L. Kulp [5], K. Rankama [6] and H. A. Shillibeer and R. D. Russell [8] have investigated the present amount of ^{40}A in the atmosphere for various geochemical considerations aimed at defining the age of the earth or some of its geospheres.

The present author attempted an evaluation of the reality of such speculations. The amount of ^{40r}A in the present atmosphere depends on: 1) the thickness of the outer crust of the earth, the potassium of which is the source of atmospheric ^{40r}A; 2) the average K content in that zone; 3) the present ^{40}K content in terrestrial potassium; 4) the period which has elapsed since ^{40r}A began to be accumulated in the atmosphere: 5) the rate of escape of ^{40r}A produced in the earth's crust to the atmosphere; and 6) the decay constant of ^{40}K. Only the values mentioned under 3) and 6) are known with sufficient accuracy, whereas the others can be estimated with a varying degree of probability.

The author tried to establish to what degree the changes of some of the values listed above (accepted within credible limits) influence the value of the other parameters. The following possibilities for K content in the crust and in the interior of the earth were taken into consideration:

1. The earth crust

HYPOTHESIS I. *Thickness* 31 km.,

a) *continental part* (*under the continents only* $= 1.5 \times 10^{18}$cm.^{2}) *density* (d)=2.7 g./cm.^{3}, *average* K=2.6%, *total* 0.39×10^{20} g. ^{40}K.

b) *suboceanic part* (*under oceans only* $= 3.6 \times 10^{18}$ cm.^{2}) density (d)= =2.9 g./cm.^{3} *average*=0.7% K, *total* 0.38×10^{20} g. ^{40}K.

Total $a+b = 0.64 \times 10^{20}$ g. ^{40}K(HI).

Hypothesis. II. *Thickness* = 33 km., $d = 2.8$ g./cm.^{3}, *average* K *content* 2.2% [10]. *Total* 1.2×10^{20} g. ^{40}K (HII).

Hypothesis III. *Thickness* = 36 km., $d = 2.8$ g./cm.^{3}, *average* K *content* 2.6 [4]. *Total* 1.55×10^{20} g. ^{40}K (HIII).

2. The mantle

Mass = 4×10^{27} g.

A) The dunitic hypothesis: average 0.004% of K (according to Ahrens et al. [1] for ultrabasic rocks), total 0.2×10^{20} g. ^{40}K (HA).

B) The chondritic hypothesis: average K = 0.09% [1], total 4.3×10^{20} g. ^{40}K (HB).

For the values thus obtained of the amount of ^{40}K the following calculations were made:

a) The total amount of ^{40r}A produced up to now on the earth or in its crust and mantle. The results of calculations for various values for the age of the earth are shown in Fig. 1. Two separate calculations were made for every definite value of t and ^{40}K: (i) for $R = \lambda e/\lambda\beta = 0.089$, and (ii) for $R = 0.125$. Not single curves, but strips broadening with the increasing distance from the zero point and limited by the lines for $R = 0.089$ and for $R = 0.125$, represent the variation of ^{40r}A.

b) The age of atmospheric argon is expressed by the time that has elapsed since the initiation of the process of origination of the present ^{40r}A from the decay of ^{40}K. However, this time is not necessarily identical with the time that has elapsed since ^{40r}A started to accumulate in the atmosphere, because it is possible that a certain part of ^{40r}A in the present atmosphere existed previously in the interior of the earth and only later after a certain lapse of time reached the atmosphere. Thus, if we identify the time of existence of ^{40r}A in the present atmosphere with the age of this atmosphere, then "the age of atmospheric argon" will correspond to a value intermediate between the age of the atmosphere and the age of the earth and will fix the higher limit for the former and the lower for the latter:

age of atmosphere < age of atmospheric argon < age of the earth.

The age of atmospheric argon was calculated only for the assumption that all the argon derives exclusively from the earth's crust. This assumption was thought correct. The present knowledge of the amount of K in the mantle and of the participation in the atmosphere of argon formed in the mantle is far too inaccurate to serve as a basis for such calculations. The amount of ^{40r}A in the present atmosphere is only a part of the total amount of argon produced in the earth's crust during a time t_0 equal to the "age of atmospheric argon". This is so because the rest has remained within the crust.

(1) $$^{40r}A_{atm} = {}^{40r}A_{total} - {}^{40r}A_{crust},$$

but

$$^{40r}A_{total} = {}^{40}K \times \frac{R}{1+R}(e^{\lambda t_0} - 1), \quad (2)$$

where ^{40}K is the amount of ^{40}K in the earth's crust and t_0 is the "age of atmospheric argon".

It is impossible to determine directly the value of $^{40r}A_{crust}$, but it can be done by introducing after Schillibeer and Russell [8] the value t_{av} = "average age of the earth's crust". This concept as introduced by the

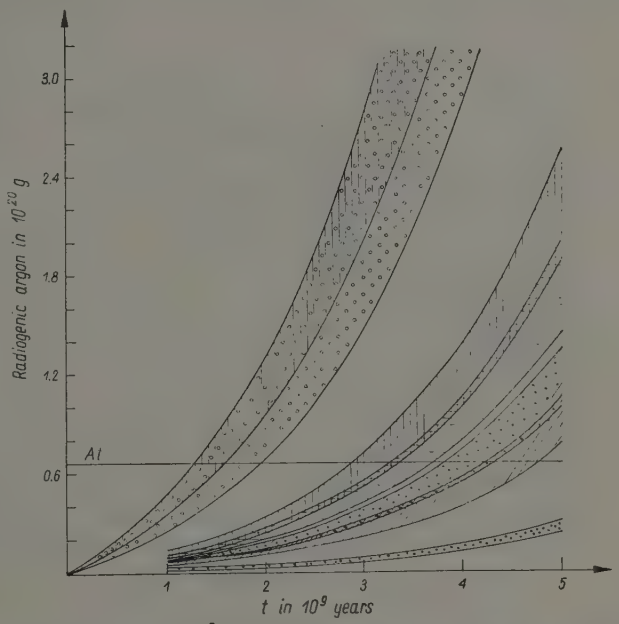

Fig. 1. Rate of change of total amount of radiogenic argon (^{40r}A) with growing time t

Earth's crust	Mantle	Total earth
hypothesis I (H I)	hypothesis II (H II)	hypothesis B (H B)
hypothesis A (H A)		
hypothesis I+A	hypothesis III (H III)	hypothesis III+B

present author has no real geological meaning but is used only as a mathematical means of expressing the value $^{40r}A_{crust}$. The "average age of the earth's crust" is, therefore, the "age" which would be revealed by the argon method, if the dating was based on the present amount in the earth's crust of ^{40}K and ^{40r}A.

Thus,

$$(3) \qquad {}^{40r}A_{crust} = {}^{40}K \frac{R}{1+R} (e^{\lambda t_{av}} - 1),$$

$$(4) \qquad {}^{40r}A_{atm} = {}^{40}K \frac{R}{1+R} (e^{\lambda t_0} - e^{\lambda t_w}).$$

By changing t_{av} over a wide range, the limits within which lieś the amount of ^{40r}A in the earth's crust are fully accounted for.

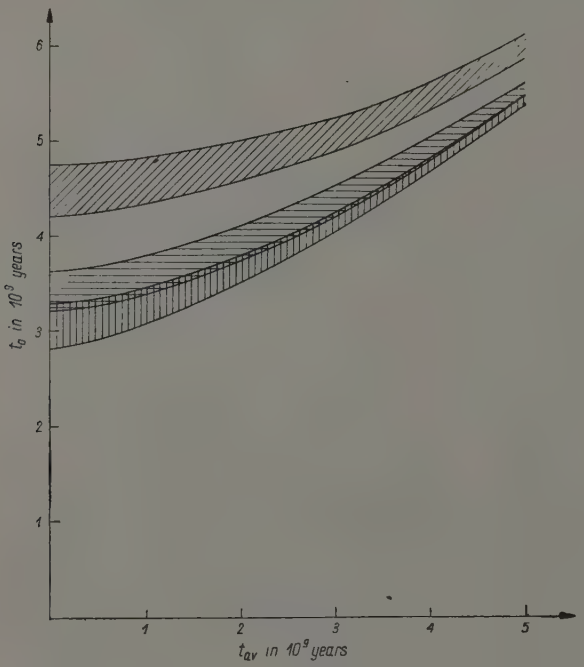

Fig. 2. Dependence of value t_0 on value t_{av}

hypothesis I (H I)

hypothesis II (H II)

hypothesis III (H III)

Fig. 2. shows how the "age of atmospheric argon" (t_o) depends on the various values of the "average age of the earth's crust" (t_{av}) when the different values assumed by the author for the amount of K in the earth's crust (HI—HIII) are considered. This diagram is based on the same principles

as Fig. 1, i. e., in both cases it is assumed that R changes within limits of 0.089 to 0.125.

The following conclusions are to be made when the two diagrams are considered:

1) The computed results for the total amount of ^{40r}A on the earth depend primarily on the value assumed for the age of the earth (t), on the amount of ^{40}K in the particular geospheres and to some extent on R. In the present state of our knowledge of these values it is impossible to reach any real values on the total amount of radiogenic argon 40 which has been produced up to now on the earth. Hence, it is impossible to determine what part of that amount corresponds to the ^{40r}A in the present atmosphere and consequently the rate of escape of ^{40r}A from the interior of the earth to the atmosphere cannot be estimated.

2) There is no means for determining whether the now existent atmospheric argon was produced entirely from potassium present in the earth's crust, or if the potassium accumulated in the mantle contributed in its formation. The extent to which this latter source contributed to the amount of atmospheric argon is impossible to define. It is to be noted, moreover, that the values for the amount of K in the earth's crust accepted here are not the only ones which could be considered. For instance, if it were assumed – in accordance with the latest geophysical data – that the thickness of the suboceanic zone is only 5 km., then the values in hypothesis I would change and the value for K in the earth's crust would be somewhat lower. Indeed, from the now available data it is impossible to decide if all the ^{40r}A in the atmosphere is derived solely from the earth crust's or partly from the mantle, since such other parameters as the age of the earth, or even the physical constants of potassium, are not known with sufficient exactitude.

3) Calculations of the "age of atmospheric argon" cannot be made with sufficient reliability, even if the rather doubtful assumption is made that all atmospheric ^{40r}A derives entirely from potassium in the earth's crust. Here, too, the lack of knowledge of the necessary data is the decisive factor.

4) In the light of the considerations outlined above it seems premature to attempt actual computations based on the amount of ^{40r}A in the atmosphere. For this reason all speculations made hitherto in that field, though very interesting and highly ingenious as some of them are, must be approached with caution since they are not free of much uncertainty. The following examples may be quoted to illustrate the point: a) the proof given by Kulp [5] for the interior origin of the hydrosphere based on the assumption that the escape of argon from inside the earth is 14 per cent; b) the attempt of Rankama [6] to determine the amount of weathered igneous rocks ($= 6462$ kg./cm.^{2}) based on the assumption that all the atmospheric ^{40r}A has its source in the ^{40r}A libe-

rated during the weathering processes of these rocks; c) the calculations of the age of the earth (5.3×10^9 years) made by Shillibeer and Russell [8] and based on the assumption that all atmospheric ^{40r}A comes solely from the earth's crust. In all these instances the amount of ^{40r}A in the atmosphere was used for calculations in which the assumed numerical values were by no means more reliable than the a priori results obtained with these methods.

LABORATORY OF GEOCHEMISTRY, MINERALOGY AND PETROGRAPHY,
GEOLOGICAL INSTITUTE, POLISH ACADEMY OF SCIENCES

REFERENCES

[1] L. W. Ahrens, W. H. Pinson, M. M. Kearns, *Association of rubidium and potassium and their abundance in common igneous rock and meteorites*, Geochim. et Cosmochim. Acta **2** (1952), 229.

[2] Fr. Birch, *Recent work on the radioactivity of potassium and some related geophysical problems*. Jour. Geophys. Research **56** (1951), 107.

[3] K. F. Chackett, K^{40} *and the age of the atmosphere*, Phys. Rev. **81** (1951), 1057.

[4] V. M. Goldschmidt, *Geochemistry* (edited by A. Muir). Oxford 1954, Clarendon Press.

[5] J. L. Kulp, *Origin of the hydrosphere*, Bull. Geol. Soc. Am. **62** (1951), 326.

[6] K. Rankama, *A calculation of the amount of weathered igneous rocks*, Geochim. et Cosmochim. Acta, **5** (1954), 81.

[7] A. Rostagni, *Radioattività del potassio ed età della terra*, Geofis. pura et applicata, **18** (1950), 128.

[8] H. A. Shillibeer and R. D. Russell, *The argon-40 content of the atmosphere and age of the earth*, Geochim. et Cosmochim. Acta, **8** (1955), 16.

[9] H. E. Tatel, *Argon*^{40} *and the age of earth*, Jour. Geophys. Research, **55** (1950), 329.

[10] Fr. E. Wickman, *The "total" amount of sediments and the composition of the "average igneous rock"*, Geochim. et Cosmochim. Acta, **5** (1954), 97.

BULLETIN DE L'ACADÉMIE
POLONAISE DES SCIENCES
Cl. III — Vol. V, No. 5, 1957

PETROLOGY

Metasomatic Evolution of the Granite-Gneiss of Wądroże Wielkie (Lower Silesia)

by

M. KOZŁOWSKA

Presented by K. SMULIKOWSKI on March 2, 1957

The granite-gneiss of Wądroże Wielkie *) emerges from under schist formations in the foreland of the Sudeten, SE of Legnica. The age of the schists is assumed as Ordovician. With the exception of a few outcrops the granite-gneiss is covered by Pleistocene sediments and forms a flat dome only slightly contrasting with the gentle landforms of the region.

Most German workers are of the opinion that the gneiss of Wądroże is of an intrusive character and define it as orthogneiss.

In 1917 G. Gürich [3] described the gneiss of Wądroże Wielkie as a marginal metamorphic facies of the Strzegom-granite ("Striegau") and almost of the same age, i. e. Variscian. Gürich believed that the gneiss was formed in the initial stages of the Strzegom-granite formation as a result of metamorphism of schists in the roof of the liquid magma.

On the other hand, some years later H. Cloos [1] was of the opinion that the origin of the gneiss of Wądroże Wielkie was purely magmatic and intrusive. The granite intruded in the course of the Caledonian orogenetic movements and was foliated during the cooling of the magma. A similar view was expressed in 1938 by H. J. Fabian who considered the gneiss of Wądroże Wielkie to be a late tectonic Caledonian intrusion submitted at a later stage to post-crystalline deformations.

In respect to the age and origin, the gneiss in question is compared by most German workers with the Iser granite-gneiss.

The main and typical gneiss presents a grey, coarse-grained rock. The foliation and linear elongation of the rock are weak. The rock is composed of bluish quartz grains, tabular grey-white, frequently Karlsbad twinned felspars, and flat, dark mica aggregates. Black schist enclosures

*) German name — Gross Wandriss.

are frequent in the gneiss. They are composed of small mica scales and are more or less concordant with the direction of the gneiss. The size of the intercalations is variable and may be as much as several centimetres.

All the schist enclosures and even the mica spots have proved, after microscopic examination, to be relics of diffluent garnet-mica schists. They are composed of compact small mica scales (mostly muscovite), sometimes aggregating into long usually parallel streaks. Occasionally the streaks wind around garnet grains, larger biotite porphyroblasts or lenticular quartz-mica aggregates. A part of biotite which had been originally mixed with muscovite in the form of small scales recrystallised into large olive-brown, strongly pleochroic plates frequently containing rutile needles (sagenite) and inclusions of zircon surrounded by pleochroic halos. The evidence for the crystalloblastesis of the large biotite plates from the primary small scales is supplied by the muscovite inclusions and by the fringes of scaly mica aggregates surrounding the biotite plates.

Microscopic examination shows that, in opposition to the opinion of German workers, the gneiss of Wądroże Wielkie cannot be considered as proper orthogneiss, since it originated in the course of complex process of metasomatic granitisation of mica schists.

The granitisation took place in several successive stages and at every one the schists were transformed more and more, reaching finally their present granite-gneiss appearance and composition.

In the first stage of metasomatic activity the rocks were enriched in sodium. The growing plagioclases (up to 8 per cent An) corroded the biotite replacing it with phengite and epidote. At first small cavities filled with a microlitic aggregate of phengite and epidote were formed (Photo 1). The further course of this process led to the development of pseudomorphs replacing biotite. They were composed of phengite closely interwoven with vermicular epidote especially frequent at their rims (Photo 2).

Meanwhile an ever increasing inflow of sodium made possible an extensive growth of plagioclases. Large plagioclases were formed. They contained abundant inclusions of parallel mica scales and roundish garnet grains. The latter ones were partly biotitised at their rims during this process (Photo 3).

The next stage of granitisation consisted in an invasion of microcline, which to some extent attacked plagioclase and penetrated it sinuately (Photo 4). Where the process was far advanced perthite structures could be formed with relics of the replaced plagioclase enclosing mica scales and forming veins within the microcline.

In the rock here considered there is also another, somewhat later metasomatic perthite. It was caused by a veiny infiltration of albite

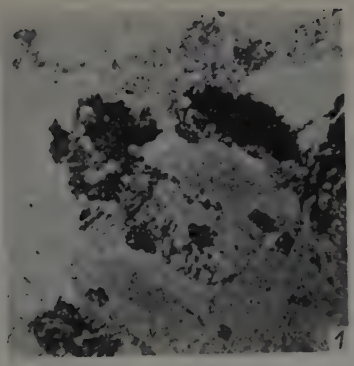

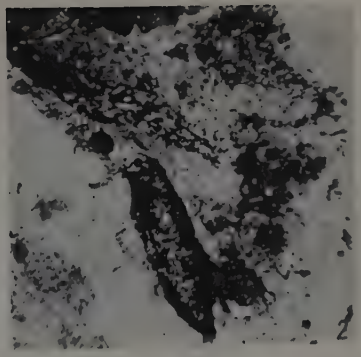

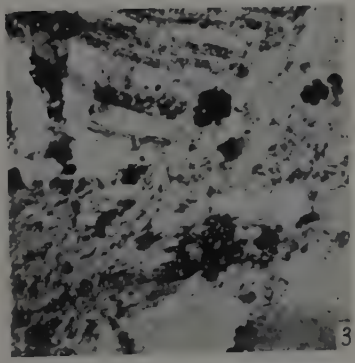

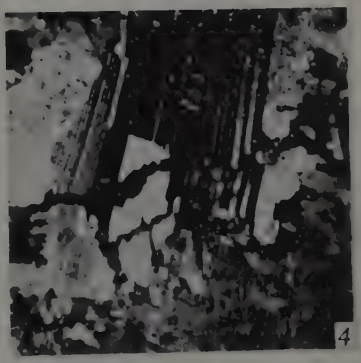

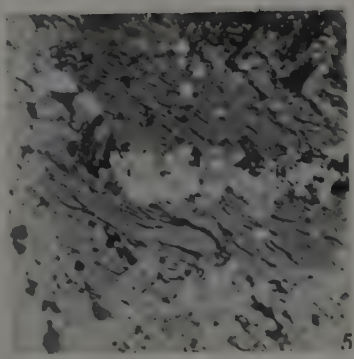

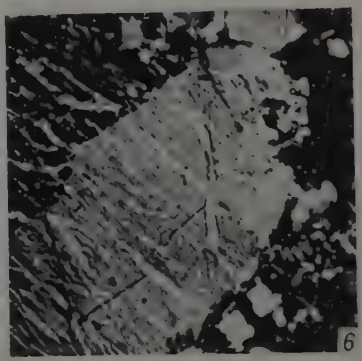

1. Plagioclase enclosing micas and garnets and penetrating into biotite. Cavities filled with microlitic aggregates of phengite and epidote are visible. Ordinary light, magnif. 17×
2. Phengite-epidote pseudomorphs replacing biotite. Ordinary light, magnif. 22×
3. Digestion of a garnet bearing mica schist relic in plagioclase. Crossed nicols, magnif. 22×
4. Old plagioclase attacked by microcline. The plagioclase is cut by the fissure filled with fluorite and albite. Crossed nicols, magnif. 38×
5. Quartz and albite growing in a fissure in metasomatic perthite gradually replace the perthite. Myrmekite is visible at the foot of the photo. Crossed nicols, magnif. 35×
6. A late quartz vein in microcline perthite cuts across infiltration veins of albite. Crossed nicols, magnif. 20×

into already formed microcline. It is not always possible to make the distinction between the two kinds of perthite. Yet, when the plagioclase veins are closely interwoven with micas, and simultaneously show throughout the whole microcline the same optic orientation as the attacked older plagioclase, there can be no doubt that it is the older secondary perthite that is present.

It is noteworthy that in these interfelspathic reactions myrmekite was produced only exceptionally and not in the typical form.

The gneiss, which had been formed by metasomatic granitisation of schists, was later submitted to dynamic deformations, and the solutions circulating in the thus loosened structure deposited various hydrothermal contistuents reacting partly with the minerals already present in the rock. At this stage small limpid albites containing no micas and frequently accompanied by quartz were crystallised from the solutions. Crystallisation probably started in the small fissures, but later it extended, and while dislodging the surrounding felspars, it produced granoblastic aggregates of small crystals in the form of veins, streaks and cavities usually in microperthite. Very often it is possible to discern that this albite was later than the perthite albite because it cuts the perthite veins within the microcline (Photo 5).

Usually, these late albites are concentrated on the edges of microperthite grains which sometimes contain untypical myrmekite. In some cases it is difficult to discern myrmekite and the products of quartz corrosion of felspars. The thin quartz veins are somewhat younger. They cut across the albite infiltration veins in perthites, thus showing that they are younger than the metasomatic albitisation of microclines (Photo 6). May be, the small fluorite-albite or fluorite-quartz veins cutting across older felspars are of the same age. Photograph 4 shows older plagioclase attacked by microcline and afterwards crushed; the fissures are filled with fluorite and albite (black). Sometimes a single crystal of fluorite together with chlorite scales fills the cavity in mosaiclike desintegrated quartz. Crystallisation of chlorite and quartz in fissures is followed by pyrite. In contrast to the scaly chlorite which occurs with fluorite or replaces biotite, the chlorite underlying the pyrite is formed in shapeless aggregates.

Quartz is present in almost all the veins, i. e. as well in the albite — as in the pyrite ones. It is, therefore, to be inferred that the influx of silica was repeated several times. There is, however, some doubt as to the source of the main mass of quartz forming large grains with strain shadows or a compact mosaic of small grains. The quartz could either invade the rock in the course of granitisation or it could be a rock-forming component of the pre-existing schists. The circumstance that the relics of schists contain only 1—3 per cent of quartz, whereas the total proportion of quartz in the rock is about 44 per cent, cannot be considered

as sufficient evidence that the pre-existing schists contained little of quartz, since in the course of granitisation a certain differentiation in the mineral composition of the schists could take place and above all the enrichment in the micas and garnet at the expense of other components could occur.

From the above results it follows that, contrary to the generally accepted earlier opinion, rocks with such a complicated evolutional history and derived from metamorphic para-schists cannot be considered as foliated intrusive granite. The parallel texture of the gneiss was by no means due to crystallisation under pressure out of magma, as was believed by H. Cloos [1] and H. J. Fabian [2], neither was it caused by post-crystalline deformations of granite (foliation). The parallel texture was inherited, from the schists which became gneiss in the course of granitisation. The degree of the textural parallelism is now defined by the number and the degree of conservation of the schist relics in the rock.

Quite a different problem is raised by the strong local dislocations and in some zones even mylonitic foliation which occurred much later in the already formed gneiss. A very distinct zone of such mylonitic schists almost approaching phyllonites was found in an active quarry in Wądroże Wielkie, but this has nothing in common with the earlier evolution of gneisses herein described.

The author wishes to express her very sincere gratitude to Professor K. Smulikowski for his most valuable advice in the course of her investigations.

LABORATORY OF GEOCHEMISTRY, MINERALOGY AND PETROGRAPHY,
GEOLOGICAL INSTITUTE, POLISH ACADEMY OF SCIENCES

REFERENCES

[1] H. Cloos, *Der Gebirgbau Schlesiens und die Stellung seiner Bodenschätze*, Berlin, 1922.

[2] G. Gürich, *Zur Geologie der Striegauer und Jenkauer Berge*, Jb. Preuss. Geol. L.-A. **36** (1917), 611-616, Berlin.

[3] H. J. Fabian, *Das Nordsudetische Schiefergebirge in seinem Vorlandsteil*, Jb. Preuss. Geol. L.-A. **59** (1938), 6-41, Berlin.

BULLETIN DE L'ACADÉMIE
POLONAISE DES SCIENCES
Cl. III — Vol. V, No. 5. 1957

PETROLOGY

The Metamorphic Origin of the Granite of Mount Jawornik (Lower Silesia)

by

J. BURCHART

Presented by K. SMULIKOWSKI on March 2, 1957

The Variscian orogeny extends unequally in different regions of the Sudeten Mountains. These movements are especially strong in a few narrow zones near the eastern border of the Western Sudeten, namely: the zone of Niemcza, the zone of the upper part of the Biała Lądecka River and the zone of Skrzynka-Złoty Stok. The latter divides the Carboniferous intrusive syenites from the older, precambrian metamorphic complex situated on the southern side of the zone.

This zone is assumed to be built of the same rocks which occur in the South: granulites, para- and orthogneisses, amphibolites and various schists. The Variscian orogeny turned these rocks into mylonites. This mylonitisation was succeeded by partial recrystallisation. At present the zone of Skrzynka-Złoty Stok is composed of the blastomylonitic complex, including various mica- and amphibole schists, amphibolites, blastomylonitic gneisses and mylonites. The direction of the strike is about NE/SW and the dip towards the northwest. The veins of Jawornik granite are concordant with these rocks. The "granite" is of granodioritic or tonalitic composition. The thickness of the veins varies from several centimetres up to 100 m. but it usually oscillates about 1 m. The bigger granitic bodies are found in Czechoslovakia near the Polish frontier.

According to the German geologists [1], [2] who worked on this area before and during the second World War, both the syenites of Złoty Stok and the Jawornik granites are true magmatic rocks. During the Variscian orogeny the granite magma intruded the cold wall rocks and therefore the porphyritic texture of the granites was formed. Later deformations caused some parts of the granite to resemble the older blastomylonitic gneisses.

Detailed petrographical investigations of the Skrzynka-Złoty Stok zone were undertaken in 1955. These investigations have proved the

existence of a great variety of rocks called the "granites of Jawornik". In the present stage of investigations it seems possible that these granites are not of uniform origin. In this paper the author is limited to only one small section composed of schists and granites. The map shows the localisation of section (A-B) and the geological structure of the eastern

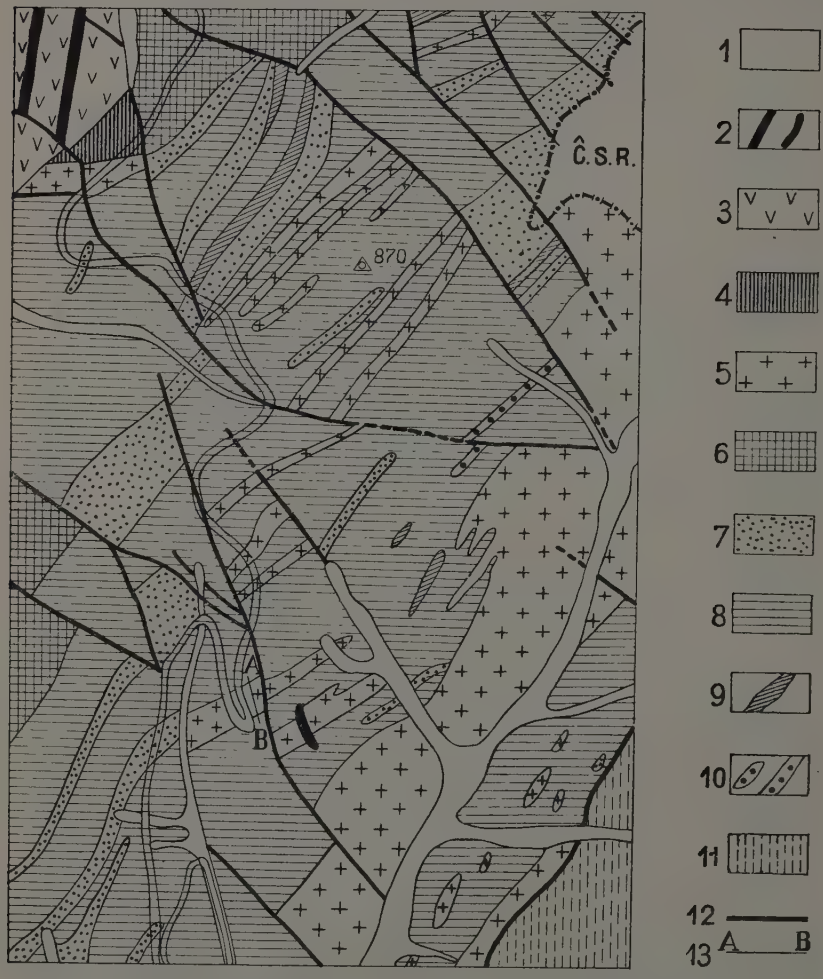

Fig. 1. Map of the eastern part of the Skrzynka-Złoty Stok dislocation zone

1. Quaternary, 2. lamprophyres, 3. syenites, 4. mylonites. 5. Jawornik granites, 6. gneisses and gneissoid mylonites, 7. blastomylonitic gneisses, 8. mica schists, 9. amphibolites, 10. graphite quartzites, 11. gneisses out of the zone, 12. faults, 13. section line

part of the Skrzynka-Złoty Stok zone. This map was drawn after a German map [3]. The thickness of the granitic veins has been exaggerated in some cases, due to indispensable generalisation, e. g., according to the map, the section in question is composed only of granite. In reality there are various schists with small granitic sills (see Fig. 2).

The mineral composition of the mica schists is characteristic for staurolite-kyanite subfacies (quartz, muscovite, biotite, garnet, kyanite and small amounts of magnetite, tourmaline, K-feldspar, acidic plagioclase and apatite). The texture of these rocks points to twofold mechanic deformations. Small veinlets and lenses of quartz and feldspars are younger than the first strong deformation stage, but older than the later,

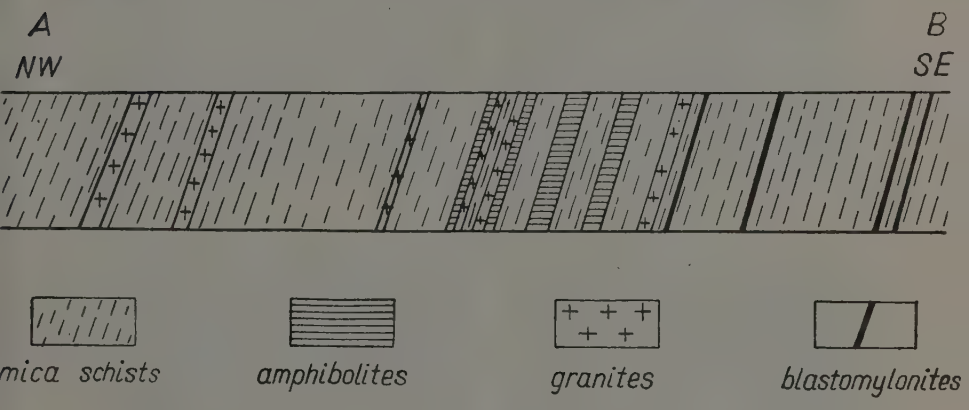

Fig. 2. Sketch showing the section described in this paper

weaker one. The mica schists are differentiated in their quantitative mineralogical composition and contain concordant interlayers of light blastomylonites. The latter are composed of a fine-crushed, rolled out mass of quartz and feldspars with traces of mica. The oligoclase porphyroblasts grew in this mass after mylonitisation (Fig. 3a). Porphyroblasts of K-feldspar are rarely seen. They contain many inclusions of mylonitic mass. Undoubtedly they are postkinematic. Sometimes the porphyroblasts are grouped (glomeroporphyroblastic texture) and the mylonitic mass appears only as a matrix (Fig. 3b). Under the microscope these parts of rock resemble the granites of Jawornik. The younger and weaker stage of deformation is rarely seen. The amphibolite appearing in this section is not a homogeneous rock, but is composed of thin layers of true amphibolite and of fine-grained granoblastic plagioclase-biotite-quartz rock. The transversal fissures are filled out with prehnite, epidote and K-feldspar.

The veins of "Jawornik granite" (strictly speaking, granodiorites and tonalites) are concordant with the schists. The borders are sharp and no differentiation is seen in the veins. The granite shows gneissoid texture owing to the directional biotite-chlorite stripes. In the thin section porphyritic texture is visible, including large crystals and fine-grained mass filling spaces (Fig. 3c). The fine-grained mass is not uniform. Sometimes it is composed only of sericitised plagioclase, but often it is accompanied by quartz and mica scales. The components are often elongated and overlap each other. Undoubtedly this fine-grained mass is the result of mylonitisation of a certain pre-existing rock, but not of the granite itself. This mass sometimes contains strongly overlapping quartz grains and mica scales and has a schistoid appearance (Fig. 3d). The oligoclase forms large crystals of a few millimetres in diameter. Zoned crystals with some reversed zoning are rarely seen. Plagioclases commonly contain inclusions of quartz and micas. They also sometimes include mylonitic mass. The centres of plagioclase grains are often sericitised, and they are surrounded by clear and fresh oligoclase rims. K-feldspars are less frequent. They fill the spaces among the other minerals, form small veinlets and replace plagioclase. The larger crystals of K-feldspars include sericitised plagioclase and round-shaped grains of quartz. Quartz is supposed to occur in two generations: the older is represented by fine grains with strong undulatory extinction, the younger creates the elongated lenses composed of coarse crystals. The coarse-grained quartz shows no traces of deformation. K-feldspars are larger and more isometric inside and near the above mentioned coarse-grained quartz lenses. Both micas and chlorite replacing the biotite form elongated slipped streaks. The slip movements are younger than the origin of plagioclase blasts. Though the rock contains mylonitic parts, in general it shows no signs of cataclasis. The feldspar porphyroblasts are not attacked by mylonitisation.

As a result of field investigation and microscopic studies the author has arrived at the conclusion that the structural and textural behaviour of the so-called Jawornik granites are due neither to the crystallisation of silicate melt intruding the cold schists nor to the cataclasis of primary coarse-grained rock. The large plagioclases originated as a result of the recrystallisation of mylonites in the solid state. The granites are not intrusive magmatic rocks but the result of feldspathisation of pre-existing mylonites. It is not necessary to suppose that the feldspathisation depended on large scale migration of alkali and silica, because the rebuilding of the old mylonitic material could play a significant role. The "matrix" is probably the relict of these old mylonites. It is striking that the mica schists, the wall rock of granitic veins, remained unchanged by the granitisation processes.

The stages of metamorphic development of these rocks are as follows:

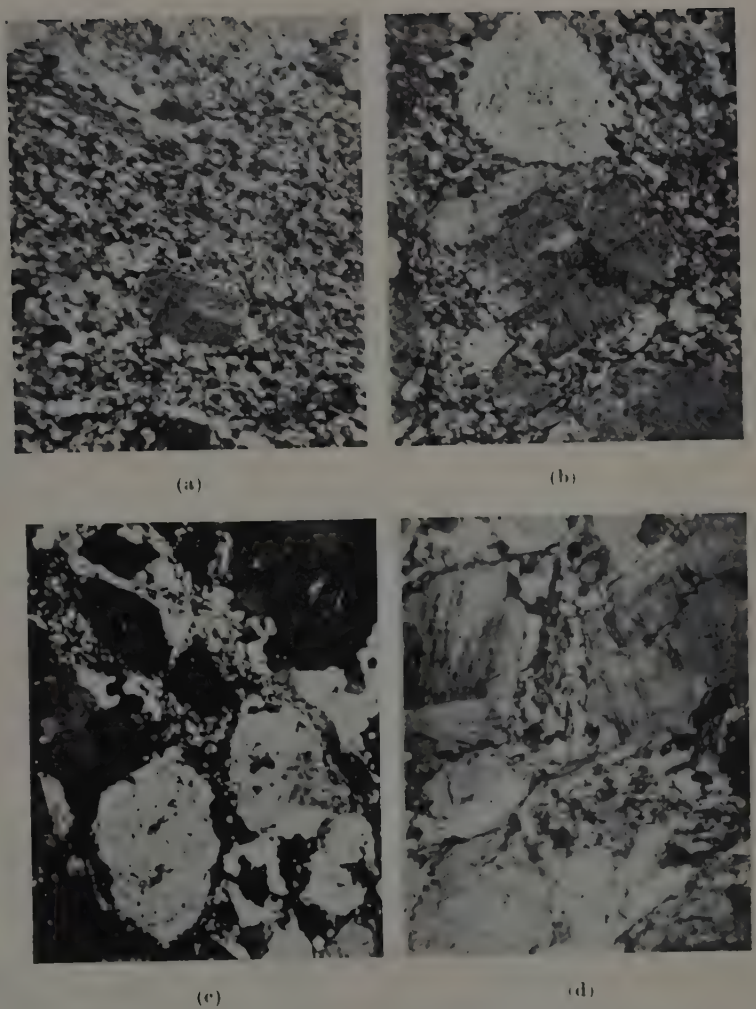

Fig. 3. (a) Plagioclase porphyroblast in mylonitic surrounding. Blastomylonite. Crossed nicols, magnified abt. 22 times. (b) Glomeroporphyroblastic texture. Blastomylonite. Crossed nicols, magnified abt. 22 times. (c) The characteristic feature of Jawornik granites: mylonitic "matrix" among plagioclase porphyroblasts. (d) Jawornik grainte. Crossed nicols, magnified approximately 17 times.

1) mylonitisation;
2) recrystallisation, origin of plagioclase porphyroblasts;
3) K-feldspar feldspathisation and enrichment in silica;
4) mica deformation due to slipping movements;
5) rock fractures more or less perpendicular to the foliation (fissures filled with prehnite, K-feldpar, epidote, quartz).

LABORATORY OF GEOCHEMISTRY, MINERALOGY AND PETROGRAPHY, GEOLOGICAL INSTITUTE, POLISH ACADEMY OF SCIENCES

REFERENCES

[1] L. Finckh, E. Meister, G. Fischer, E. Bederke, *Erl. z. Geol. Karte d. Deutschen Reiches 1:25.000, Bl. Glatz, Königshain, Reichenstein und Landeck*. Berlin, 1942.

[2] L. Finckh, Götzinger, *Erl. z. Geologische Karte d. Reichensteiner Gebirge, Nesselkoppenkamm und Neisse-Vorland, (1:75.000)*, Wien, 1931.

[3] *Geologische Karte d. Deutschen Reiches 1:25.000, Bl. Reichenstein und Landeck.*

BULLETIN DE L'ACADÉMIE
POLONAISE DES SCIENCES
Cl. III — Vol. V, No. 5, 1957

PETROLOGY

Problems of the Genesis of Granite from Kudowa

by

M. BORKOWSKA

Presented by K. SMULIKOWSKI on February 16, 1957

In the vicinity of Kudowa (Middle Sudeten) a small, but from the genetic point of view, very interesting Variscian granitic body is exposed. The outcrop lies at the bifurcation of the important and deep Pořiči-Hronov dislocation to the South West of the Góry Stołowe (Heuscheuergebirge). The granitic body forms a stock widening in the North and stretching out to the South in the form of a long, narrow and steep interformational sheet along the fault separating it from a trough filled with Lower Permian rocks (Rotliegendes) [2], [3]. Petrascheck [5], [6] is of the opinion that the granitic intrusion of Kudowa occurred at the time of the folding movements which affected also the surrounding schist series. Moreover, he considers that this intrusion forms part of a long series of intrusions approaching diorites in their composition and rich in dark minerals. The syenites of Złoty Stok (Reichenstein) are included by Petrascheck in the same type.

The table below lists results of planimetric analyses carried out by the authoress of the present paper. It shows the variability in the mineral composition of the Kudowa "granite" from different outcrops in Kudowa Zdrój and neighbouring localities.

As can be seen from Table I and from the distribution of points in the classification triangle (Fig. 1) the rock body of Kudowa is not a normal granite from the point of view of modern petrographic classification. The rocks range from monzonite granite, through granodiorites to tonalites. In almost all the rocks the content of biotite is high. Microscopic examinations show that the plagioclase belongs to relatively acid oligoclase (15—22 %) and that its preservation is much inferior to that of the undoubtedly later potash felspar which is a microcline with a very well developed grating texture (Photo 1). The quartz is almost always characterised by a mosaic structure, with elements frequently causing undulatory extinction and flattened in one direction. Only seldom concentrations of large quartz grains with normal extinction are found.

TABLE I

	Kudowa			Darnków	Dańczów		Gołaczów	
	1	2a	2b	3	4	5	6	7
Quartz	24.1	36.8	23.5	22.3	17.9	24.0	22.3	20.1
Microcline	25.6	21.9	24.8	15.8	14.4	8.4	8.4	2.9
Felspar matrix				1.1				
Plagioclase	37.7	33.3	47.4	46.3	58.5	56.9	57.7	53.4
Biotite + Chlorite	10.7	7.0	3.1	12.9	7.5	8.6	10.4	21.1
Iron ores	1.4	0.8	1.0	0.2	0.2	2.0	1.0	0.3
Other accessory minerals:	0.5	0.2	0.2	1.4	1.5	0.1	0.2	2.2
Epidote aggregate				0.5				
Zoisite	0.04			0.3	1.5			0.2
Allanite				0.03				0.3
Titanite	0.01			0.36				—
Leucoxene	—			0.15				1.5
Zircone	0.04			0.03				trace
Apatite	0.01			0.03				0.1
Calcite	0.4							0.1

Sometimes felspathic or quartz-felspathic aggregates, undoubtedly produced by later crystallisation, intrude between large felspars. These aggregates are in some cases accompanied by myrmekite which is a very frequent constituent of Kudowa "granite". In some places microcline

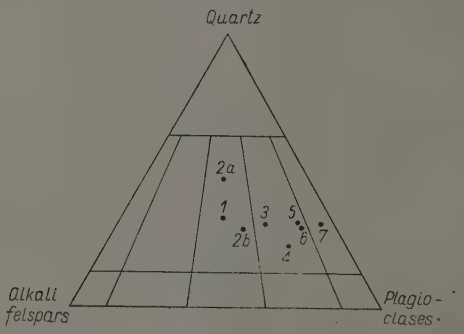

Fig. 1. Classification triangle of rocks from the granitic body of Kudowa (after Johannsen, modified by Niggli and Smulikowski [7])

perthites are abundant; they were formed by late infiltration of albite in the form of more birefringent spots and streaks intruding from the borders towards the centre of potash felspar grains.

The biotite is the only representative of micas. In some places it forms bands which cause a parallel texture of the rock, but elsewhere biotite plates develop large accumulations and dark "schlieren". A characteristic feature of the biotite in the Kudowa rock body is the multitude of pleochroic halos (Photo 2). Among the accessory constituents

1

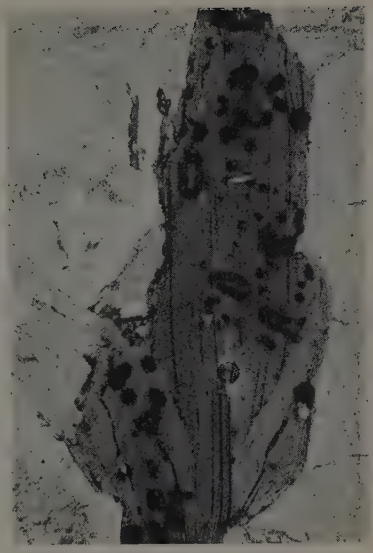

2

3

4

1. Microcline with abundant myrmekite in the monzonite granite from a quarry at the Kudowa-Radków road (crossed nicols).
2. Biotite with pleochroic halos in granodiorite from Dańczów (normal light).
3. Microcline vein cutting across a crystal of plagioclase in the granodiorite from Gołaczów (crossed nicols).
4. Microcline filling interstices between other minerals in granitised schists from an outcrop near the road at Lewin (crossed nicols).

Note: All photographs are magnified approximately 43 times.

5

6

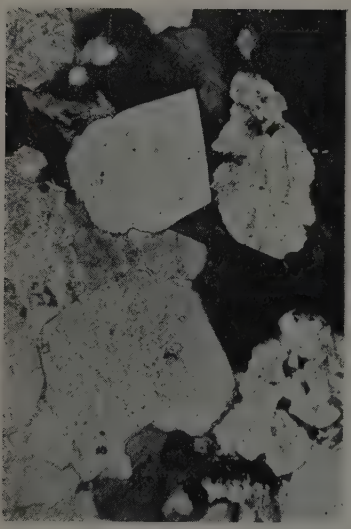

7

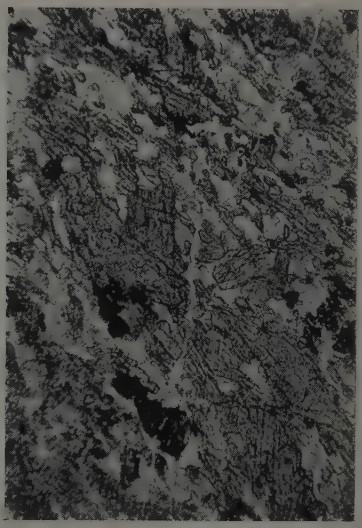

8

5. Myrmekite surrounding a grain of microcline in a paragneiss from an outcrop near the road at Lewin (crossed nicols).
6. Crystalloblastic muscovite in mica schist from an outcrop near the road at Lewin (crossed nicols).
7. Automorphic quartz crystals in a granitised mica schist from an outcrop near the road at Lewin (crossed nicols).
8. A thin clear vein filled with microcline cutting the amphiboles in a hornblende-schist from Gołaczów (normal light).

Note: All photographs are magnified approximately 43 times.

mention must be made of the minerals from the epidote group (chiefly zoisite, and sometimes allanite which in some cases is developed in the form of large, automorphic crystals) present in some places in considerable amounts, and titanite often opaque and of leucoxenic appearance.

The results of microscopic analyses do not agree with the opinion of German workers that the rock body of Kudowa belongs to the diorite group. Moreover, microscopic examinations bring out doubts on the intrusive and igneous origin of this rock. The formation of minerals in different stages — a two-fold crystallisation of felspars and quartz, microcline veins running across plagioclase crystals (Photo 3), infiltration perthites — and sometimes very apparent parallel texture bear evidence to the very intense metasomatic processes which occurred when the rocks were being formed.

As has already been mentioned, the "granite" of Kudowa is in contact with the schist series, composed of mica- and hornblende schists, mostly of sedimentary origin and metamorphosed in the epizone. The contacts of the "granite" are neither tectonic nor thermal. There are no contact minerals and this undoubtedly would have to be the case if hot liquid magma intruded into a preexisting schist series.

In the mica schists at the contact with the "granite" a twofold felspathisation is visible: first plagioclasic and later microclinic. This process caused the blastesis of felspars (primely of plagioclases) owing to which the schists were altered to paragneisses. In some places the blastesis of felspars is so intense that the rock resembles greatly the "granite" of the main body. Moreover, small lenses resembling pegmatites in their magascopic appearance are found occasionally in the schists.

The late infiltration of potassium into the schists in the course of their granitisation is supported by the presence of microcline in the interspaces between the minerals (Photo 4) and by the formation of metasomatic antiperthites in the plagioclases. Macrocrystalline microclines are found primarily in the pegmatite lenses "suspended" in the schists. These are not true pegmatites which must have the form of veins and not of small isolated and lenticular enclosures within the schists. Myrmekite is of exceptionally wide occurence and it is associated not only with the distinct and large microcline crystals (Photo 5) but is present also in places where there is no potash felspar. The formation of myrmekite was thus undoubtedly somewhat earlier than crystalloblastesis of microcline, although both processes were directly connected with one another, the latter following immediatly the former [4].

Blastesis of muscovite (Photo 6) visible in the mica-schists adjacent to the paragneisses was probably caused by the penetration of potassium when folding movements had ceased. The last stage in metasomatism of wall-rocks undergoing granitisation is the occasional formation of automorphic quartz crystals (Photo 7).

The hornblende schists of the environs of Kudowa, generally less frequent than mica schists, are usually also of sedimentary origin. The underlying garnet-bearing para-mica-schists probably belong to the same series as the mica schists mentioned previously. In the narrow contact-zone with the "granite", the hornblende schists show distinct signs of migmatisation. The "granite" lying closest to them is almost entirely deprived of potash felspar. Neither is such felspar found in the pink infiltrations penetrating into the adjacent schists. On the other hand, microscopic examinations reveal its presence in the narrow veins (Photo 8) cutting across the amphiboles and the other primary minerals of the schists. The biotitisation of hornblende, visible in some places, is probably also due to a later invasion of potassium into the rock. Under the migmatising effect of the Kudowa "granite" recrystallisation and blastesis of hornblende grains occurred in the schists and this is most apparent in the vicinity of most abundant accumulations of the light veins.

The study of the contacts of the Kudowa "granite" with the crystalline schists confirm the doubts raised earlier in this paper in respect to its intrusive nature. Indeed, microscopic examination has stressed the significance of some facts which contradict the formation of the Kudowa "granite" through normal differentiation from a silicate melt and suggest another genetic hypothesis. Signs of metasomatism are very distinct in the mica schists. Selective migmatisation visible in the series of hornblende schists (the pink veins penetrating into the schists are entirely composed of plagioclase or of plagioclase and quartz) is undoubtedly also the result of metasomatism. The question thus arises whether or not the whole granite body owes its origin to metasomatism, and where is the source of the matter which caused it to be looked for?

It seems somewhat unlikely that the whole "granite" body of Kudowa was formed simply by normal metasomatism consisting solely in penetration of, first, sodium – and then potassium emanations into the older crystalline schists under conditions of relatively low temperatures. This supposition is contradicted by the compact nature of the body deprived of any schist intercalations. The contact effects at the boundary with the mica schists found in the flanks of the body are confined to a narrow zone: over a space of about 4 m. there are on the one side granite rocks and on the other – unaltered schists. It follows, therefore, that the processes involved in the formation of the granite body of Kudowa had to occur in deep regions at high temperatures, where a sedimentary complex was granitised. The complex was so extensively metasomatised that it is impossible at present to define the chemical nature of its primary rock-components. Inasmuch as the composition of the granite body of Kudowa is varied (monzonite granite—granodiorite—tonalite) it seems that the susceptibility of the preexisting rocks to granitising factors was se-

riously differentiated. Possibly, the primary sedimentary rocks of different facies varied in their conductivity of the granitising emanations. The penetration of the primitive sediments by immigrating matter led to an increase of their volume and consequently to their mobilisation, i. e., rheomorphism [1]. The results of these processes were differential movements and plastic folding, and finally an intrusion in the direction of least resistance.

In the light of the above hypothesis the "granite" of Kudowa is neither a magmatic rock, nor a product of metasomatism *in situ* of surface rocks. The rocks from Kudowa defined as granite are in fact rheomorphites, i. e., the products of extreme granitisation and plastic mobilisation of some deep sedimentary complex.

The author is sincerely grateful to Professor K. Smulikowski for his kind advice in the course of this work.

DEPARTMENT OF GEOCHEMISTRY, MINERALOGY AND PETROGRAPHY,
GEOLOGICAL INSTITUTE, POLISH ACADEMY OF SCIENCES

REFERENCES

[1] H. G. Backlund, *Zur „Granitisationstheorie"*, Geol. Fören. Förhandl. **60** (1938), 177.

[2] H. Cloos, *Das Batholithenproblem (Der Granit von Kudowa)*, Fortschr. d. Geol. u. Palaeont. (1923), 39.

[3] — *Der Gebirgsbau Schlesiens*, Berlin 1922, p. 54.

[4] F. K. Drescher-Kaden, *Die Feldspat-Quartz-Reaktionsgefüge der Granite und Gneise*, Berlin-Göttingen-Heidelberg, 1948.

[5] W. Petrascheck, *Die kristallinen Schiefer des nördlichen Adlergebirges*, Jahrb. k. k. Geol. Reichsanst., **59** (1909), 427.

[6] — *Der Böhmische Kamm*, Handbuch der Regionalen Geologie, Abt. 5, 1 (1944), 238.

[7] K. Smulikowski, *Les roches éruptives des Andes de Bolivie*, Arch. Min. **10** (1934), 122.

BULLETIN DE L'ACADÉMIE
POLONAISE DES SCIENCES
Cl. III — Vol. V, No. 5, 1957

GEOLOGY

Notes on the Geological Evolution of the Eastern Sudeten Mountains

by

K. ŁYDKA

Presented by K. SMULIKOWSKI on February 16, 1957

Petrographic examination of the detrital bed of the Culm-facies in the eastern fringe of the Sudeten Mountains yielded some information on the origin of the crystalline rocks in that mountain massif [3]. This was possible because the terrigenous material had been carried from the mountains to the Lower Carboniferous sedimentation basin. Microscopic examination referred to the material constituting the pebbles of the conglomerates in the Górny Beneszów beds (Bennischer Grauwacken) of the Upper Tournaisian sediments. The beds are made up of material from Jesioniki (Altvatergebirge) and crop out in the neighbourhood of Dobieszów (district of Głubczyce). From the results of microscopic examination of their pebbles it was possible to determine the time of some stages of tectonic evolution in the Eastern Sudeten, particularly in the Jesioniki Ridge.

Microscopic analyses of the gneiss pebbles from the Górny Beneszów beds — which in the present author's opinion correspond to the Caledonian gneisses of Desna [1], [5] — showed that they had passed through numerous metamorphic stages. It was not always possible to establish their original nature. Paragneisses, developed originally in granulite facies, are the most common component. Orthogneisses could not be distinguished with absolute certainty. The paragneisses were composed of potash felspar, quartz and garnets. Among the pebbles there are gneiss specimens showing further stages of metamorphism, i. e., the garnets were sometimes transformed into oligoclase-biotite aggregates with relic scraps of garnets. In some of the rocks the garnets had disappeared completely leaving characteristic oligoclase-biotite pseudomorphs with accessory muscovite. The traces remaining after the alteration of garnets showed that conditions had changed and that the pre-existing complex had passed from the granulite into the amphibolite facies. Oligoclase

in these rocks has the form of large blasts frequently rolled into lenticular agglomerates of small xenoblasts. This means that the rocks had been deformed dynamically in conditions of the amphibolite facies. The gneiss specimens examined showed even further stages of metamorphism: postkinematic albitisation marked by the appearance of large idioblasts of pure and clear albite containing about 4 per cent of anorthite. The last stage of metamorphism which can be observed is marked by diaphtoretic chloritisation of biotite and sericitisation of plagioclase felspars.

The presence in the conglomerates of the Górny Beneszów beds of the gneiss pebbles just described, derived from the erosion of the Jesioniki (Altvatergebirge) crystalline formations could mean only that all the particular stages of metamorphism mentioned above are earlier than Upper Tournaisian.

Further facts of much significance were exposed by analysing the pebbles of other rocks present together with the gneisses in the Culm conglomerates. In the course of microscopic investigations two main lithological types of extrusive rocks, formerly constituting one rock type only, were distinguished. Intermediate forms between both types were also identified. One type is represented by pebbles of quartz bearing extrusive rocks—mostly rhyodacites—the other consists of porphyroid pebbles. Both types were compared by the author with analogical rocks from Middle Devonian Jesioniki beds, where — similarly as in the Culm pebbles — the intermediate forms were also found. Hitherto, in earlier reports of other workers the Middle Devonian quartz-bearing extrusive rocks from Jesioniki were defined as keratophyres [4].

The presence of Middle Devonian porphyroids among the Lower Culm pebbles is of much significance, as this is the basis for dating the metamorphic transformation of quartz-bearing extrusive rocks or their tuffs which has occurred in the primary region later than the Middle Devonian and prior to the Upper Tournaisian. The porphyroids are cut by numerous thin veins filled with quartz and chlorite. The thickness of the veinlets is a fraction of a millimetre and as a rule they cut obliquely the parallel rock texture.

Rhyodacite pebbles also supply some interesting data. In several of the pebbles examined, neoformation of epidote and albite is observed. The formation of small albite blasts in the rock background and in the fissures of these rocks is due to metamorphism manifested by the decomposition of plagioclases. Epidote was formed from the anorthite constituent and the albite molecules were liberated in the form of small blasts. All these effects show clearly that the metamorphism of the preexisting rocks has occurred under conditions of the greenstone mineral facies.

Another point of much interest is that among the small fragments in the Górny Beneszów greywackes there are also fragments of Lower

Devonian graphite phyllites. The phyllites were intensely folded with symptoms of parakinematic felspathisation. New felspars correspond to acid oligoclase (12—14 per cent of anorthite).

The above facts indicate that the metamorphism of the Lower and Middle Devonian beds occurred prior to Upper Tournaisian sedimentation.

The observations and considerations reported in the present paper lead to the conclusion that the Marsian subphase of the Bretonian phase was very distinctly marked in the Eastern Sudeten. The present results throw new light on the time at which metamorphism occurred in Jesioniki. According to the opinion of Bederke [1], [2] the Upper Devonian folding was associated with the Erzgebirge orogenetic stage.

The author wishes to express his sincere gratitude to Professor K. Smulikowski for his kind assistance and criticism in the course of this work.

DEPARTMENT OF PETROLOGY, WARSAW UNIVERSITY

REFERENCES

[1] E. Bederke, *Bau und Alter des Ostsudetischen Gebirges*, Neues Jahrbuch f. Mineralogie etc., Beil. Bd. Ser. B. **53** (1926).

[2] — *Die Regionalmetamorphose im Altvatergebirge*, Geol. Rundschau, **26** (1935).

[3] K. Smulikowski, *The old crystalline formations of the Sudeten Mountains*, Annales de la Soc. Géol. de Pol. **21** (1951), No. 1.

[4] J. Stejskal, *Geologische Forschungen im Hohen und Niederen Gesenke*, Geol. Rundschau, **20** (1929).

[5] H. Teisseyre, *Some remarks on the tectonic structure of Caledonides and Variscides in the Sudeten*, Bull. Acad. Polon. Sci., Cl. III, **4** (1956), 165.